



HAL
open science

Experimental and computational analysis of REM sleep distributed cortical activity in mice

Mathias Peuvrier

► **To cite this version:**

Mathias Peuvrier. Experimental and computational analysis of REM sleep distributed cortical activity in mice. *Neurons and Cognition [q-bio.NC]*. Sorbonne Université, 2022. English. NNT : 2022SORUS199 . tel-03828203

HAL Id: tel-03828203

<https://theses.hal.science/tel-03828203v1>

Submitted on 25 Oct 2022

HAL is a multi-disciplinary open access archive for the deposit and dissemination of scientific research documents, whether they are published or not. The documents may come from teaching and research institutions in France or abroad, or from public or private research centers.

L'archive ouverte pluridisciplinaire **HAL**, est destinée au dépôt et à la diffusion de documents scientifiques de niveau recherche, publiés ou non, émanant des établissements d'enseignement et de recherche français ou étrangers, des laboratoires publics ou privés.



Thèse présentée pour obtenir le grade de docteur
Sorbonne Université



École doctorale ED 158 - Cerveau, cognition, comportement

Discipline : Neurosciences

**EXPERIMENTAL and COMPUTATIONAL
ANALYSIS OF REM sleep DISTRIBUTED
CORTICAL ACTIVITY IN MICE**

PAR : Mathias Peuvrier

Sous la direction de ALAIN DESTEXHE, Directeur de Recherche au
CNRS, Université Paris-Saclay

et de PAUL-ANTOINE SALIN, Directeur de Recherche au CNRS,
Université Lyon 1

MEMBRES DU JURY:

Rapporteur : Nathalie BUONVISO, Université Lyon 1

Rapporteur : Viktor JIRSA, Aix-Marseille l'Université

Examineur : Laure BUHRY, Université de Lorraine.

Directeur de Thèse : Alain DESTEXHE, Université Paris-Saclay

Directeur de Thèse : Paul-Antoine SALIN, Université Lyon 1

Date de soutenance : 28 avril 2022

What is REM sleep?
C'est une bonne question!

Résumé

Le sommeil à mouvements oculaires rapides, également appelé sommeil paradoxal, est un état de sommeil intrigant classiquement décrit comme présentant une activité électrique d'oscillations de faible amplitude et de fréquence rapide identique à celle de l'éveil. Chez les rongeurs, les enregistrements EEG sont caractérisés par une oscillation thêta continue et de forte puissance (5-10 Hz) qui peut refléter l'activité d'un certain nombre de zones corticales et sous-corticales telles que l'hippocampe. Cependant, des études récentes utilisant des techniques de résolution spatiale plus fines ont montré que, pendant le sommeil paradoxal, les aires corticales présentent une activité de fréquence lente proche de celle du sommeil à ondes lentes. L'objectif de la thèse est de mieux caractériser la distribution temporo-spatiale de ces oscillations lentes et rapides au cours de cet état de sommeil, puis de proposer un modèle computationnel permettant de faire des prédictions sur les mécanismes responsables de cette distribution complexe d'activité corticale. A l'aide de différents algorithmes de traitement du signal, nous avons d'abord analysé les ondes lentes du sommeil paradoxal ($<4.5\text{Hz}$) en la comparant au sommeil lent, ainsi que son activité thêta, en utilisant des enregistrements multi-sites de potentiel de champ local (LFP) dans le cortex somato-moteur, le cortex préfrontal médian (mPFC) et l'hippocampe de la souris. Nous avons montré que, dans les zones somato-motrices, l'activité du sommeil paradoxal présente plusieurs caractéristiques différentes de celle du sommeil lent. En particulier, l'activité du sommeil paradoxal a une fréquence légèrement plus élevée que celle du sommeil lent, se rapprochant ainsi des oscillations delta (2-4.5Hz). Les ondes lentes du sommeil paradoxal alternent également avec des oscillations de fréquences petites et rapides à travers les épisodes de sommeil paradoxal. Les ondes lentes sont prévalentes dans le cortex somatosensoriel primaire (S1) et dans le cortex somatosensoriel secondaire (S2), mais sont rarement présents dans le cortex moteur primaire (M1). Les ondes lentes du sommeil paradoxal sont fortement corrélées entre les zones S1 et S2 mais faiblement entre celles-ci et la zone M1. En revanche, les ondes lentes du sommeil paradoxal n'est pas observé dans l'hippocampe et le mPFC. L'activité thêta dans l'hippocampe est caractérisée par de brèves ($<2\text{s}$) périodes de fréquence accrue appelées « thêta phasique ». Nous montrons que ces périodes de thêta phasique se retrouvent dans l'EEG et le mPFC. Ce thêta phasique est fréquemment associé aux ondes lentes dans les zones S1, S2 et M1. En conclusion, cette étude suggère une nouvelle description des oscillations lentes et rapides corticales dans le sommeil paradoxal avec des périodes d'activité coordonnée entre les aires corticales. Pour étudier les mécanismes sous-jacents possibles de cette activité corticale distribuée, nous avons ensuite développé un modèle computationnel du cortex

entier de la souris en sommeil paradoxal. Ce modèle est composé de champs moyens AdEx (Adaptive Exponential integrate-and-fire) considérés comme des nœuds du réseau neuronal. Les champs moyens AdEx sont composés de neurones excitateurs à décharge régulière (neurones RS) et de neurones inhibiteurs à décharge rapide (neurones FS) dans une proportion correspondant aux données biologiques. Un paramètre important qui régule l'activité simulée par ce modèle est l'adaptation de la fréquence des potentiels d'action. Ces champs moyens AdEx ont été connectés entre eux selon le connectome de la souris (c'est-à-dire la carte des connexions entre les neurones des aires corticales ; source ouverte de l'Allen Brain Institute). Les propriétés dynamiques du réseau sont simulées à l'aide du simulateur The Virtual Brain (TVB). Pour comparer avec nos données expérimentales, la LFP est calculée dans chaque aire corticale de la souris. Nous proposons que différents niveaux d'adaptation de la fréquence des potentiels d'action soient mis en œuvre dans les différents champs moyens AdEx représentant les zones corticales, conformément à nos résultats biologiques. Dans ces conditions, les simulations du modèle reproduisent la distribution des oscillations lentes et rapides dans les aires somato-motrices et dans les autres aires corticales. Le sommeil paradoxal est caractérisé par un seuil de réponse sensorielle plus élevé que celui de l'éveil. Nous avons donc testé si le modèle de sommeil paradoxal répond différemment d'un modèle d'éveil à une stimulation mimant un stimulus sensoriel. Le modèle de sommeil paradoxal avec un niveau différent d'adaptation de la fréquence des potentiels d'action soutient l'idée que les ondes lentes du sommeil paradoxal pourraient expliquer une réponse réduite à la stimulation pendant cet état par rapport à l'état d'éveil. L'adaptation de la fréquence des potentiels d'action est liée à la signalisation neuromodulatrice et en particulier à celle de l'acétylcholine, qui est présente à un niveau élevé pendant le sommeil paradoxal. Ainsi, nous proposons qu'une distribution dynamique temporo-spatiale de la signalisation cholinergique puisse expliquer les caractéristiques spécifiques de l'activité corticale du sommeil paradoxal par rapport au sommeil lent et à l'éveil.

Abstract

Rapid Eye Movement (REM) sleep (also called Paradoxical sleep) is an intriguing sleep state classically described as having an electrical activity of small amplitude and fast frequency oscillations identical to wakefulness (W). In rodents, the EEG recordings are characterised by a continuous and high power theta oscillation (5-10 Hz) that may reflect the activity of a number of cortical and subcortical areas such as the hippocampus. However, recent studies using finer spatial resolution techniques have shown that, during REM sleep, cortical areas present a slow frequency activity close to that of Slow Wave Sleep (SWS). The aim of the thesis is to better characterise the temporo-spatial distribution of these slow and fast oscillations during this sleep state and then to propose a computational model that allows to make predictions about the mechanisms responsible for these complex activity patterns. Using different signal processing algorithms, we first analysed REM slow-wave activity (SWA, $<4.5\text{Hz}$) by comparing it to SWS, as well as its theta activity, using multi-site local field potential (LFP) recordings in the mouse somato-motor cortex, medial prefrontal cortex (mPFC) and hippocampus. We showed that, in the somato-motor areas, the REM sleep SWA has several different characteristics compared to the SWS. In particular REM sleep activity has a slightly higher frequency than that of the SWS, thus being close to delta oscillations (2-4.5Hz). REM sleep SWA also alternates with small and fast frequency oscillations across REM episodes. SWA is prevalent in the primary somatosensory cortex (S1) and in the secondary somatosensory cortex (S2), but is rarely present in the primary motor cortex (M1). REM sleep SWA are strongly correlated between areas S1 and S2 but weakly between these and area M1. In contrast, REM SWA is not observed in the hippocampus and the mPFC. Theta activity in the hippocampus is characterised by brief ($<2\text{s}$) periods of increased frequency called phasic theta. We show that these periods of phasic theta are found in the EEG and the mPFC. This phasic theta is frequently associated with SWA in areas S1, S2 and M1. In conclusion, this study suggests a new description of cortical slow and fast oscillations in REM sleep with periods of coordinated activity between cortical areas. To investigate possible underlying mechanisms of this cortical distributed activity, we then developed a computational model of the mouse whole cortex in REM sleep. This model is composed of Adaptive Exponential integrate-and-fire (AdEx) mean-fields considered as nodes of the neural network. AdEx mean-fields are composed of excitatory neurons with regular spiking discharge (RS neurons) and inhibitory neurons with fast discharge (FS neurons) in a proportion corresponding to the biological data. An important parameter that regulates the activity simulated by this model is the spike frequency adaptation. These AdEx mean-fields were connected together according to

the mouse connectome (ie map of the connections between neurons of the cortical areas ; open source from the Allen brain Institute). The dynamic properties of the network are simulated using The Virtual Brain (TVB) simulator. To compare with our experimental data, the LFP is computed in each mouse brain area. We propose that different levels of spike frequency adaptation are implemented in the different AdEx mean-fields representing the cortical areas in accordance with our biological results. In these conditions, the model simulations reproduce the distribution slow and fast oscillations in the somato-motor areas and in the other cortical areas. REM sleep is characterised by a higher sensory response threshold compared to wakefulness. We therefore tested whether the REM model responds differently to a stimulation mimicking a sensory stimulus than an awake model. The model of REM sleep with different level of spike frequency adaptation supports the idea that REM sleep SWA could explain a reduced response to stimulation during this state compared to the awake state. The spike frequency adaptation is linked to neuromodulatory signaling and in particular to acetylcholine, that is present at a high level during REM sleep. Thus, we propose that a dynamic temporo-spatial distribution of cholinergic signalling may explain the specific characteristics of REM sleep activity compared to SWS and wakefulness.

Remerciements

A ma famille, mes amis, et tous ceux qui m'ont aidé. Sans vous cela n'aurait pas été possible.

A mes professeurs, mes camarades, et tous ceux avec qui j'ai pu échanger. Ce que j'ai écrit, ce sont aussi vos idées.

Merci

Ce travail a été supporté par l'*Agence National de la Recherche* (ANR PARADOX), le *Human Brain Project*, ainsi que par la *National Science Foundation* (bourse *AccelNet*).

Summary

Résumé	v
Abstract	vii
I Introduction	1
1 Neurophysiology of Rapid Eye Movement sleep	3
1.1 sleep generalities	3
1.1.1 What is a brain state? - REM as example	4
1.2 The sleep-wake cycle	5
1.3 REM sleep regulation	7
1.3.1 Brainstem and REM regulation	8
1.3.2 Neuromodulation in REM	8
1.3.3 A central structure: the Thalamus	8
1.4 More about REM sleep	9
1.4.1 REM, a classical description	9
1.4.2 The hippocampus and theta rhythm in rodent REM	10
1.4.3 REM is a complex sleep state	11
1.4.4 Neurobiological substrate of dreams	13
1.4.5 Recent perspectives related	15
2 Modelling mouse REM	17
2.1 What is a model?	17
2.1.1 Popular models in neurosciences	18
2.1.2 Neuron model - the single unit scale	19
2.1.3 Network model - multiple units interacting	20
2.1.4 Spiking neuron network	22
2.1.5 Mean-fields - a population model	22
2.2 About the model in this thesis	23
2.2.1 Adex integrate and fire neurons	24
2.2.2 Adaptation	24
2.2.3 Adex network	25
2.2.4 Adex mean-fields	26
2.2.5 LFP modelling	28

2.2.6	TVB - integration into whole brain network	29
II	Objectives	31
III	Experimental analysis of mouse REM sleep	35
IV	Model	53
V	Discussion	71
2.3	Result summary	73
VI	Bibliography	81

PART I

Introduction

Neurophysiology of Rapid Eye Movement sleep

1.1 sleep generalities

Sleep is a fundamental state existing in the whole animal kingdom from worms to primate. Compared to wakefulness, it is characterised by complex changes in physiological and behavioral processes; it is a reversible and recurring global state typically characterised by postural recumbency, fundamental loss of awareness and responsiveness, behavioral quiescence, but also closed eyes, decreased temperature, slow respiration and others. . . [21, 25, 10]

Sleep, and its fine structure, occurs on a circadian rhythm, in alternation with wakefulness, and is homeostatically regulated (coordinated with physiological processes tracking the evolution of “sleep pressure”). The interaction of those two mechanisms will regulate the timing, the duration and the quality of sleep and wakefulness [24, 11, 1, 34]. This sleep pattern is specific for all species, and large deviations from what is considered ‘standard’ can be seen as unhealthy or even pathological [21]. Finally, in a number of mammalian species, sleep is consolidated with a prolonged period of wakefulness of several hours alternating with sleep cycles (e.g. in carnivores and primates). On the other hand, in other mammals sleep is not consolidated, i.e. wakefulness is frequently interrupted by sleep episodes (in prey animals such as rodents).

The discovery of sleep Modern era of sleep science began with the electroencephalography (EEG) and the recording of sleeping humans [38, 58, 59], which revealed that sleep is not uniform but composed of multiple states characterised by specific patterns of cortical activity. The two main states are described as “small EEG waves as in the alert waking state” from Derbyshire 1936 p582) [42] on one hand, and an EEG with slow, high amplitude waves on the other hand. Those are the Rapid Eye Movement (REM, also referred to as Paradoxical sleep) sleep and the Slow Wave Sleep (SWS also called Non-REM (NREM), sleep).

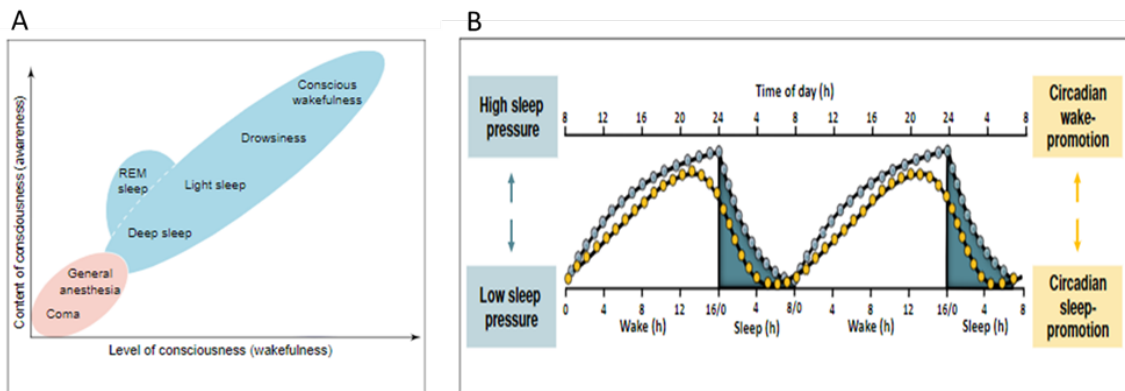


Figure 1.1: **Sleep generalities.**

(A) Oversimplified illustration showing the specific place of REM when compared to the different physiological states classified according to the two major components of consciousness. In blue-green the healthy physiological states and in red the pathological or pharmacological coma. Figure adapted from [55]

(B) Schematic illustration of the classical two process model for the sleep-wake regulation [24] extracted from C Reichert [19]

1.1.1 What is a brain state? - REM as example

In an article trying to understand brain states, Brown [17] cites Pogler 2004 to remind that “the identity conditions for a thing [...] are the boundary conditions for that thing”. The identity conditions do not need to be exact and exhaustives, but we have to know what sorts of properties are relevant to tell if something belongs to the kind of things in question. This means that the discriminative method, that depends on the observation technique, we use to assess sleep states is actually central in the description of this state. A good example of the importance of that is about the discovery of REM sleep.

The discovery of REM In the 50’s the discovery of REM sleep has been of great importance to our understanding of states of vigilance and consciousness. [42]. Surprisingly, in less than ten years, the sleep stage is defined by two different teams, with two different perspectives. First, Aserinsky, Dement and Kleitman published study polysomnography recordings of human sleep and published multiple papers about the sleep stage. They describe a state with low-voltage EEG associated with eye movements, relate those eye movements to dream content and recall, and show that episodes of this sleep stage increase in duration during the night. They thus called it, the Rapid Eye Movement sleep.

On the other hand, Jouvet et al published a series of articles about sleep electrophysiology in different cat preparations. They describe a paradoxical stage of sleep with loss of muscle tone, rapid EEG, theta activity in the hippocampus, changes in heart rate and breathing and jerks of the paws and tail. They also describe PGO waves, which are large LFP deflection recorded from the pontine brainstem (P), the lateral geniculate body of

the thalamus (G), and the occipital cortex (O), and propose that they could be internal signals of significance for dream theory [46]. This description of the sleep state is centered on the apparent opposition of a rapid brain activity associated with a muscle atonia, while it is only on the third article about this sleep stage that eye movements are reported, thus the name of Paradoxical Sleep. These two definitions are not exclusive but rather complementary.

1.2 The sleep-wake cycle

REM is usually presented in contrast to W and SWS, and the identification of vigilance states based on physiological recordings, called sleep scoring, is essential for sleep researchers and clinicians. So before defining REM, we will contextualize it by presenting the sleep-wake cycle of healthy humans, as illustrated with the schematized sleep hypnogram figure 1.2,B(*top*) (also fig 1.4 and 1.7,A for a full human hypnogram). Although sleep scoring methods are still debated among the scientific community [5, 32] they usually rely on EEG and EMG recordings, as illustrated on figure 1.2, where we can observe the important electrophysiologic oscillations typically associated to each state.

Wakefulness (we do not make distinctions in different W states here) is characterised by a small amplitude desynchronized EEG and a high muscular activity. It is the state of maximal consciousness and awareness[55]. Then sleep begins with SWS and progresses through deeper stages indicated by a progressive dominance of low-frequency high voltage synchronous EEG and multiple electrophysiological signatures associated such as the Delta waves/K-complex, spindles and hippocampal sharp waves ripples. This progression through a deeper sleep state is accompanied by very little muscular activity and with a decrease in the content and level of consciousness. Then comes the first REM episode, with its desynchronized EEG similar to W, and muscle atonia. Several studies (memory of dreams after waking up during REM or SWS; lucid dreaming during REM also suggest that it is during this state that dreaming activity takes place in a privileged way [46, 100], although dreams can also take place during SWS [85]. Because of this complex phenomenology, this state usually deviates from the other natural states in the relation between wakefulness and awareness! REM is then generally followed by a small awakening and the sleep cycle repeats over the night[21]. The amount of SWS and REM in each cycle varies across the night, dominated by SWS and its deepest stages in the first part of the night, while REM is prevailing in the last part.

The general principles of the sleep-wake cycle are the same in rodents, although some differences should be noted. First, as mentioned above, the sleep-wake cycle is shorter and more fragmented (or less consolidated) than in humans and it occurs at a different circadian time. Second, the W period considered is not exactly the same. While in humans it is mostly the pre-sleep period of W that is considered in the sleep studies, in rodents a

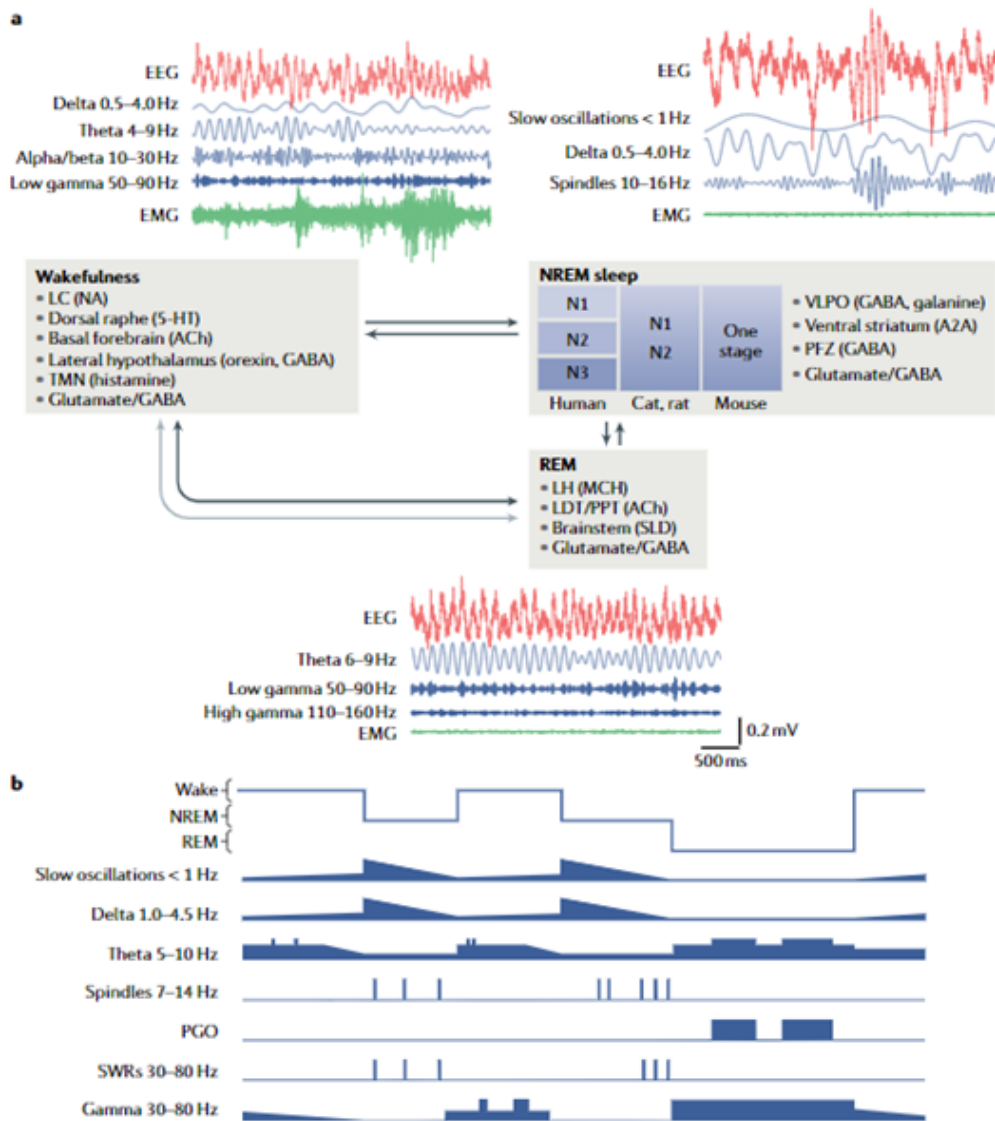


Figure 1.2: **Summary of the sleep state specific oscillations**

(A) Typical electroencephalography (red), electrophysiologic oscillations (blue) and muscular activity (green) associated to the different sleep-wake states. The boxes highlight important elements of the different states regulation and shows that SWS (NREM) can be decomposed into multiple substates in human and cat. [55]

(B) Representative hypnogram of the mouse sleep-wake cycle, showing network oscillations associated with vigilance states. We see that REM is relatively uniform, with some long PGO occurring in relation with an amplified theta. We can notice when looking at the different frequency bands described in this unmodified picture from a review that the exact definition of a frequency band is not standardized and definitive as well as the fact that different oscillatory band can overlap according to some authors definition.

Extracted from [2].

larger portion of the total W is considered, usually pulled together it is sometimes splitted into active and quiet W periods [31]. Finally, SWS is classically considered as a single state in rodents, although some work considered it as multiple stages or some identified another sleep state referred to as intermediary sleep (between SWS and REM). In this work about REM we will simply consider the three classical states, W, SWS and REM without further distinctions in the W and SWS states.

1.3 REM sleep regulation

Major work looked at the mechanisms regulating those sleep states and a lot of findings point to the important role of subcortical structures in this regard. While this is not the subject of our work, we will briefly overview some of the findings that are important to understand REM sleep and the cortical activity in this state. Our short review is summerized on the figure 1.3 and can be complemented by [62] for the interested reader

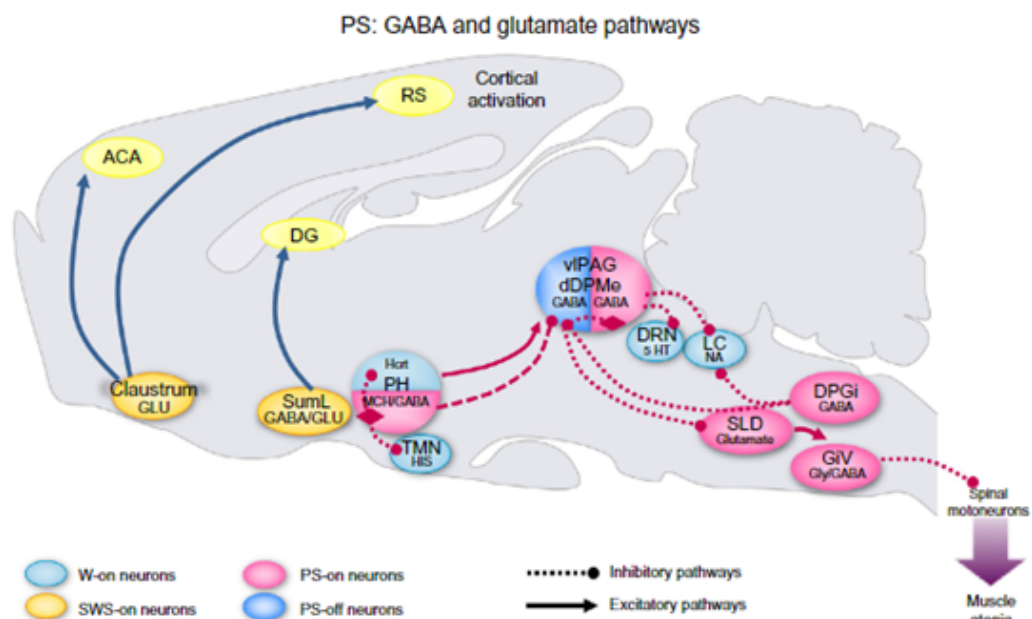


Figure 1.3: **Neuronal networks responsible for paradoxical sleep**

This figure show the different neurons from the pontine reticular formation that are involved in the generation of REM sleep. We can notice different structures we evoke: the ventro-lateral periaqueductal gray (vIPAG) and the sublatero-dorsal tegmental nucleus (SLD), the orexin (Hcrt) and melanin-concentrating hormone (MCH) neurons of the posterior hypothalamus

Extracted from [62].

1.3.1 Brainstem and REM regulation

We will first mention the ventro-lateral periaqueductal gray (vlPAG) and the sublaterodorsal tegmental nucleus (SLD). Those structures have a mutually inhibitory relationship that is ultimately responsible for the muscle atonia in REM [62], making them an essential element of REM sleep regulation. The activity of these structures is influenced by the lateral and posterior hypothalamus, where neurons producing melanin-concentrating hormone (MCH) are mixed with orexin neurons. Both neuron groups receive afferents from many components of the ascending arousal system, and send axons to the brainstem, basal forebrain and the thalamus to some extent. While they participate in the same brain circuitry, Orexin neurons fire preferentially during wakefulness and are thought to regulate the sleep-wake cycle perhaps by their excitatory action on the neurons of the locus coeruleus. In contrast, MCH neurons fire mainly during REM sleep and inhibits target neurons, thus the two populations have the exact opposite activity profile.

1.3.2 Neuromodulation in REM

Neuromodulation by acetylcholine, noradrenaline, histamine, dopamine or other neuromodulators from several brainstem nuclei, drives the activity of large neuronal populations in the brain and is essential for the transitions between sleep states. Among them, Pedunculopontine (PPT) and laterodorsal tegmental nuclei (LDT) are cholinergic nuclei that innervate the thalamus, lateral hypothalamus, basal forebrain and prefrontal cortex. With a suggested role in driving cortical activation, neurons of those nuclei fire mainly during W and REM [83, 65, 90, 64]. Close by, multiple monoaminergic cell groups can be found, such as the noradrenergic cells in the Locus Coeruleus or the histaminergic neurons in the tuberomammillary nucleus. As for cholinergic nuclei they innervate multiple cortical and subcortical structures, but contrary to the first one, monoaminergic cells fall silent during REM. While the actual role of neuromodulation in the switching mechanism from SWS to REM is questioned by lesional studies [61], it is most likely that neuromodulation, and Acetylcholine particularly, plays an important role in the modulation of the brain activity in REM [83, 56].

1.3.3 A central structure: the Thalamus

Finally, the Thalamus is essential in shaping cortical activity. The Thalamus is a structure that occupies a large part of the diencephalon and is composed of several nuclei with specific roles each. It is a key structure in most sensory processing acting as a relay between peripheral sensory inputs and the cortex, and is also involved in arousal, attention and motor control. While its role in the transition from one state to another might be questioned, the thalamocortical neurons (TC, the thalamic relay cells from the Thalamus

nuclei) is the most important source of subcortical glutamatergic afferent to the cortex. Another important area of the Thalamus is the reticular nucleus. These Inhibitory cells do not contact the cortex but modulate the activity of TC neurons, thus shaping the thalamocortical transmission.

Thalamic TC neurons receive inputs from the different neuromodulators we evoked before and thalamocortical exhibits two distinct activity states: a tonic activity during W and REM that is conducive to sensory processing and cognition, and synchronized rhythmic activity with slow waves, delta and spindles during SWS [72, 95, 94]. The exact activity and implication of the Thalamus in REM cortical activity remains outside the scope of this thesis although this structure is a key component in order to understand what is going on in the cortex. Also it should be noted that, we know less about the thalamic activity in REM compared to W and SWS and the similarity of activity in REM and W should certainly be contrasted.

In an article we can find: "With the exception of the theta rhythm, all sleep and wake brain oscillations are generated in the thalamocortical (TC) system" [94]

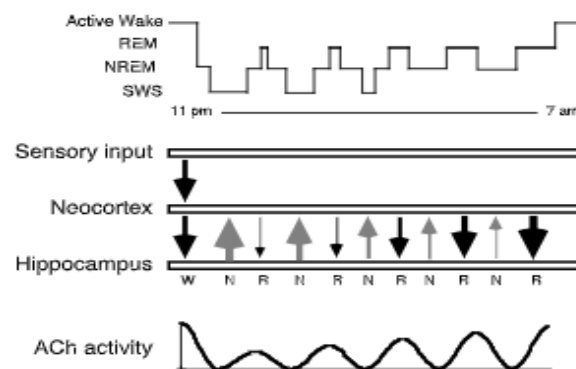


Figure 1.4: **Simplified sleep wake cycle and information processing**

Changes in cholinergic neuromodulation and hippocampo-neocortical communication are superimposed on the human sleep cycle.

Extracted from [91].

1.4 More about REM sleep

1.4.1 REM, a classical description

Since its discovery in the 50's, we know a lot more about REM sleep. Although usually described in comparison to W and SWS, REM is a very unique and complex state and descriptions such as "A 'dreaming state' characterised by an awake brain with a sleeping body", as we implied earlier, we don't really consider many aspects that happen in that state.

1.4.2 The hippocampus and theta rhythm in rodent REM

Theta (5 – 10 Hz, or sometimes broader) rhythm is a prominent coherent oscillation (monochromatic) present in all mammals, especially in rodents. Especially evident in the hippocampus, theta is observed during spatial navigation and exploration in W but also during REM and it plays an important role in the formation and retrieval of episodic and spatial memory (fig 1.5, 1.6) [101].

During W navigation, hippocampal place cells, that are pyramidal neurons that encode the animal location, progressively spikes in coordination with the local theta frequency oscillation while the animal moves toward the related place field. This mechanism, known as phase precession, compresses the spatial trajectories of an individual into the timescale of theta cycle and is theorized as a way for the brain to represent sequential experiences [79].

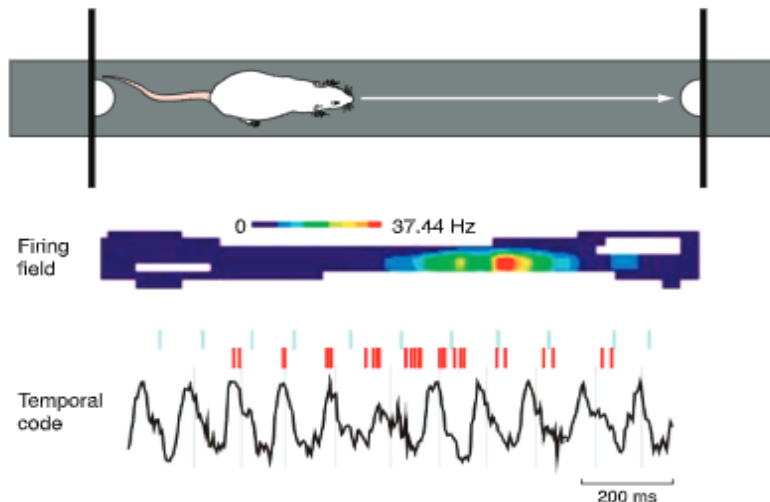


Figure 1.5: **Theta rhythm in the hippocampus during spatial navigation**

In a task the rat moves back and forth along a linear track. The color-coded trace shows the firing field of a place cell created from multiple runs. At the bottom, the EEG theta rhythm in black and the place cell firing (in red) for the same cell in a single run. Ticks above indicate the phase for each theta cycle.

Extracted from [101].

In rodents, REM presents a sustained theta that is suggested to support information transfer from neocortex to hippocampus where can be observed the replay of long temporal sequence of neuronal ensemble firing rate seen in W [60]. This mechanism is supposed to support memory consolidation strengthening the connections previously established in W. Recent studies strengthen this idea by showing a decrease in memory consolidation following an optogenetic inhibition of theta in REM [13]. However it should be noted that in REM, the transfer of information between the hippocampus and the neocortex is inhibited rather than facilitated [18, 80], as illustrated figure 1.4. Theta rhythm is also observed in various neocortical sites such as the frontal midline, including the anterior

cingulate cortex[101].

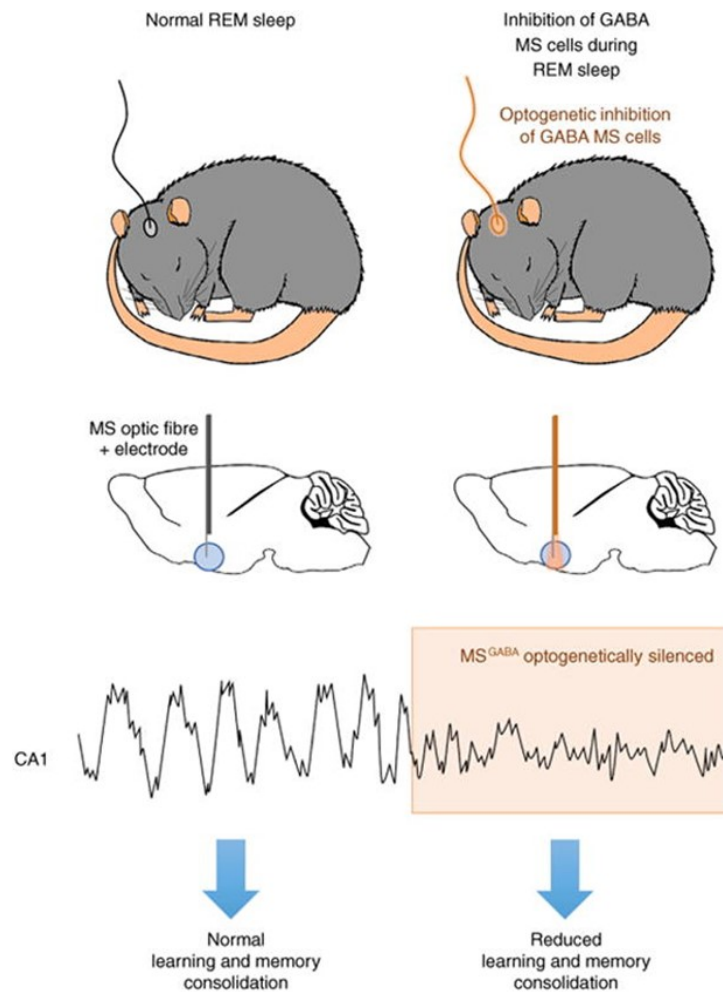


Figure 1.6: **Theta in REM and memory consolidation**

Schematic diagram showing how optogenetic inhibition of GABA cells in the medial septum (MS) result in the abolition of the hippocampal theta rhythm and in turn affects the acquisition of new memory associations.

Extracted from [77].

1.4.3 REM is a complex sleep state

Indeed, the view of a global and homogeneous state should be balanced with a myriad of corporal and neurophysiological transient events. Today, an increasing amount of study challenge the view of REM as a uniformly desynchronized state (those will be discussed later), and some work such as [87] propose to look at the microstructure of REM to better conceptualize it as the heterogeneous state it is. This implies the alternation of close, but distinct neural states that would occur throughout REM. In this article, Simor et al propose a distinction of human REM based on the eye movement that occurs in burst during this phase, with ‘phasic’ periods of eye movement and the ‘tonic’ periods without. This distinction is illustrated figure 1.7. Such distinction is thought to possibly

bear different functions of REM. While we think this distinction is very relevant and the results of Simor’s work will be detailed later, we would first discuss two points regarding this distinction.

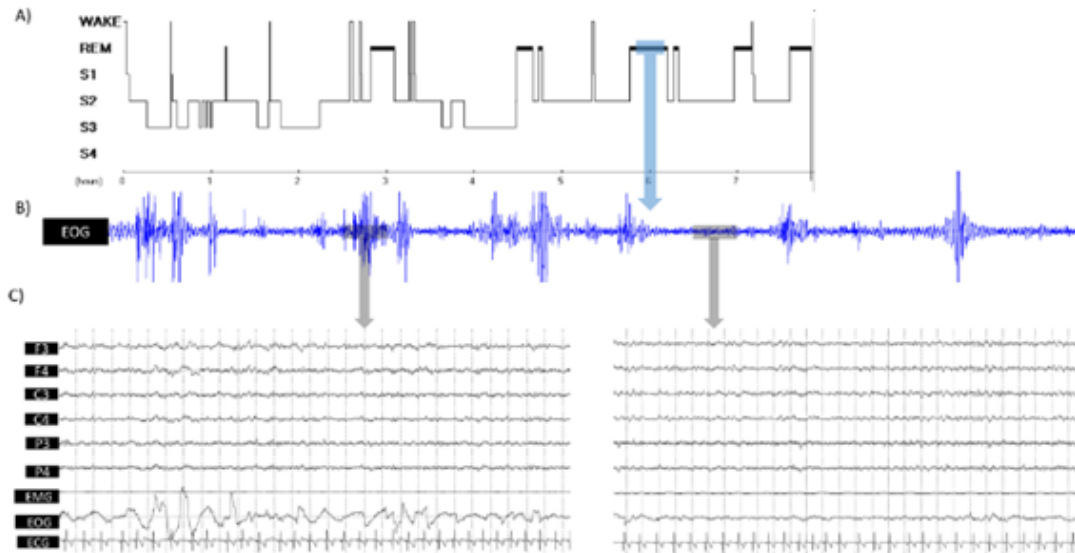


Figure 1.7: **REM sleep microstructure**

(A) Hypnogram of healthy human sleep.

(B) 15 min long REM sleep segment of EOG activity.

(C) 30 sec period of phasic (period with rapid eye movement, on the left) and tonic (no eye movement, on the right) REM sleep with different electroencephalographic (electrode derivation F3, F4, C3, C4, P3, P4), electromyographic (EMG) electrooculographic (EOG), and electrocardiographic (ECG) activity

Extracted from [87].

Transient events in REM First, it is interesting to notice that in order to find relevant distinct neural states, one can be tempted to look at the activity of sensory organs, which are not part of the central nervous system. This reminds that outside of the nervous system, the body activity is not only characterised by the strong and continuous muscle atonia exerted by the vIPAG and SLD inhibition of the motor commands, but also with other major events. Here the authors looked at the eye movements that are well studied and iconic of the state, but other aspects, such as the irregular cardiac and respiratory activity [51], the twitching in distal muscles [81], penile erection or changes in temperature [76] could be as many factors that could influence, or be the reflection of particular transient brain activity depending or not on the parasympathetic activity observed during this state. Second, while the visual system is very important in humans, this is less true in other animals that also exhibit REM, such as the rodents, for which a distinction based on rapid whisker movement (whisking) could be more relevant while still comparable.

Although limited, a distinction based on eye movement is extremely relevant, especially

considering the large amount of research that was initiated with the earliest descriptions of REM. Indeed Dement and Kleitman described the relationship between eye movement and dream content in humans, while Jouvet et al described the PGO waves that appeared as a brain electrophysiological correlate to the eye movements in REM. Since then, significant work on the subject. Here we will look at the synthesis proposed by Hobson and colleagues regarding the PGO waves and the neurobiological substrate of dreaming.

PGO waves PGO are large biphasic EEG deflections typically identified as propagating activity between the pontine brain stem P, lateral geniculate body of the thalamus (G) and occipital cortex (O), although they can arise in response to external stimuli, PGO are primarily of internal origin.

Extensively studied in cats, PGO waves provide a model system for understanding predictive processes in the brain. Studies suggest that PGO are also found in rats and primates although the regions involved vary from species to species, such that in rodents where the visual system is less developed than in cats, the PGO waves are referred to as Pontine waves (P waves) [41].

Largely associated with REM, PGO waves are also observed following unpredicted stimuli in W. Nelson et al 1983 identify PGO burst cells in the pons that have a higher excitability, about six times, in REM compared to W, and show that their bursting anticipated the actual eye movement. This led to the sensorimotor integration paradigm emphasized in [46], with the idea that the PGO network conveys information about the eye movements. Thus, the difference between W and REM proposed by Hobson is summarized on figure 1.8. In rats, the PGO wave generation is localized in the Nucleus Subcoeruleus of the pons [27], an area that send dense projections to the Amygdala, the Hippocampus, the Entorhinal and the Piriform cortex, suggesting a potential relationship between PGO waves and other cognitive functions, including sensorimotor, emotional and memory functions.

Hobson et al suggest that the prevalence of PGO waves in REM is due to its unique neuromodulation such that acetylcholine might play a role in PGO generation while aminergic neuromodulators would have an inhibitory role [47]. The enhanced excitability of the PGO system hints at a function of surprise or prediction error reduction in REM, and combined with the absence of external visual input, it could be a way for the brain to generate internal percepts in REM.

1.4.4 Neurobiological substrate of dreams

To explain features of dreams, some REM sleep researchers point toward three neurophysiological characteristics of REM [91]. First the specific neuromodulatory balance that occurs in REM is considered essential to support multiple neurophysiologic characteristics of the dreaming brain, such as we have seen with the PGO. Second, as shown in some studies

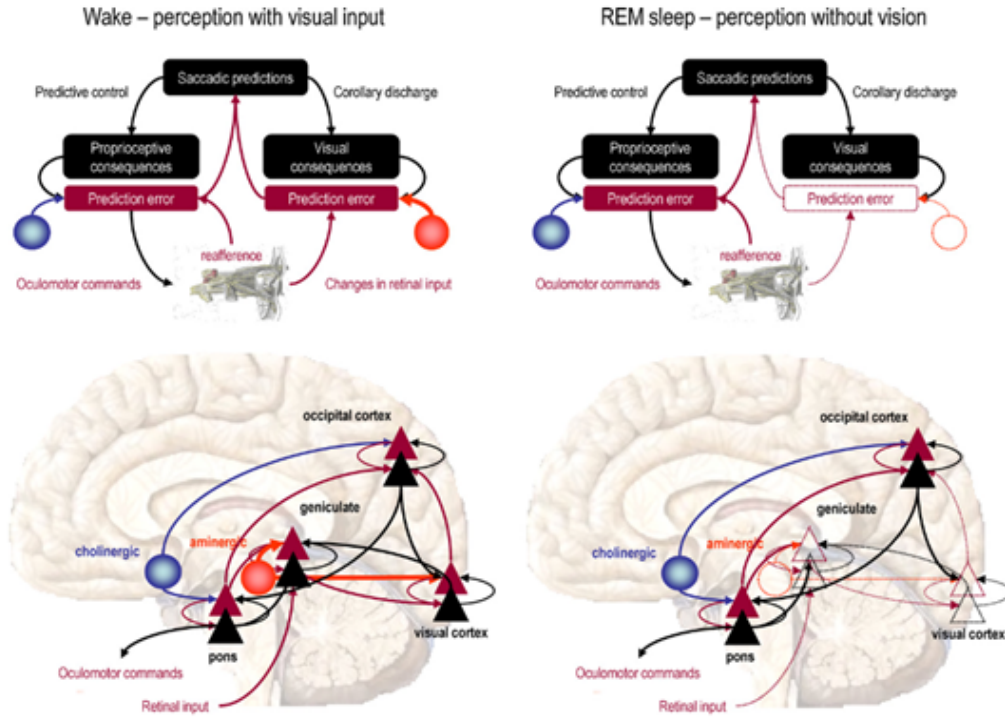


Figure 1.8: **Eye movements in W and in REM** Functional anatomy of visually guided eye movements during waking (left) and REM (right). The upper panels summarize the implicit functional differences in terms of active inference. Bottom panels show the simplified functional anatomy network. The triangles corresponding to superficial (dark red) and deep (black) pyramidal cells and the blue and pink corresponds to cholinergic and aminergic projections respectively. The visually guided movement of REM are associated to PGO phenomenon in this figure. Figure extracted from [46].

[15, 66], there are important heterogeneities in the level of activation of cortical regions in REM. Such that, the decreased activity of the dorsolateral prefrontal cortex (dlPFC) to allocate attentional resources (thus reducing the attention to dream incongruities), while the increased activity in the amygdala and limbic forebrain structures cortex would bias the brain toward emotional processing. Third, they point to the decreased outflow of information from the hippocampus to the neocortex in this state [18]. This would prevent reactivation of episodic memories. Thus dreams may reflect the contribution of certain cortical areas that remain active.

Together, these neurophysiological aspects would support essential housekeeping functions upon which primary consciousness depends. What is referred to as primary consciousness can be seen as a virtual reality system. In this regard, high-order cognitive functions can emerge from internal simulation of external sensory information synthesized by high-order regions and functional networks within the brain. Not only active in REM, the neurophysiological substrates of this synthesis are unveiled and amplified in this state, promoting a shift towards a volatile experience of mind [45].

As we have seen, PGO is a good example of systems tuned specifically in REM that

can contribute to transient cortical activity in this state. Associated with multiple other neurophysiological characteristics (summarized figure 1.8) they are proposed to support part of the volatile experience of dreams in REM. However this model for the constructions of dreams suffer from some simplifications. First, as we evoked for the phasic and tonic microstructure of REM proposed by Simor et al, the association of visually related event to major cognitive events is more relevant to species as cats or humans than it is for mouse, while the fundamental mechanisms in action for the sensory synthesis in REM should be relatively comparable. Thus it seems important to balance the importance of the different sensory systems when looking at the cortical dynamic in REM. Especially considering that non-sensory structures such as the Amygdala or the hippocampus could have an important role in the events observed in the neocortex.

Also, recents study points toward a more dynamic evolution of the neuromodulation than what was presented in the Hobson's model. It is likely that other cortical phenomena, non identified in Hobson's work, can drastically change the available neocortical associations for the construction of dreams.

1.4.5 Recent perspectives related

About the complex neuromodulation While classical neurochemistry study (using microdialysis) conceptualized neuromodulatory signaling as slow acting and spatially diffuse, Lusing and Sarter propose that cholinergic signaling is more likely phasic, lasting from milliseconds up to a second, with specific target regions. Examples of short transient cholinergic signaling have been found in rodent somatosensory cortex during whisking in W [30, 73], or in the hippocampus where the frequency of transients is the highest in REM compared to W or SWS (respectively 0.4 vs 0.1 and 0.25 transients/min) [84]. Thus the actual neuromodulation that occurs in REM and its implication remain to be explored and new insights such as the implication of dopaminergic activity in sleep should be considered.

Phasic theta In REM, although tonic and sustained activity are present most of the time, short phasic theta bouts occur with higher theta-gamma activity. Suggesting enhanced dentate processing with limited CA3-CA1 coordination during the tonic periods such that the hippocampal-neocortical dialog is biased and mainly comes from the neocortex to the hippocampus. These phasic periods are characterised by transient high synchrony of theta and gamma oscillations between the different areas of the hippocampal formation, closing the hippocampal loop[18, 75]. This would provide a short window for increased output to cortical targets, such that information could be replayed and encoded in tonic REM could be transferred in the neocortex [60]. It should be noted, however, that in contrast to SWS, the transfer of information between the hippocampus and the neocortex is inhibited

rather than facilitated during REM [80]

Karashima et al [52] suggest an acceleration of theta several hundred milliseconds before the peak of PGO wave in cats and rats. It is likely then that associations between hippocampal theta frequency and cholinergic signaling could be observed [89, 26], as the latter is supposed to support PGO waves. Similar increases in theta frequency have been also associated with the muscle twitches, irregular heartbeat rate and respiration.

Thus, with its phasic theta burst the REM hippocampal theta could be a central component in the coordination and integration of irregular physiological and behavioral events occurring in that state. It has also been proposed that hippocampal theta oscillations have an important role in pattern separation and recombination of previous memories, facilitating novel inferences. Because of it, Montgomery et al hypothesize that tonic theta support offline mnemonic processing while the short phasic burst would promote memory consolidation and could be involved in the generation of dream.

Modelling mouse REM

2.1 What is a model?

I would say that models are the pragmatic description of scientific theories

A tool for neuroscience Models are among the main tools used in neuroscience. One aspect that can be mentioned is that computational modelling is now conceived as being in some cases an alternative approach to experimental studies insofar as it can replace the use of animal models (Replace is one of the 3 R's of ethical protocols). Moreover, in an essential way, computational models have made it possible to better understand and interpret complex or apparently contradictory experimental results, such as those of David Marr in the field of the mechanisms of memory and vision in the 1980s. Used to explain a phenomenon by fitting it into the basic framework of a grand theory, the relevance of a model is dependent on the sociohistorical context. As there is a tight link between the scientific question, theory, theoretical framework, field of research and models, the latter have to be updated according to the newest scientific discoveries.

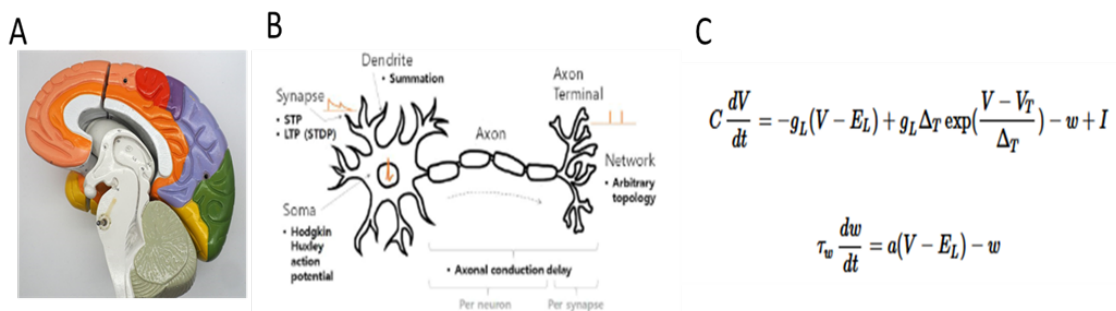


Figure 2.1: **Different models used in Neurosciences**

(A) An educational, physical, model of the brain [https://commons.wikimedia.org/wiki/File:Brain_Anatomy_Model_\(50692876848\).jpg](https://commons.wikimedia.org/wiki/File:Brain_Anatomy_Model_(50692876848).jpg).

(B) The features of a model neuron, extracted from [3].

(C) The two differential equations that describe the Adaptive exponential integrate-and-fire model (Adex).

The object "model" A model is a well-defined structure that can be interpreted to represent an observed or theoretical phenomenon. A variety of things can be referred to

as models. It can be a physical object (such as an educational brain or neuron model), a fictional object, a set-theoretic structure, a stylized description of the relevant system, or a set of equations. Models perform two representational functions: a representation of a selected part of the world and a representation of theory in the sense that it interprets the laws and axioms of that theory, the two being not mutually exclusive. Although models can be of a variety of forms, one version of the semantic view of theories that builds on a mathematical notion of models, posits that a model and its target, what it represents, have to be similar, if not isomorphic.[35]. There is no consensus on the classification of models, some are based on the explanations the model gives, representational style, or other key dimension, but many authors emphasize the importance of explicitly stating the goal, the function, of the model as clearly as possible. [57, 35, 6]

2.1.1 Popular models in neurosciences

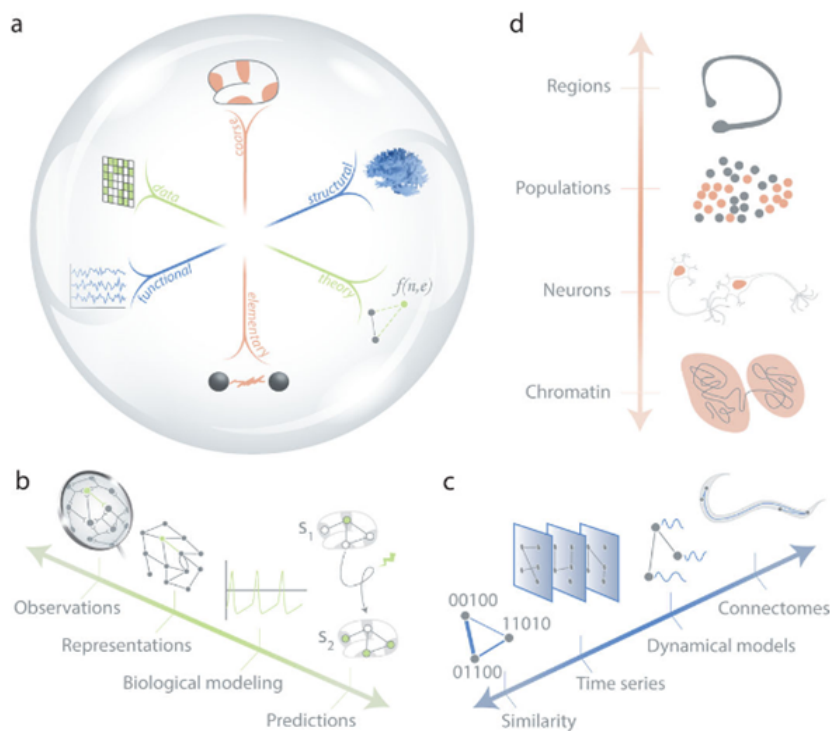


Figure 2.2: **Three dimensions of network model types**

Efforts to understand mechanisms of the brain can be organized along three key dimensions of model types. (b,c,d) represent the three key dimensions, respectively the representation, the functional realism and the scale of description.

Extracted from [6].

As models are so tightly related to scientific process, it is no surprise that they cover a wide range of neuroscience topics and can be of many forms. Here we will first discuss general aspects of three classes of models that represent different observatory levels encountered in experimental neurosciences, from microscopic to macroscopic scales. Then

we will introduce the model we used in this thesis in order to highlight the theoretical aspects it covers and the biophysical realism it supports.

2.1.2 Neuron model - the single unit scale

In 1952 Hodgkin and Huxley explained for the first time the ionic mechanisms underlying the initiation and propagation of action potential in squid giant axons with a mathematical description: the well known Hodgkin-Huxley model.[48] Still among the most popular and powerful models in neuroscience, it is now used as a mechanistic model for the spike generation of different neuron classes [78, 20], showing that models with the same structure can be used for different purposes.

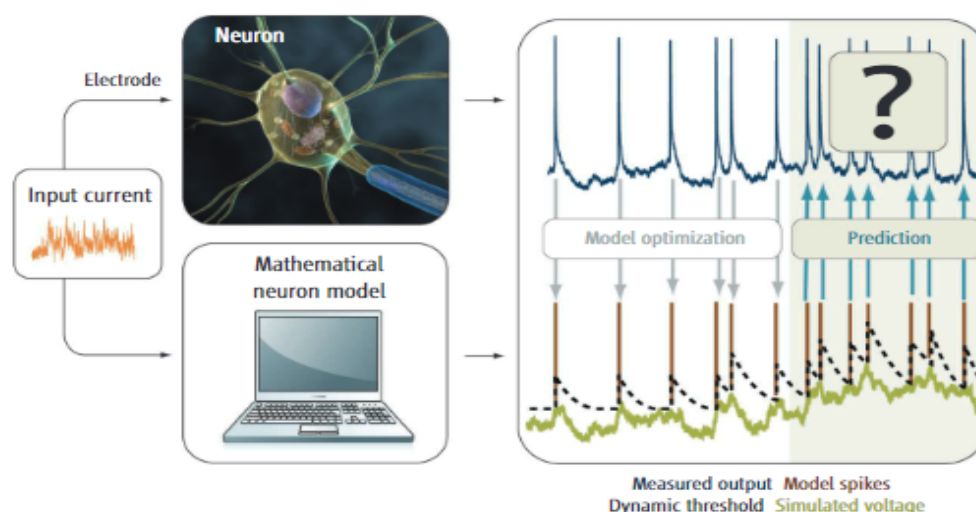


Figure 2.3: **Testing single neuron model**

The same input current is injected into a live neuron and a model neuron. A part of voltage time course data is used to parametrize the model, then the performance of the model is evaluated according to its capacity to reproduce the live neuron response to the input current.

Extracted from [37].

In the cerebral cortex of mammals, the two main neuron classes of interest are the Regular Spiking (RS) and the Fast Spiking (FS) neurons. Corresponding mostly to excitatory pyramidal and inhibitory GABAergic cells respectively, these classes are the same as the one usually observed from large electrophysiological recordings [67, 63].

The idea is that a neuron model, with a parameter tuning constrained by biological data, can match the rich and complex dynamic features observed in in vitro experiments with simple pulse currents[50], as shown in figure 2.3.

Since Hodgkin-Huxley, many descriptive neuron models have been proposed. In his effort to review models available at that time, Izhikevich [50] highlighted (figure 2.4) the trade-off between the number of neuro-computational features a model can simulate and the

computational cost of it, which can still today be a technical issue when it comes to use the neuron model in larger networks[68, 3].

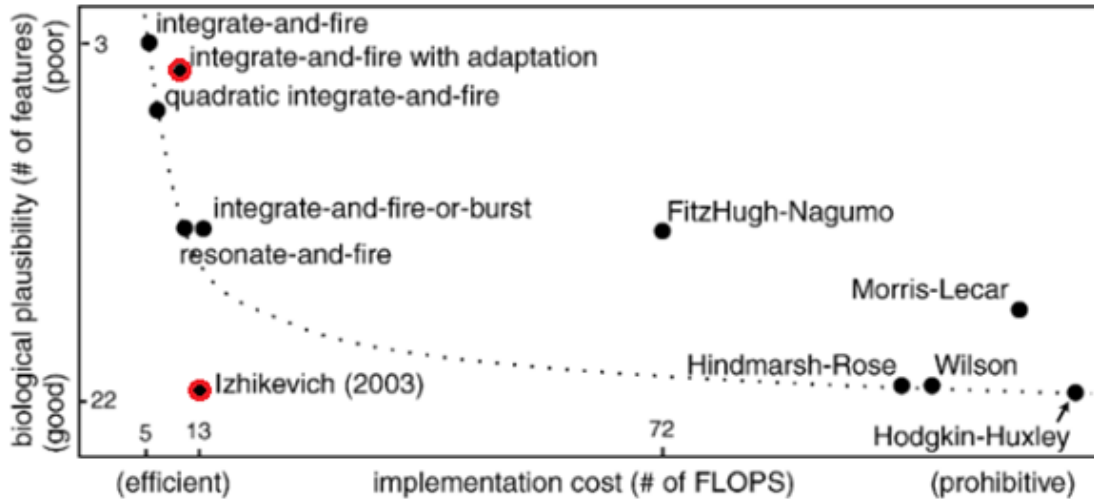


Figure 2.4: **Comparison of neuro-computational properties of spiking and bursting models**

This shows the how many neurobiological features a neuron model can reproduce and the computational cost of the implementation of this model. In red are circled two models that inspired the Adex model [16]

Adapted from [50].

There are two kinds of neuron models that stand out: biophysical detailed models, with strong biological insights with the embedding of data on the ionic conductances present in the neurons and the specific neuronal geometry are generally preferred by in vitro electrophysiologists. However such complex models, in addition to being computationally expensive, make parameter tuning extremely difficult, hence they are very specific and are difficult to generalize and integrate in a larger context. By contrast, theoreticians tend to prefer simple point neuron models, with few parameters they neglect the dendritic morphology and reduce the neuron to an extensionless mathematical construct. Although providing a weaker link to the underlying biophysical causes of the electrical activity, those models are easier to tune and to generalize into larger networks, while they provide excellent phenomenological description of the neural behavior when confronted with new biological data. [37]. Similar considerations can be done at the different scales, where often too many detailed parameters lead to complex and difficult to generalize models.

2.1.3 Network model - multiple units interacting

In contrast to approaches focusing on elaborate computational modelling of a single neuron with multiple dendritic compartments, network neuroscience seeks to understand systems defined by units, called nodes, and their relations, interactions, or connections, that are

referred to as edges. Together, the units, the connections and associated dynamics, form a network model that can in turn be used to describe, explain, or predict the behavior of the neurobiological network it represents. Many features of networks are summarized figure 2.5

Thus network models are extremely powerful when it comes to represent complex systems as the brain [22]. We somehow already covered one of the most advanced network models of cortical activity in REM when we discussed Hobson's theory about dreaming consciousness. Indeed the schematic representation used fig 1.8, is an annotated network. Although it proposes key concepts to understand the neuronal activity in REM, the underlying neuronal activity is only assigned from theoretical knowledge we have from neurophysiological experimentation, and is not generated by the model itself.

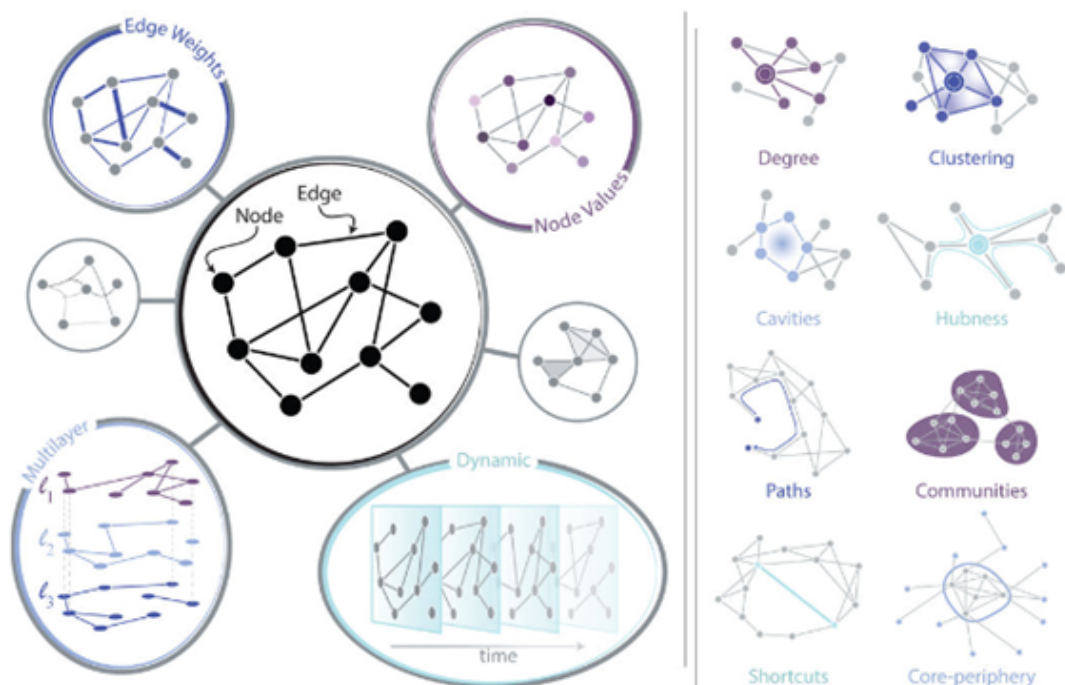


Figure 2.5: **Schematic of network models used in neuroscience**

(Left). The simplest network model used to represent neural systems is constituted of nodes and edges as shown in the middle. More sophisticated models can be constructed by adding some of the properties shown around: edge weights, node values, multilayer organisation, or temporal dynamic.

(Right) Common measures to describe networks. This shows the different interesting phenomenon that can emerge at the network scale.

Extracted from [6].

Network models can tackle many kinds of problems in neurosciences. As presented in figure 2.5, while simply composed of nodes and edges, network models can become extremely sophisticated when those elements are considered with temporal dynamic and heterogeneous parameterization, thus enabling the study of reconfigurable dynamical systems that evolve over time.[6]

2.1.4 Spiking neuron network

Spiking neuronal networks are extremely useful to understand the dynamics of cortical activity [103] and it is a cornerstone for the construction of our model. Neuronal networks are networks with neuron models assigned at each node and with specific connectivity rules determining the edges. Neuronal networks can be used to describe the neuronal activity that supports the neurophysiological phenomenon that is modeled, such as the up and down state dynamic of SWS.[44, 29] It can be used to test and explain the relation between the network properties and the generation of collective oscillatory phenomena [99]. But also to understand information transmission within the network with stimulation and predict the neuronal response elicited[71, 105].

As introduced here, spiking networks can be extremely insightful to understand and simulate brain activity. However the limitations we discussed for neuron models only scale up with the number of neurons and the complexity of the model. While theoretically scaling from two to an infinity of neurons, very large models as proposed by [68] already reach some limits, being computationally extremely expensive and difficult to use and make sense out of it for an experimentalist in neuroscience.

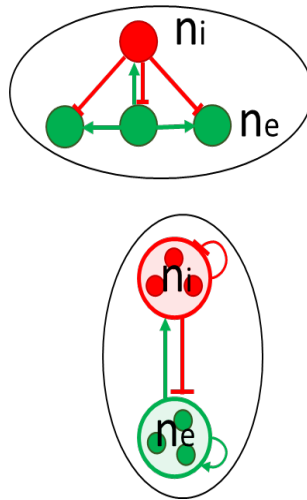


Figure 2.6: **schema of a spiking network and the related mean-field**

This figure schematises very simple models. At the top, a spiking network composed of two different neuron populations (red and green) with each neuron represented by a specific set of equations describing its dynamic, how it receives inputs and send output. At the bottom the equivalent mean-field model. Here the model is constituted of only two set of equations, each describing one population dynamic and its global input/outputs.

2.1.5 Mean-fields - a population model

To overcome such problems, another important theoretical approach that allows us the study of neural oscillations is the mean-field models, also called neural mass models or

rate models. In those models, the smallest unit (a node) is not a neuron but a population of neurons [28]. The difference between the two type of models is shown on the schema 2.6. This general mean-field approach was introduced specifically to model networks of spiking neurons, simulating only the average firing rate of the neuron population. It describes the system with a Master Equation formalism [12], which consist of a few equations about the underlying population activity and the network synaptic activity that are somehow independent to the number of neurons considered. It therefore greatly reduces the computational cost for large models. By eliminating information at the neuron scale, we have simple but very insightful information about the system dynamic that corresponds to the temporal resolution of real-time imaging techniques and of LFP recordings (lowpass filtered below 300 Hz). The mean-field models are the model of a spiking network. The quality of a mean-field is its ability to capture the properties of the spiking network it represents, and its biological relevance is closely related to this spiking network. Thus the scale of a mean field corresponds to the scale of the complete spiking network it represents, but contrary to this one it is not composed of a large number of smaller units and is thus easier to use and to integrate in a larger network of macroscopic scale.

2.2 About the model in this thesis

A model for REM In this thesis, we want to model the dynamic of brain activity we observed during REM. This means to build a model able to produce simulations that match observation of LFP recordings in mouse cortical areas during REM.

It should be noted that in neural modelling, as with the neurophysiological studies, REM has received less attention than the other brain states. There are some models about the genesis, the regulation or the general cognitive processes in this state but they don't have real temporal dimensions. To our knowledge there is no model about the dynamic of the cortical activity in REM. On the other hand, several studies have presented simulations of W and SWS cortical activities [8, 44, 29]. The modelling method we present here is based on the work of [40] that performed such approaches to generate asynchronous irregular (AI) and Up Down dynamics, corresponding to W and SWS cortical activity respectively, in a model of the whole human brain. This modelling approach rely on The Virtual Brain (TVB) <https://www.thevirtualbrain.org/tvb> project that simulates dynamics of the whole brain activity in a biologically structured network model in which the units reflect the activity of the underlying neuronal population. In this model, the activity of each unit (node) is simulated by the adaptive exponential integrate-and-fire model (Adex) mean-fields. In addition, in mouse TVB [74], the network's topology is constrained by the connectomic data of the mouse cortex obtained from the Allen brain Institute.

Model features at the different scales This simulation method synthesizes many advances in computational neurosciences and relies on a large theoretical framework spanning from micro to macro scales. We will not detail all aspects of this model but we will review the important biological parameters of the different scales, from the single neuron to the whole cortex.

2.2.1 Adex integrate and fire neurons

The work in this thesis will use the Adaptive Exponential (Adex) integrate and fire neuron model. Introduced by Brette and Gerstner in 2005 [16], it combines the two-variable integrate and fire model as proposed by [49] with the exponential integrate-and-fire model of [33].

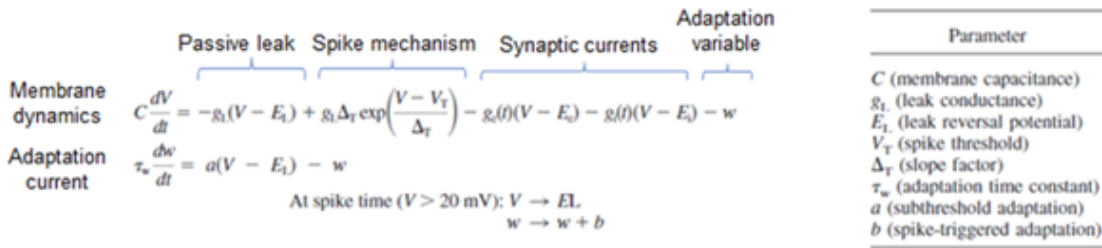


Figure 2.7: **The adaptive exponential integrate and fire neuron model**

It is a relatively simple conductance based point neuron model described by two equations (see figure xx 2.7). In addition a reset rule is associated with these equations. The first differential equation describes the membrane dynamic according to the passive membrane properties of the neuron, the spike mechanism that include an exponential non-linearity around the spike threshold [33], the synaptic currents and the global adaptation variable w . The second equation with the reset rule actually consider the adaptation current dynamic as a function of the subthreshold adaptation a and the variable w which is increased by an amount b at each firing time, accounting for the spike-triggered adaptation [16, 49]. Thus, this model is able to capture different neuronal dynamics by tuning a limited number of parameters. As we will show, the spike-triggered adaptation parameter b is of particular interest.

2.2.2 Adaptation

In the Adex neuron, the global adaptation variable w is related to two different adaptation parameters. The subthreshold adaptation a , and the spike-triggered adaptation b . Changes in parameter subthreshold adaptation a can lead to bursting activity as observed in neurons such as thalamic cells, but this is not something we are looking for to simulate the cortical neurons thus we use a small subthreshold adaptation in this work. On the other hand, a

tonic firing as observed in either RS or FS cortical neurons can be obtained by changing the b value (i.e. the spike-triggered adaptation parameter).

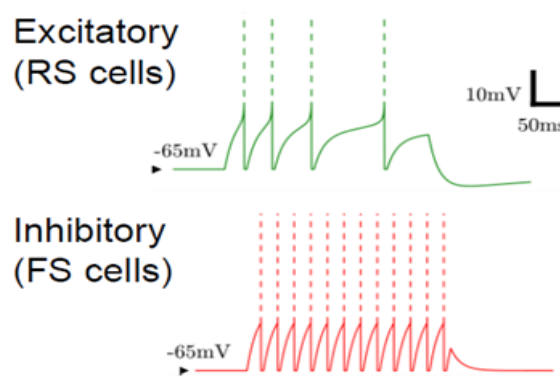


Figure 2.8: **Single cell model using the adaptive exponential formalism**

The figure shows how the Adex model can generate two typical firing patterns of regular spiking (RS, green) and fast spiking (FS, red) cortical neurons.

Extracted from [105].

With high b the neuron fires regularly when stimulated, but each spike significantly increases the refractory period before the next one, thus the spike frequency is high at the onset and then it adapts. This is similar to RS neurons of the mammalian cortex [86, 50, 29].

Thus, increasing or decreasing b modulates the post-spike refractory period. Several biophysical mechanisms can cause spike-triggered adaptation such as activity dependent activation of slow hyperpolarizing currents (i.e. voltage-dependent potassium currents such as the non inactivating potassium current I_m ; I_m is modulated in particular by acetylcholine) and inactivation of depolarizing currents (i.e. Na channels inactivation). It is suggested that in pyramidal neurons, the spike frequency adaptation is mediated by currents (i.e. I_m) that are deactivated by acetylcholine and the spike-triggered adaptation b strongly relate to these currents. Thus the b value can be seen as inversely proportional to the supposed concentration of acetylcholine and its action on muscarinic receptor and voltage dependent and calcium-gated afterhyperpolarization potassium channels [4]. Finally the suppression of the spike-triggered adaptation produces a fast and tonic firing, similar to FS cells (ie parvalbumin GABAergic interneurons).[29]. The two type on neuron are illustrated figure 2.8

2.2.3 Adex network

At the network scale, it is well described that the interaction between nodes can generate unexpected dynamics. Here the network we will use has to be biologically relevant regarding the brain state simulation. The network must also be generalized in a mean-field model. We consider a network of ten thousand Adex neurons, with a proportion of 20% of inhibitory

FS cells and 80% of excitatory RS cells[29, 105]. This corresponds approximately to a few hundred micrometers of cortical tissue and could correspond to a generic cortical column[67, 63].

With an external noisy drive that is connected to both populations and the afferent inputs such a network of Adex neurons can switch from asynchronous irregular (AI) to Up and Down regimes, that are comparable to W and SWS, by changing the spike-triggered adaptation of RS cells. Indeed while at the neuron scale the spike-triggered adaptation influences the post-spike refractory period, at the network scale high b value results in a global bistable Up and Down firing pattern with synchronous and regular oscillations. With lower adaptation neurons fire tonically without silent period and without apparent synchrony [40, 29].

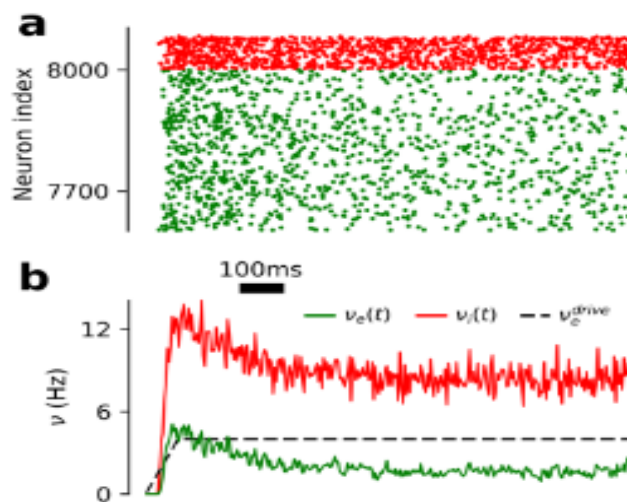


Figure 2.9: **Adex network**

Simulation of the activity of an Adex network.

(A) Raster plot of a portion of the network. In green the RS and in red the FS neurons.
 (B) Average firing rate of the different regular spiking (RS) and fast spiking (FS) neurons.
 Extracted from [105].

Similar spiking networks are also used to study stimulus-driven responses. When excitatory RS neurons are submitted to an afferent input, that would be an equivalent to thalamic input, the network produces a response that is more intense for FS than for RS neurons [104]. Similar stimulation experiments can be done in networks with Up and Down states, or in the corresponding mean-field models [97, 98, 40, 39]. This is also an approach we will use in our ‘REM model’.

2.2.4 Adex mean-fields

The Adex mean-field model results from the application of the Master Equation formalism [12] to the Adex network we discussed above. This model describes the network behavior

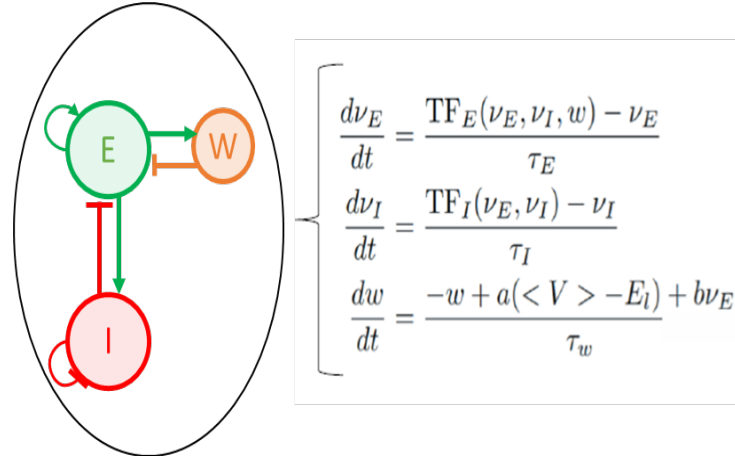


Figure 2.10: **Adex mean-field with adaptation**
Modified from [97].

using only three equations corresponding to the dynamic of the excitatory population, the inhibitory population and the adaptation variable (that is applied only to the excitatory population) (presented figure 2.10). $\nu_{E/i}$ being the firing rate of the population derived with a time resolution T . (A Markovian dynamic is considered for the network, hypothesizing that the system is memoryless over the timescale T [97, 12]. $\text{TF}_{E/i}$ stands for Transfer Function of each neuron type. It contains the whole dynamics of the network as it describes the firing rate of the neuronal population as a function of excitatory and inhibitory inputs (and is therefore essential for the model to produce oscillatory behavior).

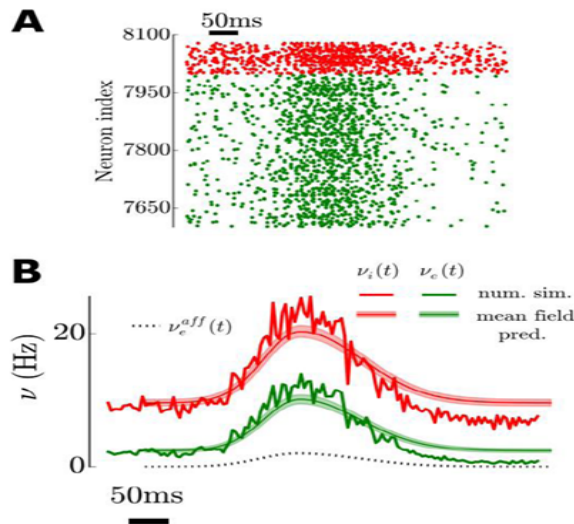


Figure 2.11: **Simulation of stimulus evoked responses in a network of RS-FS cells and its associated mean-field**

The external excitatory input was Gaussian distributed (bottom dotted trace) and was randomly distributed to all cell types. The response was well captured by the AdEx mean-field model (continuous lines in B).

Adapted from [105].

In Di Volo 2019 the Adex mean-field is built with the objective to account for con-

ductance based interactions and spike-frequency adaptation. The mean-field is not only able to correctly capture the fine time course of the network's response to external stimuli (figure 2.11), but it can also reproduce both AI and Up/Down states activity (2.13).

2.2.5 LFP modelling

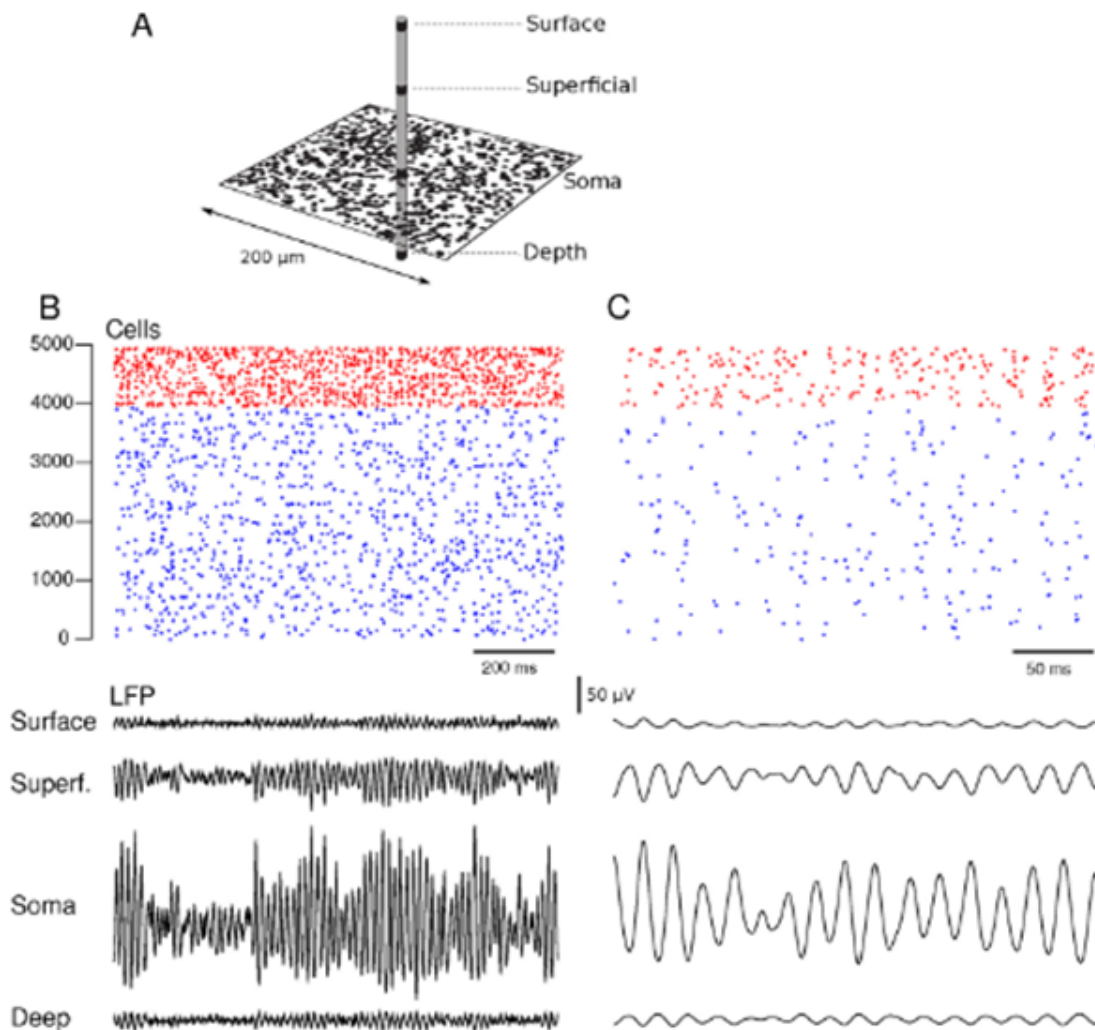


Figure 2.12: **Kernel-based method to calculate local field potentials**

Example of a LFP calculated from a network of spiking neurons.

(A) shows the placement of the electrode according to the cells.

(B & C) The top raster plots shows the same spiking network at different temporal resolution, while the two bottom panels shows the corresponding simulated LFP calculated at the different placements shown in A.

Extracted from [92].

The Local Field Potential (LFP) is an extracellular electric potential (usually < 300 Hz) recorded in the brain tissue (especially in cortical areas that are organized in layers of neurons with excitatory cells having a parallel arrangement of dendrites) and is used to measure locally the synchronized activity of neurons. Sampling the electric potential

in close vicinity it can be different for electrodes separated by a few hundreds microns. (Katzner et al., 2009) This can be observed laterally, but also when moving in depth large changes in amplitude or even in signal polarity can be observed. LFP reflects both action potentials and slower extracellular events such as synaptic potentials of a large number of neighboring neurons. Experiments from the hippocampus or from the cortex in different animal models indicate that inhibitory neurons largely contribute to LFP signal [7, 93]. A method to compute LFP from neuron firing rate was proposed by [92] consists in calculating the LFP of the network as a convolution of spiking activity with micro-LFPs (uLFPs) waveforms determined in in vivo experiments (a micro-LFP is an LFP evoked by a single neuron). This method has been successfully implemented for mean-fields by F.Tesler in prep.

2.2.6 TVB - integration into whole brain network

As we saw, the Adex mean-field is a good tool to simulate what is observed experimentally with LFP during *W* and *SWS*.

The whole cortex simulation we propose here consists in a network of Adex mean-fields arranged in a network with the connectivity extracted from mouse connectome [22]. To do this we use the mouse version of TVB [74] that allows the parcellation and extraction of data from the Allen brain to be used in the simulation environment. However no study on the Adex integration into the mouse TVB has been published yet. Therefore we will present this model on its human counterpart here that is based on fMRI data [40] as our modelling approach is the same.

In this model, the two-populations Adex mean-field model is expanded. The mean-fields are connected together by excitatory interactions while the inhibitory connections remain only local, within the mean-field. The transfer function is adapted accordingly with the excitatory firing rate considered. The transfer function is the result of the firing rate of every mean-field excitatory population modulated by the distance and the connectivity strength of each mean-field pair. These two parameters (distance and connectivity strength) are determined according to the connectomic information from the Allen Brain institute.

Similarly to what is observed with the single mean-field, AI and Up and Down states are observed in the whole brain model. This time, with low adaptation the AI is not only irregular but we can see that the activity produced by the different mean-fields is poorly correlated. With high spike-triggered adaptation b , the Up and Down dynamic is observed in this model with the different mean-fields synchronized together. We can also see the global adaptation W of each mean-field dynamically rises at the beginning of the Up period and is relaxed during the Down. The authors were also able to perform a neuronal stimulation experiment with the model and showed that the stimulus-evoked dynamic was dependent on the model state in a manner consistent with experimental data obtained

with transcranial magnetic stimulation (TMS) in human [70, 69]

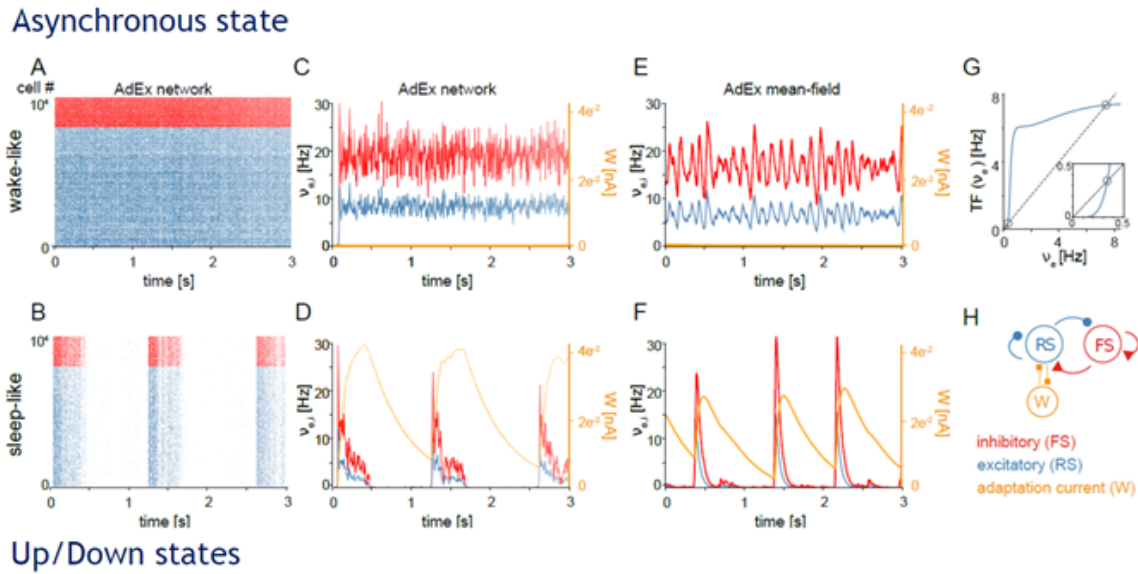


Figure 2.13: **Asynchronous and synchronous dynamics produced by networks of microscopic AdEx neurons and their mesoscopic approximations.**

Raster plot (A-B) and mean firing rate (C-D) from network compared to its mean-field approximation (E-F).

A,C,E represent the asynchronous irregular regime, while B,D and F represents the Up and Down state.

(G) Input-output firing rate relations are given by the mean-field model transfer function.

(H) schematic representation of the mean-field as seen before.

Extracted from [39].

PART II

Objectives

The objectives of this thesis are to explore in detail the cortical activity of REM by comparing it with that of the two other states of vigilance in order to feed a computational model allowing to predict the mechanisms responsible for this activity. As we saw in the Introduction, the classical view of REM largely relies on old studies and is challenged by recent findings, questioning previous conceptions about the cortical activity in REM. We will first try to describe the diversity of mouse cortical activity regimes that occur in REM by analysing a LFP dataset (Fernandez et al citeFernandez2016), looking for REM SWA and phasic theta events as described in [36, 75] respectively. We will present the important aspects of those very different phenomenons using standard spectral analysis, but also with a closer examination at the individual components of those phenomenons with a cycle by cycle analysis adapted from [23]

This approach allows us to precisely describe the signals but also to tackle our second objective: questioning the spatio-temporal organisation and the co-existence of the different REM cortical regimes. Indeed our first analysis reveals important differences between areas that seem engaged in a similar cortical regime. Indicative of some heterogeneity at a spatial but also temporal point of view. Moreover, even one of the more iconic and stable brain oscillations observed in rodent REM, the hippocampal theta, presents notable neurophysiological transient events. As the cortex is a structure extremely connected, it is likely that different cortical transient events are coordinated or influence each other, resulting in a particular temporal organisation.

The last objective of this thesis is to propose a model of REM in order to investigate the mechanism that underlies the delta oscillations. As described in the introduction, we lack computational models simulating the dynamics of brain activity in REM. Therefore, we propose to use a computational modelling approach that was proven successful in simulating large scale brain models of W and SWS and adapt it to match the heterogeneity of REM delta activity described in the data analysis. We then show how this model can be used to question biological hypotheses and predict the cortical response to stimulation in REM. Although somehow incomplete and limited, as it focuses mainly on the presence of Delta waves, we believe that such a model could be used as a basis to implement other aspects of this state and could in turn be used to interrogate many aspects of the mysterious state that is REM sleep.

PART III

Experimental analysis of mouse REM sleep

Résumé de l'article Le sommeil à mouvements oculaires rapides (REM) (également appelé sommeil paradoxal) est classiquement décrit comme similaire à l'éveil (W), avec une activité à l'EEG de faible amplitude et de fréquence rapide. Chez les rongeurs, les enregistrements EEG sont caractérisés par une oscillation thêta continue et de haute puissance qui peut refléter l'activité d'un certain nombre de zones corticales et sous-corticales telles que l'hippocampe. Cependant, deux études récentes ont montré que, pendant le REM, les aires corticales présentent une activité à fréquence lente proche de celle du Sommeil lent (SWS). Ici, nous avons analysé l'activité REM à ondes lentes (SWA) en la comparant à SWS, ainsi que son activité thêta, à l'aide d'enregistrements multi-sites de potentiel de champ local (LFP) dans le cortex somato-moteur et l'hippocampe de la souris. Nous montrons que le REM SWA a plusieurs caractéristiques différentes par rapport au SWS. En particulier, il a une fréquence légèrement plus élevée que le SWS, étant ainsi proche du delta, et une forme d'onde différente. Le REM SWA alterne avec des oscillations plus rapides au sein des épisodes de REM, et est répandu dans le cortex somatosensoriel primaire (S1), ainsi que dans le cortex somatosensoriel secondaire (S2), et il est rarement présent dans le cortex moteur primaire (M1). Les accès REM SWA sont fortement corrélés entre les zones S1 et S2 mais faiblement entre celles-ci et la zone M1. En revanche, le REM SWA n'est pas observé dans l'hippocampe ou dans le cortex préfrontal médial (mPFC). L'activité thêta dans l'hippocampe est caractérisée par de brèves périodes (<2s) de fréquence accrue appelées thêta phasique. Nous montrons que ces périodes de thêta phasique se retrouvent dans l'EEG et le mPFC. Ce thêta phasique est fréquemment associé à des accès SWA dans les zones S1, S2 et M1. En conclusion, cette étude propose une nouvelle description du SWA cortical dans le REM en tant qu'activité Delta alternant avec des oscillations de faible amplitude à fréquence rapide. De plus, de brèves périodes d'activité corrélée sont observées entre le cortex somato-moteur et l'hippocampe qui peuvent refléter le transfert d'informations entre les aires corticales pendant le thêta phasique.

ANALYSIS OF REM SLEEP DISTRIBUTED CORTICAL ACTIVITY IN MICE

A PREPRINT

 **Mathias Peuvrier**

French National Centre for Scientific Research (CNRS), Institute of Neuroscience (NeuroPSI)
Paris-Saclay university
91198 Gif sur Yvette, France
mathias.peuvrier@cnrs.fr

 **Alain Destexhe***

(CNRS), Institute of Neuroscience (NeuroPSI)
Paris-Saclay university
91198 Gif sur Yvette, France
Alain.Destexhe@cnrs.fr

 **Laura Fernandez**

(UNIL)
Paris-Saclay university
Lausanne
r

 **Sylvain Crochet**

EPFL
Lausanne
Alain.Destexhe@cnrs.fr

 **Paul Salin**

(CNRS), Institute of Neuroscience (Forgetting)
Lyon 1 University
69675 Bron, France
paul.salin@sommeil.univ-lyon1.fr

March 31, 2022

ABSTRACT

Rapid Eye Movement (REM) sleep (also called Paradoxical sleep) is classically described as similar to wakefulness (W), with an activity at the EEG of small amplitude and fast frequency. In rodents, the EEG recordings are characterised by a continuous and high power theta oscillation that may reflect the activity of a number of cortical and subcortical areas such as the hippocampus. However, two recent studies have shown that, during REM, cortical areas present a slow frequency activity close to that of Slow Wave Sleep (SWS). We analysed REM slow-wave activity (SWA) by comparing it to SWS, as well as its theta activity, using multi-site local field potential (LFP) recordings in the mouse somato-motor cortex and hippocampus. We show that the REM SWA has several different characteristics compared to the SWS. In particular, it has a slightly higher frequency than the SWS, thus being close to delta and a different waveform. REM SWA alternates with faster oscillations across REM episodes and is prevalent in the primary somatosensory cortex (S1) and in the secondary somatosensory cortex (S2), and is rarely present in the primary motor cortex (M1). REM SWA bouts are strongly correlated between areas S1 and S2 but weakly between these and area M1. In contrast, REM SWA is not observed in the hippocampus or in the medial prefrontal cortex (mPFC). Theta activity in the hippocampus is characterised by brief (<2s) periods of increased frequency called phasic theta. We show that these periods of phasic theta are found in the EEG and mPFC. This phasic theta is frequently associated with SWA bouts in areas S1, S2 and M1. In conclusion, this study proposes a new description of cortical SWA in REM as Delta activity alternating with fast frequency small amplitude oscillations. In addition brief periods of correlated activity are observed between the somato-motor cortex and the hippocampus that may reflect the transfer of information between the cortical areas during phasic theta.

*Use footnote for providing further information about author (webpage, alternative address)—*not* for acknowledging funding agencies.

Keywords REM sleep · Experimental analysis · Delta oscillation · Computational model

1 Introduction

Slow oscillations and Delta Vigilance states are characterised by oscillation patterns recorded by electroencephalography (EEG). In mammals, in wakefulness and rapid eye movement sleep (REM or paradoxical sleep) the EEG activity is desynchronized while it is synchronised and of large amplitude in Slow Wave Sleep (SWS).

The slow waves of SWS are composed of delta oscillations of 2-4 Hz and the slow oscillations (SO <2 Hz). This Slow oscillatory activity corresponds to the coordinated spiking activity of a large population of neurons, alternating between active (upstates) and silent (downstates) periods. Taken together, these oscillations make up the slow wave activity (SWA) which reflect the homeostatic processes of sleep. Thus with an increase of the sleep pressure, the power of SWA increases and conversely when the sleep pressure decreases this power of SWA also decreases. Several studies suggest that the slow and delta oscillations observed are generated in the neocortex ([26, 32]). Brain activity during SWS is accompanied by a phasic activity, spindles, which are brief and of rapid frequency (1s, 10-14Hz) ([31]).

In contrast, REM activity is associated with low amplitude higher frequency theta (5-10 Hz) and gamma (35-80Hz) activity ([20]). Thus the brain states of SWS and REM examined with EEG recordings appear entirely opposite. It is only recently that phasic events of faster theta with strong gamma coupling were observed in the hippocampus [21, 5, 28]. Previous work on cat associated increase in theta frequency and power with PGO, rapid eye movement and other body phasic activities [16, 18, 22, 24, 29, 25]. Montogmmery et al hypothesise that phasic bouts may provide windows of opportunity for the transfer of information from the hippocampus to the neocortex, opening new ways to consider phasic cortical events with specific functional implications in REM.

Delta oscillations in different brain states Advances in in vivo electrophysiological techniques (intracellular recordings, multisite local field potential (LFP) and spike recordings and high-density EEG recording) have revealed that in the neocortex W is characterised by sub-states alternating SWA and desynchronized activity during quiet and active wake respectively. These SWA in quiet wake share some common features with delta oscillations in SWS and are generated in sensory, motor and associative cortical areas ([9, 35, 36, 11]). Intriguingly, SWA is also observed in REM in LFP recordings in the superficial layers of primary areas of the mouse sensory cortex ([12]). In contrast, the activity of the secondary sensory, motor and associative cortical areas would be desynchronized as in EEG and hippocampal recordings ([12, 21]). This finding seems to be opposed to EEG work showing that REM activity is characterised by rapid oscillations of low amplitude. However, the results of Funk's study may help explain the REM "paradox": an EEG activity close to wakefulness that is associated with high sensory threshold due to synchronised slow activities in the primary sensory cortices. If SWA are present in these primary cortical areas they could filter sensory perception during REM like during SWS. Thus, this finding leads to reconsider the importance of SWA in REM as compared to SWS and W.

Very few studies have characterised the differences between SWA in REM and those in SWS and W. A detailed analysis of cortical SWA in REM versus SWS and wakefulness has not yet been performed. Are REM slow waves different in amplitude and shape compared to SWS and W? Furthermore, is functional connectivity between cortical areas during REM modulated during these slow waves compared to SWS and wakefulness? Is this activity modulated by the phasic theta events previously identified? Given the essential role of functional connectivity in cognitive processes, one may wonder whether REM slow waves facilitate or inhibit the transfer of information between cortical areas. By recording LFP activity in several cortical areas using multi site recordings it becomes possible to directly address these questions and to determine similarities and differences in the scale of the individual slow wave as well as in the temporal and spatial distribution of SWA in REM compared to SWS and W.

Using multisite LFP recordings, we first analyse REM SWA in comparison to the SWA of SWS and W in the mouse somato-motor cortex. Since this SWA is important in this cortex, we examined whether it is correlated between these cortical areas on the one hand, but we also determined whether it is correlated to other areas where faster oscillations are predominant such as the hippocampus. We show that REM SWA is characterised by Delta waves in primary and secondary cortical somatosensory (S1 and S2 respectively), as well as in primary motor areas (M1), and that SWA alternates with faster low voltage oscillations during REM episodes. This Delta activity is often surrounded by periods of hippocampal phasic theta. Indicating potential coordination in the different cortical regimes in place, it gives us new insights into the brain capacity for information integration in REM.

2 Methods

2.1 Electrophysiological signal analysis

The data analyzed in the present study come from a database acquired in unanesthetized head restrained mice recorded by L F and S C. Part of this dataset has been recently analyzed and published to characterize the cortical slow waves of wakefulness and NREM [11].

Animal preparation and surgery Briefly, nineteen C57BL/6 male mice (Janvier SAS, St. Berthevin, France), aged of 6 to 8 weeks at the time of surgery, were used for the study. All procedures were approved by the University of Lyon 1 Animal Care Committee (project DR2013-4) and were conducted in accordance with the French and European Community guidelines for the use of research animals.

The data of only seven out of the nineteen mice is analyzed here. LFP for those mice were recorded at the following sites: the barrel field of the primary Somatosensory cortex (S1), the secondary Somatosensory cortex (S2), the primary Motor area (M1), the prelimbic area of the medial prefrontal cortex (mPFC), and the area CA1 of the dorsal hippocampus (dCA1). In addition to the LFP microelectrodes, two surface EEG were implanted over the parietal (AP 2.0, lat 1.5) and

Area	S1	S2	M1	A1	V1	PtA	mPFC	dCA1
Antero-Posterior	2.8	3.1	5.1	1.3	0.5	1.8	5.7	1.3
Lateral	3.2	4.0	1.8	4.0	2.5	1.8	0.3	2.0
Depth	0.5	0.8	0.4	0.6	0.4	0.4	1.85	1.3

Table 1: LFP implantation coordinates. In bold is highlighted the areas that will be studied in this article.

frontal areas (AP 5.3, lat 1.5) onto the dura mater of the contralateral hemisphere, two EMG electrodes were inserted bilaterally in the neck muscles, and two silver wires were inserted on both sides of the cerebellum for reference and grounding. Then, to allow for painless head-fixation during recording sessions, a light-weight metal head-post was cemented to the skull.

Habituation and recording Habituation and recording sessions were performed between 12AM and 5PM, during the light period in a semidark light condition, with ambient room temperature ($22\pm 2^\circ\text{C}$), in an electrically shielded recording chamber.

After recovery from surgery, mice were progressively habituated to head-restraint conditions with repetitive daily training. The recording sessions started when the first NREM sleep episodes were observed.

Sleep scoring Epochs of wakefulness, NREM and REM were scored using EEG and EMG. REM sleep was identified by theta oscillations on the EEG and neck muscle atonia on the EMG. Artifacts, drowsiness periods and intermediate sleep were discarded. Therefore, each episode of vigilance states (W, SWS, PS) showed a clear separation.

LFP dataset For each mouse we have sets of brain state episodes, determined with the sleep scoring, corresponding to specific brain states with the following data: EEG, EMG and a set of 5 to 6 LFP (all sampled at 1kHz). LFPs implanted in each mouse corresponded to the configuration presented in the previous table. In this study, we only use the first configuration, with 7 mouse recordings in: S1, S2, M1, mPFC, dCA1. This allows the study of interactions between S1 and other areas of the somatomotor cortex.. Quantitatively this database includes 341 episodes of W (total duration of 14866 s, mean episode duration: 43.6 ± 36.05), 318 episodes of NREM (total duration 12274.08s; mean: 38.6 ± 25.1 s) and 120 episodes of REM (total duration 7418.68s (mean: 61.82 ± 40.1 s)).

Spectral analysis To compute the spectrogram of LFP, from the dataset or from the model, we used the Welch method. The power spectral density is estimated using a Hamming window of 4 seconds with 2 seconds overlapping, with the exception of 1000ms windows with 300ms overlap for the phasic theta analysis. The power spectrum is expressed in V^2 . One spectrogram is computed for each brain state episode recorded, and they are used to compute band power and to find frequency peaks in the delta band.

The maximum frequency peak is the highest peak in the frequency range. The absolute delta power is the integral of the area, between the frequency bands and below the periodogram line. To integrate this area, we approximate it using the composite Simpson's rule. The idea behind it is that the area is decomposed into several parabola and then summed up their area.

Delta cycle segmentation of the signal To detect and analyze Delta cycles in our data, we used a method inspired and based on the Bycycle algorithm (for cycle-by-cycle analysis) and python library ([7]). In this method, the LFP signal is segmented in cycle periods in a few steps illustrated in supplementary figure 6. The signal is bandpass filtered, and the zero-crossings are indexed, then back on the raw data peaks and troughs were found as the minima and maxima between two zero-crossing time points. Finally, flank midpoints are the point halfway between the peak and trough voltage. Instantaneous phase is estimated by interpolating between extrema (the peaks and troughs) and flank midpoints. Here, to find delta cycles, we used the algorithm to compute cycles from trough to trough, centered on the peak with a narrow bandpass filter between [2 and 4.5 Hz] for the first step. Once we found the extrema and flank-midpoint for each cycle, we computed cycle features such as the period, the peak and trough duration or voltage, the rise-decay and peak-trough symmetries.

Determination of delta cycle Then a second algorithm is used to determine if a delta cycle is a part of a delta oscillatory bout according to the similarity of cycle features for multiple consecutive cycles. However, delta cycles were frequently interspersed with faster activities and we observed some isolated cycles. Therefore we used permissive settings for the algorithm proposed by the library. Using a simple amplitude threshold, cycles with amplitude high enough, compared to the rest of the episode signal, were classified as putative delta without regard to other detected cycles. This threshold was not restrictive at all and captured many false positives. But it was only used to calculate the actual amplitude threshold, as the median amplitude value for all putative delta cycles found in S1 and S2 during SWS for the specified individual.

This second decision parameter restricts the delta cycles to those above [thresh percentil] of the amplitude of the Slow wave sleep Delta cycles recorded in S1 and S2 for each mouse. The cycle-by-cycle analysis of delta oscillations has been progressively optimized and verified by direct observation of the dataset by 2 authors (MP, PS).

Delta bouts To determine the temporal distribution of Delta, we describe LFP signals in delta and non-delta bouts. Validated delta cycles that are close enough were gathered together, adding non-detected cycles if they were surrounded by delta cycles and at least 75% of the bout is made of validated delta cycles. Then the delta oscillations were validated as delta bouts if they lasted at least 1 second and were constituted of at least 3 delta cycles. Separately from the delta bouts, we defined signal portions that had no delta oscillations for at least 1s as Non-Delta bouts. Therefore, isolated delta cycles and too short periods of non-delta were excluded from the analysis.

detection of phasic theta Phasic periods of theta were also detected using the same cycle Bycycle algorithm using a phasic theta detection criterion very similar to Montgomery's [21, 19]. We did not use the complete validation approach proposed by Voyteck and Cole to detect theta burst but we used the algorithm to delimit the single theta cycles and their properties. For simplicity we considered that all cycles found were about real theta signals, which is relatively close to reality and was validated visually by MP and PS. The theta band is filtered between 5 and 10 Hz. Phasic theta bursts are then considered for periods lasting a minimum of 500 ms and with at least three successive cycles with 75% of the shortest period (thus with highest frequency) compared to the other theta cycles of this signal. Then we try to extend a bit those small by, first appending the direct adjacent cycles, and then other short theta cycles (with period smaller than the phasic threshold used) that are close enough (less than 1 cycle and 500 ms apart) to the phasic theta burst.

Wavelet transform We use Morlet wavelet transformation only to illustrate the distribution of the phasic theta bouts. Time windows of 4 seconds are considered. The transformation is performed with 3 to 15 cycles wavelets for a total of 200 frequencies spanning between 0.5 and 20 Hz. On the time frequency graphs, the phasic theta and delta bouts are displayed by thick lines. Thus, phasic theta bouts are displayed by a red line (at 9.5Hz), and delta bouts (at 3Hz) are displayed by dark blue lines. Finally isolated Delta events are illustrated by a grey line.

3 Results

We first analyzed the occurrence and distribution of slow-waves in REM sleep, and then the correlation of activity between the hippocampus and the neocortex during this sleep state.

3.1 Analysis of slow-waves in REM sleep

S1 signal in different brain states Figure 1 shows the three states of the wake-sleep cycle in mice, wakefulness (W), slow-wave sleep (SWS) and rapid eye movement (REM) sleep. W and SWS classically display two drastically different activity states, asynchronous and synchronized slow-waves respectively. During REM sleep, however, one can see that the situation is less clear. While asynchronous activity usually dominates in EEG and in some brain areas, other brain areas exhibit local slow-wave activity, in middle and superficial layers of primary cortices, as pointed out

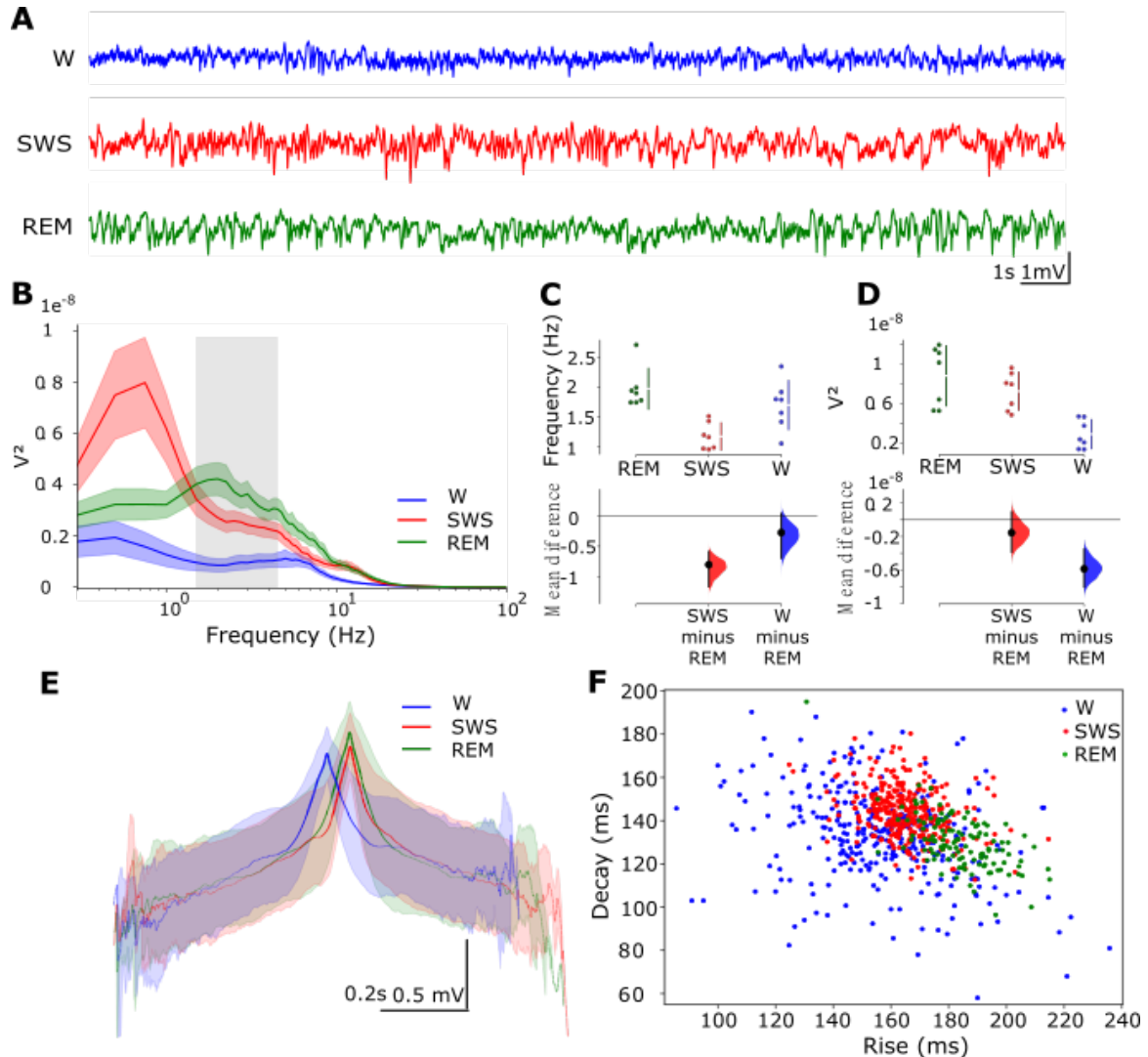


Figure 1: **Delta in the somatosensory cortex across brain states** (figure A to G colour code: blue for W, red for SWS and green for REM).

(A) Twenty seconds of LFP examples recorded in area S1 during sleep and wakefulness. (B) Mean power spectrum of S1 recordings. The grey area corresponds to the delta band, between 1.5 and 4.5 Hz. (C) Average frequency of the highest peak in SWA band (0.5-4.5Hz) Each point corresponds to the mean, for one subject of the frequency peak found in the power spectrum. (D) Delta band (1.5-4.5 Hz) power amplitude in S1 across states. delta bandpower is shown for each subject, with colours corresponding to the brain state. (E) Average Delta cycle detected in S1 for each state. The ratio $N_{datapoint}/totalN_{cycles}$ is reported as the α (intensity) of the line plotted (with a minimal value when less than 30% of the cycles are involved). (F) Scatter plot of Delta cycles rise and decay time in S1 across states: Each dot corresponds to the mean rise and decay time of delta cycles detected during one episode of the three brain states This figure shows the dispersion of Delta cycles rise-decay symmetry.

previously ([12]). The differences between these states is also apparent in the power spectral density (PSD) of the LFP signals (Fig. 1B). Here, the broad low-frequency peak, culminating in the Slow Oscillation (SO) band (<1.5Hz), during SWS contrasts with the absence of clear peak in W, while in REM, a low-frequency peak appears around 2-4 Hz (Fig. 1C.). The REM slow-waves seem thus faster than the classic slow wave complexes of SWS. This difference in frequency is characterized further in respect to the Delta component of the slow activity. Traditionally considered characteristic of SWS, the power in the delta frequency band is very similar, if not higher, in REM [Fig. 1D.). But the actual shape of the Delta cycles detected on our LFP signals is different in REM (Fig. 1E.). In regard to the average rising and decay duration of the Delta cycles, REM Delta oscillations takes longer to rise (Delta mean rise time: REM = 185.43+-13.06ms, SWS = 167.66+-12.35ms), while SWS Delta takes longer to decay (Delta mean decay time: REM = 131.09+- 11.9ms, SWS = 146.19+-11.80ms). Therefore there is a clear difference in the ratio between rise and decay time of Delta cycles in REM compared to SWS. As illustrated in Fig. 1F the distribution of rise and decay time of Delta cycles in the two sleep states overlap poorly, and REM delta is more biased toward high rising time and low decay time. Rise and decay time of delta cycles that were observed during W (i.e. quiet wake) were shorter than those of the SWS and REM.

Delta in different cortical areas in REM To investigate the spatial distribution of REM sleep slow-waves, we next compared recordings in different areas during REM sleep.

To investigate the spatial distribution of REM sleep slow-waves, we compare recordings in different areas during REM sleep. Figure 2 shows the typical LFP activity observed in REM in simultaneously recorded areas. Important differences in the amplitude as well as in the oscillation rhythms were observed. The area S1 and S2 presented bouts of large amplitude delta oscillations, intermingled with periods of smaller and faster signal fluctuations. In the area M1 we also found some large amplitude Delta waves, but sparser than those of the somatosensory areas, and most of the signal is of small amplitude with no clear prevalent oscillation. The mPFC area displays the signal of smallest amplitude in REM with no delta event, nor a clear oscillatory pattern. Finally, the hippocampus shows a sustained theta oscillation along the REM episodes, which is extremely characteristic in rodents ([6]). Almost no delta events were found in the hippocampus LFP. These differences in cortical pattern of activity in REM can also be found in the spectral analysis (Fig 2.B). The spectra of S1 and S2 are very similar with an important peak in the Delta frequencies. In M1 there is also some power that goes above the 1/f trend of the spectrum and peak in the Delta band, but its amplitude is considerably smaller than what we have in the somatosensory areas. dCA1 exhibits a clear peak in the theta band and no power in the Delta. The EEG spectrum is very close to that of the dCA1 (Figure 4). As for dCA1, mPFC did not have a delta peak. Thus given the lack of delta oscillations in these areas we analysed only the areas of the somato-motor cortex.. In panels D and E of the figure 2 we can respectively see the averaged Delta cycle centred on their peak, and the distribution of the rise and decay duration of those Delta cycles. From those, it appears that the delta cycles found in S1 and S2 are extremely similar, with a bias toward long rising and short decay time, while Delta cycles from M1 are less stereotyped. They have a tendency to have a longer time decay, which might be due to the fact that Delta events in M1 are much more isolated and rarely immediately followed by another event.

Temporal distribution of REM-sleep delta bouts Next, to determine the temporal distribution of REM-sleep delta waves, we detected delta waves and found that bouts of delta alternate with periods of asynchronous activity which we characterised in Fig. 3.

Our detection of Delta bouts allows us to discriminate periods of at least a second that are dominated by Delta activity from periods without any Delta activity, while excluding periods that would be considered as mixed-activity. With this approach we can describe at least 80% of any of our REM signals. This can be seen in Figure 3.A as the thick green and red lines, that represent the Delta bouts and Non-Delta bouts respectively, occupy the major part of the signals. While in S1 the Delta bouts occupy almost half of REM episodes and last about 2.9seconds, it describes only 7.36% of the LFP signal of M1 in REM and lasts only 2 seconds on average. The result is intermediate for S2, where Delta bouts describe a large part (about 30%) of the signal and mean duration of the Delta bouts is 2.49sec in this area.

	S1	S2	M1
Delta bouts	47.33%	30.373%	7.362%
Non-Delta bouts	41.441%	53.25%	84.283%
Mean Delta bout duration	2.951s	2.494s	2.006s

Table 2: Percentage of somatomotor REM sleep LFP signal characterized by Delta and Non-Delta bouts.

Then, we determined if Delta bouts occurred simultaneously in the different areas Thus, we assessed the level of temporal overlap of the delta bouts in the area S1, S2 and M1. Looking at the overlap of S1 on S2 we can see that the

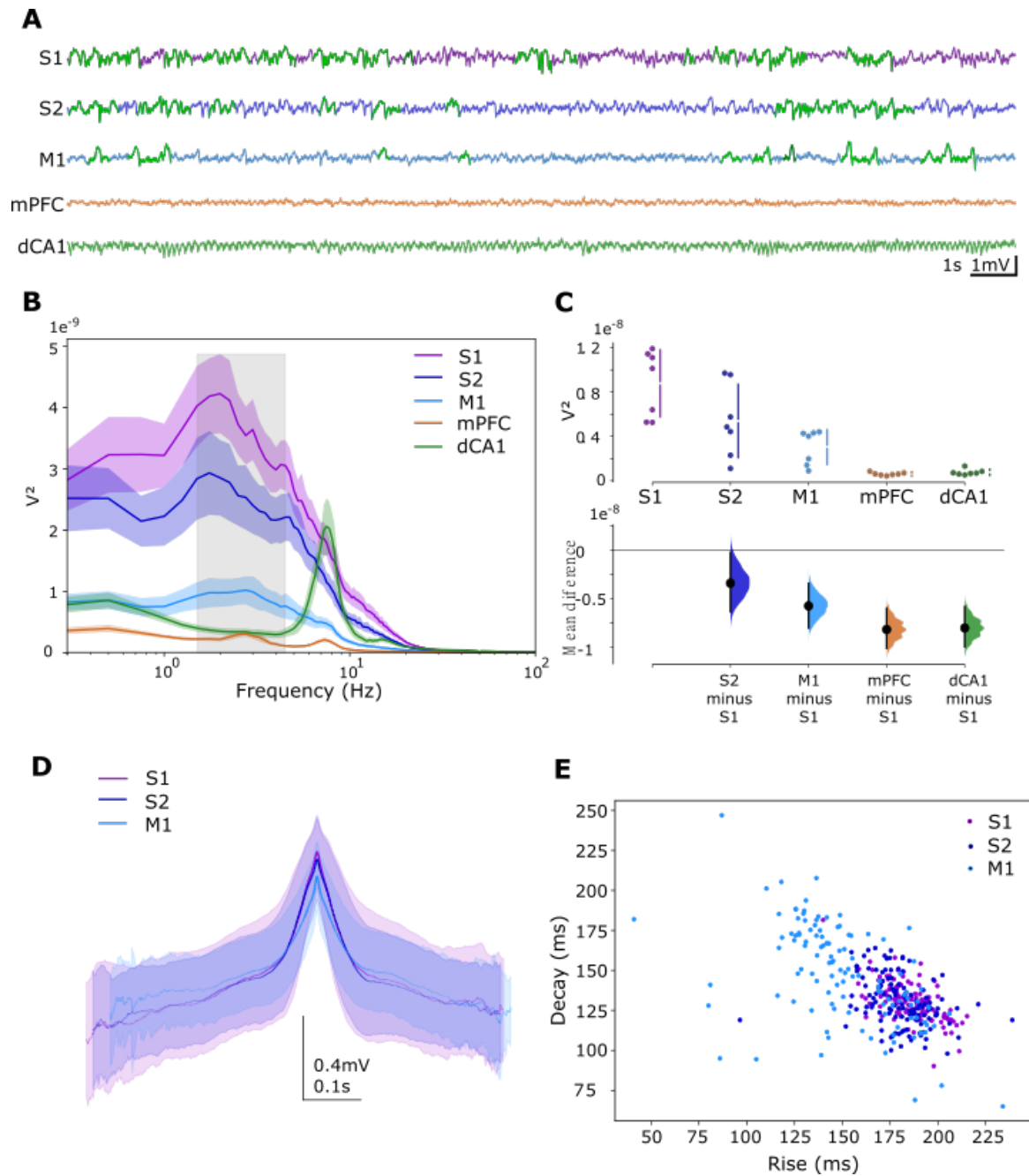


Figure 2: **REM sleep delta oscillation in the cortex** (Figure colours: Purple: S1, dark blue: S2, light blue: M1, green: dCA1, orange: mPFC)

A) 20 seconds of simultaneous LFP recording in 5 different areas during REM. Signals are shown with a common scale. Delta cycles detected in the signal are highlighted in green. (B) Average Power spectrum for the different areas for all REM episodes. Grey square shows the 1.5-4.5Hz delta band. (C) Delta band power, averaged for each mouse, in the different areas. Below is the Delta power compared to its distribution in S1. (D) Representation of the mean delta cycles, centred around their peak, over all detected cycles in the somatosensory and motor area. Line intensities represent the portion of delta cycle from the total pull recorded at specific area used for each datapoint. (Approximate number of cycles considered in each area: S1: 10000, S2: 8000, M1: 5000). (E) Scatterplot of the rise, decay symmetry of delta cycles in the somatosensory and motor area. Each dot corresponds to the mean values for delta cycles recorded in a REM episode.

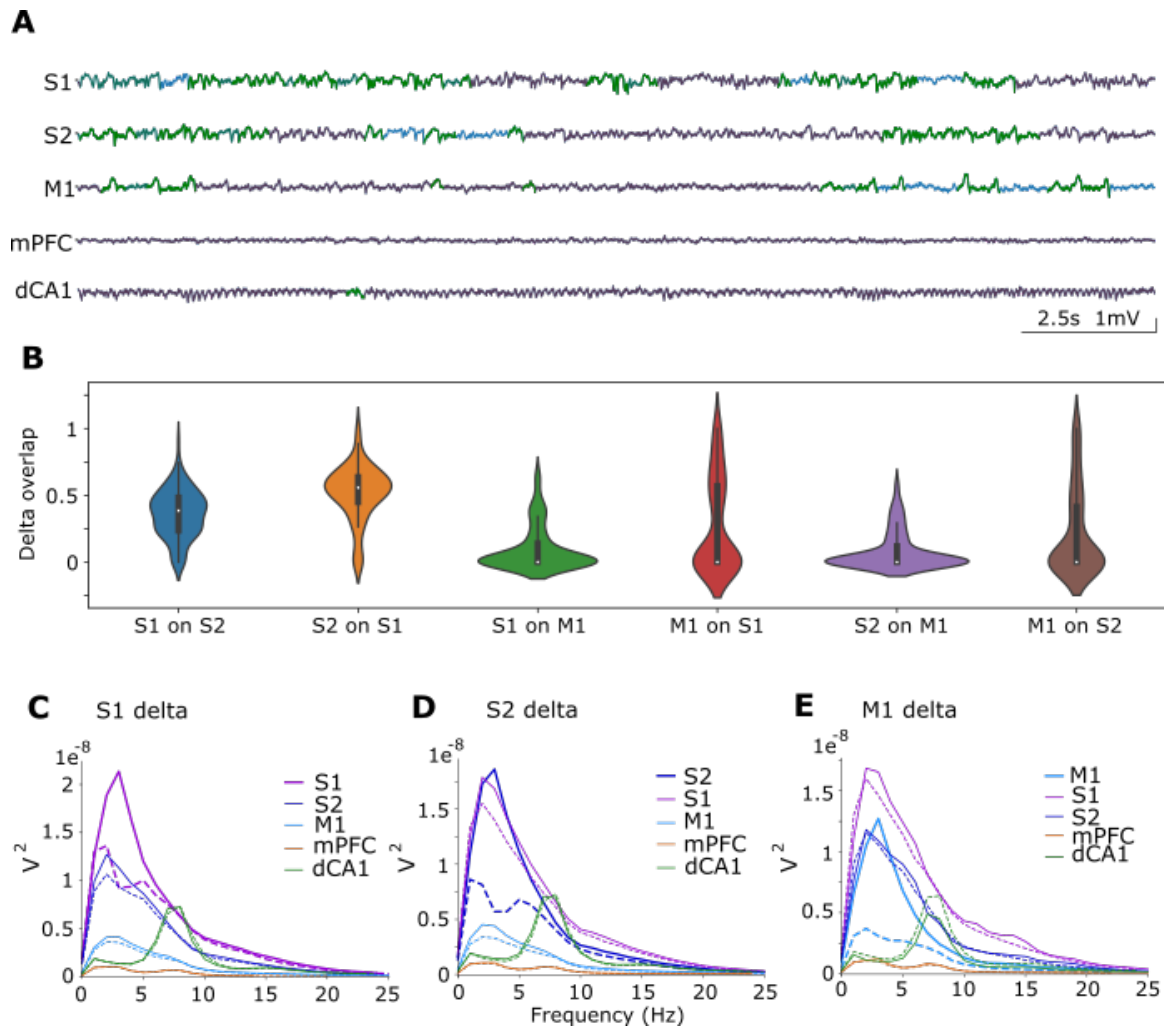


Figure 3: **Temporal presence of Delta in REM.**

A) Same LFP recording as shown before. Colours corresponding to the delta chunk analysis result. Isolated delta cycles are in light green, Delta bouts in bold green and non-delta bouts in red. In blue are the non-scored & non-delta parts. (B) Delta bouts overlap between areas. On the y axis is the percentage overlap of delta chunks from the origin to the target (S1 on S2: % of S1 delta chunks with simultaneous delta bouts in S2). Values are scaled between 0 and 1 (100% overlap). For each directed pair of areas the distribution of this overlap measure calculated for every delta chunk period of the origin area is shown in the form of a violinplot to illustrate data variability. (C) we analysed only the areas of the somato-motor cortex. Power spectrum of S1 Delta and Non-Delta bouts. For each area (with the same colour code as in figure2), the power spectrum shown is the average power spectrum of this area, for the Delta chunk periods of S1 in plain line, and for the non-Delta bouts periods of S1 in dashed line. The thickest line highlights S1, the area from where the Delta / non-Delta bouts periods are determined for this figure. (D) Same as C centred on S2. (E) Same as C centred on M1.

distribution peak is around 0.5, meaning that about 50% of S1 Delta bouts have simultaneous delta bout in S2. This is relatively important considering that S1 Delta bouts are longer and occupy a larger part of the REM signal. Looking at it the other way around, we can see that the overlap is even higher with very relatively few low values of overlap, meaning that the majority of S2 Delta bouts happened at the same time as S1 Delta bouts. In contrast, the distribution of overlaps from either S1 or S2 on M1 Delta bouts was bimodal, with a large majority of overlaps centered at zero, and a tailed distribution with values going up to slightly above 0.5. Meaning that there is a relatively poor overlap between M1 Delta chunks and those of the somatosensory areas. (when a M1 Delta bout happened in synchrony it can have a good overlap value as it is usually shorter than the bouts of its counterparts.)

So it is not surprising to see that when we look at M1 Delta power from the perspective of S1 Delta and Non-Delta

chunks we find no real difference. In S2 there is an increase in Delta power during S1 Delta chunks, but it is very small compared to the difference we have in S1 itself. A similar observation can be made when we look at the power spectra from the perspective of S2 Delta/Non-Delta chunks, however then there is also a small increase in M1 Delta power (Fig 3.C,D). As Delta chunks occupy a small fraction of REM episodes in M1 compared to the somatosensory areas, it is thus logical that there is no clear spectral difference when observed from the perspective of M1 Delta/Non-Delta chunks. Surprisingly, we found that during periods of M1 Delta bouts the theta power of the hippocampus was slightly reduced (Fig 3.E). Therefore, the Delta activity we observe in REM was neither constant nor synchronous in cortical areas, except between S1 and S2.

Detection of phasic theta in REM In rodents during REM a monotonic theta oscillation was observed in the EEG, hippocampus, limbic areas (mPFC, amygdala) and some neocortical areas. 4

Using a method inspired by [21, 19, 5] and the approach proposed by [8, 7], we searched for bouts of theta oscillations that would correspond to the previously identified phasic theta. We focus on the temporal properties of the phasic theta and did not specify the search for cycles of high amplitude as proposed by [21], yet our detection of phasic theta periods still shows a substantial increase in theta power. This method was also carried out on the other LFP signals of the cortical areas. It should be noted that this phasic theta wave is found on the background of a continuous theta oscillation (i.e. tonic theta). Therefore using this method we were able to select bouts of phasic theta in the different cortical area recordings.

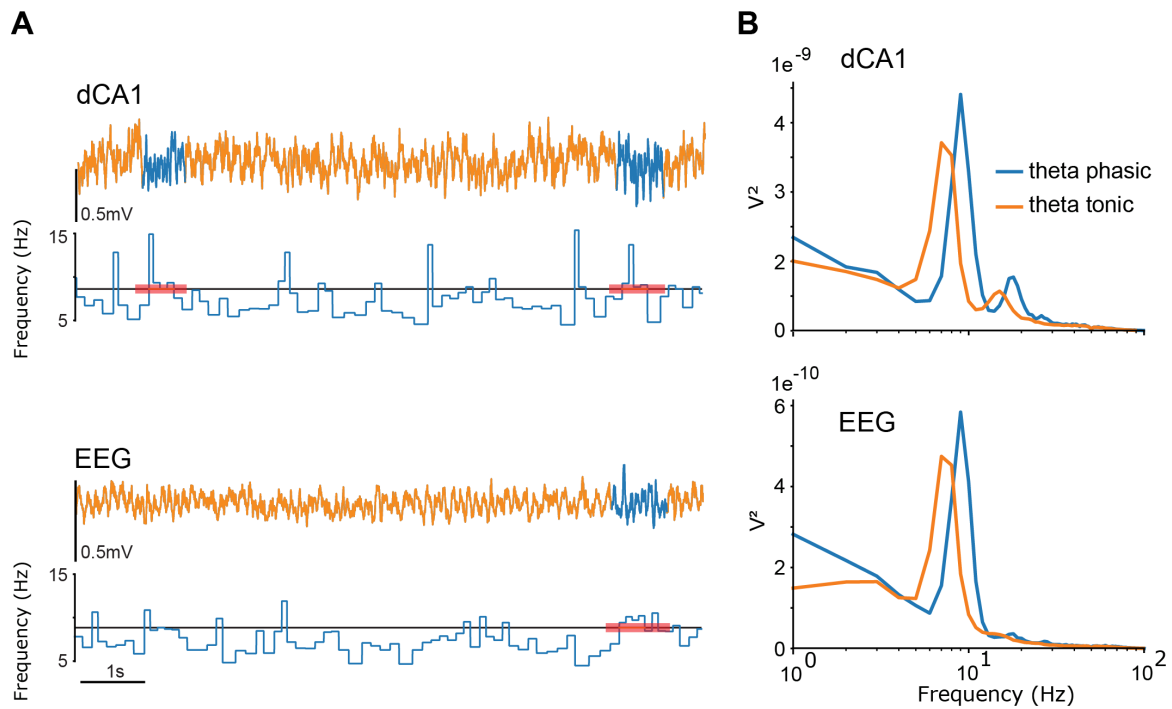


Figure 4: **Phasic and tonic REM theta in the hippocampus and the EEG**

(A) Top panel: Raw dCA1 LFP REM signal (top) with each theta cycle frequency, as 1/cycle period (below). Successive cycles above the threshold (75% fastest theta cycles, in black horizontal line) are considered as phasic theta, in blue on the signal and in red on the cycles frequency plot. Bottom panel: Same as before for the EEG signal. (B) Power spectrum of dCA1 (top) and the EEG (bottom) for REM phasic and tonic theta periods (in blue and orange respectively)

Phasic theta bouts (detected with this method) represented in dCA1 between 5 to 15% of the duration of REM episodes. Theta phasic bouts were also observed in EEG but represented a shorter duration overall. Interestingly we observed that most of the EEG phasic theta bouts occurred simultaneously to hippocampal phasic theta. As expected, it suggests that the hippocampus and its related areas largely contribute to the REM EEG signal.

Phasic theta periods was short, hundreds of milliseconds up to a few seconds for the longest (stat?). It is because of this observation that we adapted our detection method to extend the bouts as much as possible while keeping the principal properties of the phasic period, such that we could perform relevant spectral analysis, although with reduced precision compared to the first results shown in this article. From the power spectrum presented 4B we can see that both results from dCA1 and EEG were very similar and characterised by a prominent peak in the theta band. We can also see that

the difference between phasic and tonic theta is very close in both signals, with the phasic theta being faster and with a higher peak power. Two differences between dCA1 and EEG spectra can be observed. First, in dCA1 we observe a second peak of smaller power that also shifts to faster frequencies at 15 and 20 Hz, close to the sigma band. The second and main difference is about the power and amplitude of the observations in the EEG that are much smaller than what we observed in the dCA1.

Hippocampal phasic theta and sensory cortices Delta Following the observation that in M1 Delta periods are related to lower power in hippocampal theta we examined the relation between phasic theta bursts in the hippocampus and Delta activity in the somatomotor cortex.

In 5A we show the temporal distribution of dCA1 phasic theta in line with the Delta activity (both Delta bouts and isolated delta events) in S1, S2 and M1. Most theta phasic periods occurred very close to Delta periods, either at the beginning or the end. However the overlap between the two kinds of periods was infrequent and most of the phasic theta occurred outside of Delta periods. These results suggest loose correlations between these events. As if phasic theta, the fastest of the two kinds of event, could mark the beginning and or the end of the longer sequences of Delta events. With a closer look at the raw data of a phasic theta event, we can observe clear changes in the dynamic of the somatomotor area activities. From the beginning of the event we saw a decrease in the slower and larger signal fluctuations. We still observe some Delta wave in S1 but of reduced amplitude and the last of the marked Delta wave of this Delta bout end synchronously to the end of the theta phase. In line with the end of the phasic theta event, we can also observe a large fluctuation in S2. But surprisingly, shortly after we can also notice a synchronised Delta wave that occurs in the three sensory areas, although less marked in S1 than the previous Delta activity. Thus it seems that the dCA1 phasic event marked a change toward smaller LFP fluctuations and the end of a previously established Delta bout of S1. This suggests that LFP activities during REM sleep were coordinated between dCA1 and the somatomotor cortex.

4 discussion

In this paper, we have analysed mouse REM sleep cortical activity focusing on SWA which is predominant in the somato-motor cortex. The analysis showed that the REM SWA was mostly constituted of delta oscillations. This analysis also shows that REM SWA differed from the SWA of SWS. On a spatial scale, REM sleep expresses Delta waves only in some cortical areas but not in others, in contrast with SWS. On a temporal scale, again in contrast to the SWS, REM Delta bouts alternate with periods of asynchronous activity. Finally, our results suggest a relationship between the somatomotor cortex Delta oscillations and the hippocampal phasic theta. Below we relate these findings to previous works and delineate possible perspectives to follow-up on this work.

The occurrence of local slow-waves during REM was reported in humans and mice ([2, 4, 12, 30]), but our work reveals important differences with the work of Funk et al. First, REM slow-wave activity is significantly faster than that of SWS and is mostly made of Delta activity, and not slow oscillations (SO). It reinforces the idea that SWS SWA is the association of SO and Delta waves ([1, 17]) and proposes that, contrary to SWS, REM Delta(2-5Hz) is relatively dissociated from slower activity (<1Hz). Second, it was claimed that REM slow-waves occur only in primary sensory areas and therefore not in secondary or association areas. The clear occurrence of delta oscillations in S2 during REM (fig 2) appears to contradict this statement. Thus, it seems that Funk et al have wrongly generalized their result obtained in the visual cortex. Moreover, while we found clear evidence of Delta activity in S1 and M1, we did not find it in the primary visual cortex (V1) or in the primary auditory cortex (Au1, data not shown). In these areas theta oscillations were prominent during REM sleep. This topological organisation is in line with the multisite LFP recordings of [30]. These results suggest that LFP recordings in the neocortex result from a competitive combination of two oscillation generators, one close to the hippocampal theta and the other to the delta prominent in some cortical areas. Such differences were Delta power in V1 compared to S1 is also observed in human in the REM episodes at the end of the night[2]. It is also likely that one of the multiple experimental differences (chronic vs acute recording, silicon probes vs tungsten LFP, the detection methods. . .) could explain those apparently opposite results. Finally a major structure not yet studied is the thalamus which is known to play a key role in SWS oscillations. It is indeed likely that the thalamus connected to the different sensory modalities dictate in an essential way the alternation between delta and desynchronized activities. Unpublished work by Nadia Urbain's team (CRNL, Lyon), using intra- and extracellular recordings, shows that the activity of relay neurons in thalamic nuclei connected to S1 and S2 areas changes during REM episodes in a coordinated manner with the LFPs of these cortical areas. Interestingly, in humans, thalamic activity is characterized by continuous delta waves as recorded by intracerebral EEG [23].

One of the essential highlights of Funk et al study is the large neuronal silence observed in the superficial layers of the sensory cortex during REM SWA. This silence period would participate in the decreased responsiveness of REM by making the cortical areas less prone to integrate inputs [12], but we saw that REM delta is not constant and alternate

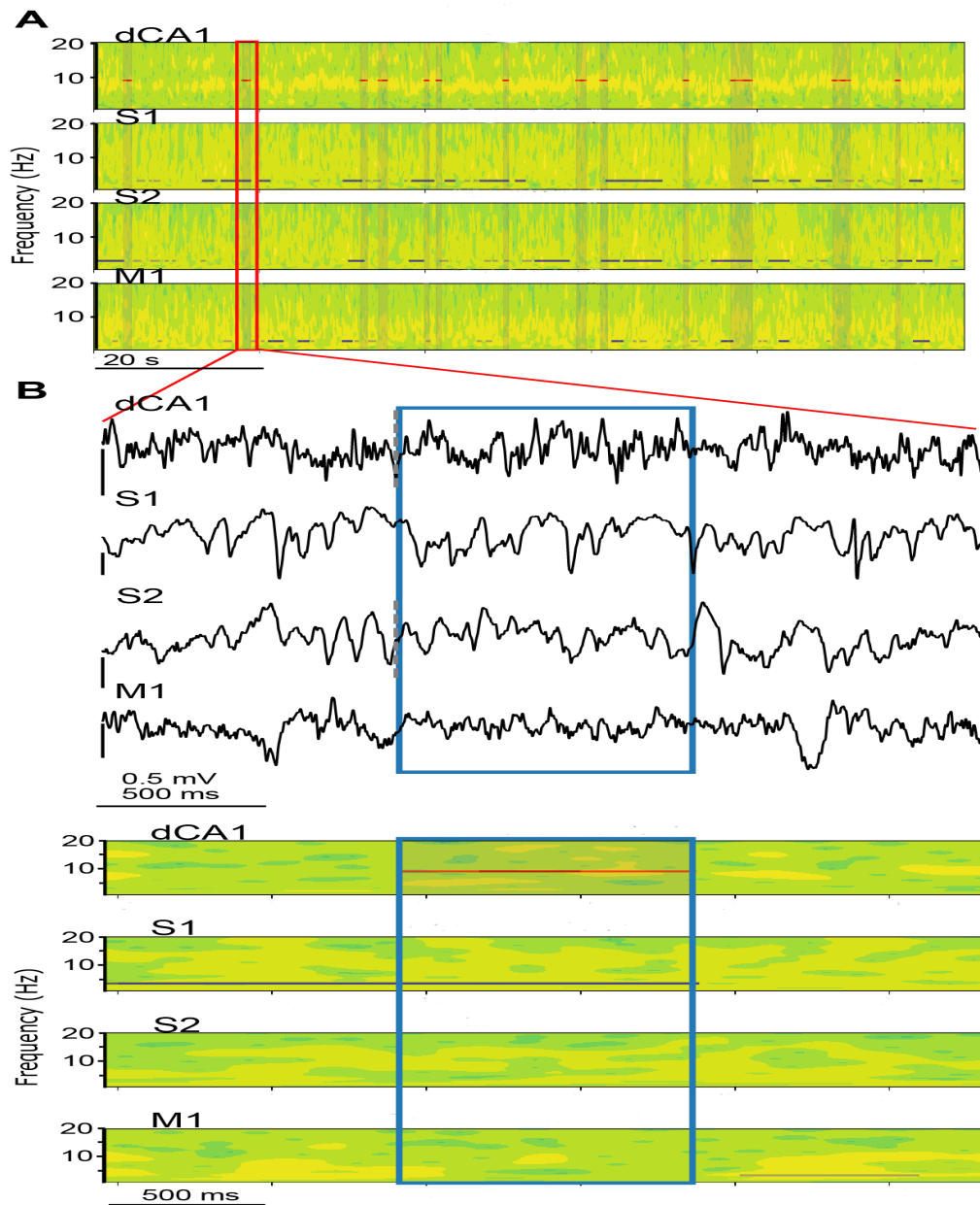


Figure 5: Hippocampus phasic theta and sensory cortices delta bouts.

(A) Time-frequency representation of the LFP signals from one REM episode simultaneously recorded in the hippocampus dCA1, the primary somatosensory cortex S1, the secondary somatosensory cortex S2 and the primary motor area M1 (from top to bottom). The periods shadowed in gray correspond to phasic theta bouts detected on dCA1 signal (also shown with the horizontal red traces at 10Hz on the top panel). On S1, S2 and M1 panels, delta bouts are shown with dark horizontal lines at 3Hz, and isolated delta waves are in gray. (B) Zoom on a single phasic theta bout (Red frame figure (A)). The part of the signal considered as phasic theta is framed in blue. Top: raw LFP of the 4 areas. Bottom: same time-frequency representation as in (A).

with periods of asynchronous activity which may reflect of a cortical state of increased neuronal excitability. The hippocampal activity might be coordinated with the alternation of Delta bouts periods of different activities. Our results suggest that phasic theta often occurs at the beginning and/or end of Delta bouts and might thus participate in the switch from Delta/non-Delta bouts. It has been proposed that phasic theta may be a window of intense synchronization correlatingly activating populations of neurons in the hippocampus and possibly in the neocortex during brief periods of REM. Thus, phasic theta periods during REM sleep could also correspond to short windows of increase in neuronal activity in cortical sensory areas.

The presence of REM SWA in some cortical areas could also be related to a heterogeneous temporo-spatial distribution of neuromodulatory signaling in the neocortex or thalamus. In classical study the unique neuromodulation of REM is associated with elevated Acetylcholine (Ach) [15, 14]. But it is shown that SWA occurs when cholinergic signaling in S1 is blocked during wakefulness [10]. Therefore if we consider neuromodulation as global, slow and tonic, in REM, the high Ach should prevent SWA. But, with recent technical advances using no longer microdialysis but choline microsensors, Lustig and Sarter[27] suggest in contrast that neuromodulatory signalling is phasic, short duration and very local (synaptic). This conceptual shift help to relate the overall high Ach with the Delta bouts we observed. We hypothesize that in REM the cholinergic signalling toward the somatosensory and motor cortex, or the thalamic nuclei connected to these areas, is low and short duration compared to other brain regions.

In this article we used a previously established experimental dataset [11] to question recent findings about REM cortical state. Natural follow-up to this study would be experiments designed to detail some of the observations and interactions we described.

A first study is to better determine the neocortical-hippocampal relations in REM sleep, and in particular with respect to SWA. Our results suggest that, in REM, the hippocampus activity is coordinated with the neocortical activity. Moreover, thalamic activity is clearly an important missing link in determining which structure -hippocampus or thalamus- plays the essential role in the temporo-spatial distribution of cortical activity during REM. During REM the sensory activation threshold is higher, especially for the sense of touch. One may therefore wonder whether SWA in S1 and S2 do not play a role as a sensory filter.

However this should be questioned with respect to the thalamic transmission to sensory cortices in REM. Knowing if the thalamus transmits sensory stimulation similarly as in W is a key to assess how much cortical delta is really about decreasing the responsiveness.

Another follow-up would be to understand the relation between the different transient events that occur during REM, which concern the whole body. REM sleep remains a global phenomenon affecting the whole individual. Multiple organs work together and many factors, such as natural whisking, respiratory or cardiac rhythm could potentially affect brain oscillations ([9, 13, 3, 34, 33]).

More experiments could be planned as the cortical activity in REM has received little attention since the transition from cat to rodent as a biological model and is often discarded as just ‘similar to wake’. We also lack specific computational models to question and understand the phenomenon we discussed. With the recent advances, models of W and NREM become more sophisticated and can span multiple scales. New dynamical model of the brain in REM could help to integrate the complex and heterogeneous cortical oscillations we discussed into a larger theoretical framework that could be questioned for new insights. One such model is presented in the following study.

References

- [1] F. Amzica and M. Steriade. Electrophysiological correlates of sleep delta waves. *Electroencephalography and Clinical Neurophysiology*, 107:69–83, 1998.
- [2] B. Baird, A. Castelnovo, B. A. Riedner, A. Lutz, F. Ferrarelli, M. Boly, R. J. Davidson, and G. Tononi. Human rapid eye movement sleep shows local increases in low-frequency oscillations and global decreases in high-frequency oscillations compared to resting wakefulness. *eNeuro*, 5, 7 2018.
- [3] A. Bergel, T. Deffieux, C. Demené, M. Tanter, and I. Cohen. Local hippocampal fast gamma rhythms precede brain-wide hyperemic patterns during spontaneous rodent rem sleep. *Nature Communications*, 9, 2018.
- [4] G. Bernardi, M. Betta, E. Ricciardi, P. Pietrini, G. Tononi, and F. Siclari. Regional delta waves in human rapid eye movement sleep. *Journal of Neuroscience*, 39:2686–2697, 2019.
- [5] J. Brankač, C. Scheffzük, V. I. Kukushka, A. L. Vyssotski, A. B. Tort, and A. Draguhn. Distinct features of fast oscillations in phasic and tonic rapid eye movement sleep. *Journal of Sleep Research*, 21:630–633, 2012.
- [6] G. Buzsáki, D. L. Buhl, K. D. Harris, J. Csicsvari, B. Czéh, C. Czéh, , and A. Morozov. Hippocampal network patterns of activity in the mouse. 2003.
- [7] S. Cole and B. Voytek. Cycle-by-cycle analysis of neural oscillations. *Journal of Chemical Information and Modeling*, 53:1689–1699, 2018.

- [8] S. R. Cole and B. Voytek. Brain oscillations and the importance of waveform shape. *Trends in Cognitive Sciences*, 21:137–149, 2017.
- [9] S. Crochet and C. C. Petersen. Correlating whisker behavior with membrane potential in barrel cortex of awake mice. *Nature Neuroscience*, 9:608–610, 5 2006.
- [10] E. Eggermann, Y. Kremer, S. Crochet, and C. C. Petersen. Cholinergic signals in mouse barrel cortex during active whisker sensing. *Cell Reports*, 9:1654–1661, 2014.
- [11] L. M. Fernandez, J. C. Comte, P. L. Merre, J. S. Lin, P. A. Salin, and S. Crochet. Highly dynamic spatiotemporal organization of low-frequency activities during behavioral states in the mouse cerebral cortex. *Cerebral cortex (New York, N.Y. : 1991)*, 27:5444–5462, 2016.
- [12] C. M. Funk, S. Honjoh, A. V. Rodriguez, C. Cirelli, and G. Tononi. Local slow waves in superficial layers of primary cortical areas during rem sleep. *Current Biology*, 26:396–403, 2016.
- [13] D. Heck, S. McAfee, Y. Liu, A. Babajani-Feremi, R. Rezaie, W. Freeman, J. Wheless, A. Papanicolaou, M. Ruzinkó, and R. Kozma. Cortical rhythms are modulated by respiration. *NEURON*, pages 1–30, 2016.
- [14] S. hee Lee and Y. Dan. Review neuromodulation of brain states. *Neuron*, 76:209–222, 2012.
- [15] H. H. Jasper and J. Tessier. Acetylcholine liberation from cerebral cortex during paradoxical (rem). *American Association for the Advancement of Science*, 172:601–602, 1971.
- [16] A. Karashima, M. Nakao, N. Katayama, and K. Honda. Instantaneous acceleration and amplification of hippocampal theta wave coincident with phasic pontine activities during rem sleep. *Brain Research*, 1051:50–56, 7 2005.
- [17] J. Kim, T. Gulati, and K. Ganguly. Competing roles of slow oscillations and delta waves in memory consolidation versus forgetting. *Cell*, 179:514–526.e13, 2019.
- [18] J. Lerma and E. Garcia-Austt. Hippocampal theta rhythm during paradoxical sleep. effects of afferent stimuli and phase relationships with phasic events. 60:46–54, 1985.
- [19] K. Mizuseki, K. Diba, E. Pastalkova, and G. Buzsáki. Hippocampal ca1 pyramidal cells form functionally distinct sublayers. *Nature Neuroscience*, 14:1174–1183, 2011.
- [20] K. Mizuseki, S. Royer, K. Diba, and G. Buzsáki. Activity dynamics and behavioral correlates of ca3 and ca1 hippocampal pyramidal neurons. *Hippocampus*, 22:1659–1680, 8 2012.
- [21] S. Montgomery, A. Sirota, and G. Buszaki. Theta and gamma coordination of hippocampal networks during waking and rem sleep. *The Journal of . . .*, 28:6731–6741, 2008.
- [22] T. E. Robinson, R. C. Kramis, and C. H. Vanderwolf. Two types of cerebral activation during active sleep: relations to behavior. *Brain Research*, pages 544–549, 1977.
- [23] D. S. Rosenberg, F. Mauguière, H. Catenox, I. Faillenot, and M. Magnin. Reciprocal thalamocortical connectivity of the medial pulvinar: A depth stimulation and evoked potential study in human brain. *Cerebral Cortex*, 19:1462–1473, 6 2009.
- [24] K. Rowe, R. Moreno, T. R. Lau, U. Walloppillai, B. D. Nearing, B. Kocsis, J. Quattrochi, J. A. Hobson, R. L. Verrier, and B. Koc-sis. Heart rate surges during rem sleep are associatedwith theta rhythm and pgo activity in cats. *American Physiological Society*, 1999.
- [25] M. V. Sanchez-Vives. Origin and dynamics of cortical slow oscillations. *Current Opinion in Physiology*, 15:217–223, 2020.
- [26] M. V. Sanchez-Vives and D. A. McCormick. Cellular and network mechanisms of rhythmic recurrent activity in neocortex. *nature neuroscience*, 3, 2000.
- [27] M. Sarter and C. Lustig. Forebrain cholinergic signaling: Wired and phasic, not tonic, and causing behavior. *Journal of Neuroscience*, 40:712–719, 2020.
- [28] R. Scheffer-Teixeira, H. Belchior, F. V. Caixeta, B. C. Souza, S. Ribeiro, and A. B. L. Tort. Theta phase modulates multiple layer-specific oscillations in the ca1 region. *Cerebral Cortex*, 22:2404–2414, 2012.
- [29] H. Sei and Y. Morita. Acceleration of eeg theta wave precedes the phasic surge of arterial pressure during rem sleep in the rat. *Neuroreport*, 7:3059–3062, 1996.
- [30] S. Soltani, S. Chauvette, O. Bukhtiyarova, J. M. Lina, J. Dubé, J. Seigneur, J. Carrier, and I. Timofeev. Sleep–wake cycle in young and older mice. *Frontiers in Systems Neuroscience*, 13:1–14, 2019.
- [31] M. Steriade and I. Timofeev. Neuronal plasticity in thalamocortical networks during sleep and waking oscillations. *Neuron*, 37:563–576, 2003.

- [32] I. Timofeev, F. Grenier, M. Bazhenov, T. Sejnowski, and M. Steriade. Origin of slow cortical oscillations in deafferented cortical slabs. *Cerebral Cortex*, 2000.
- [33] A. B. Tort, J. Brankač, and A. Draguhn. Respiration-entrained brain rhythms are global but often overlooked. *Trends in Neurosciences*, 41:186–197, 2018.
- [34] A. B. Tort, S. Ponsel, J. Jessberger, Y. Yanovsky, J. Brankač, and A. Draguhn. Parallel detection of theta and respiration-coupled oscillations throughout the mouse brain. *Scientific Reports*, 8, 12 2018.
- [35] V. V. Vyazovskiy, U. Olcese, E. C. Hanlon, Y. Nir, C. Cirelli, and G. Tononi. Local sleep in awake rats. *Nature*, 472:443–447, 2011.
- [36] E. Zaghera, A. E. Casale, R. N. Sachdev, M. J. McGinley, and D. A. McCormick. Motor cortex feedback influences sensory processing by modulating network state. *Neuron*, 79:567–578, 2013.

5 supplementary figures

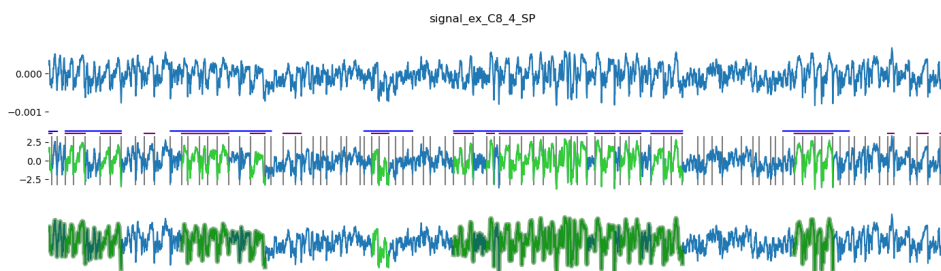


Figure 6: A: raw signal. B: Delta cycle detection, first the signal is segmented into cycles, first threshold detection (blue), second threshold detection (purple). In green are the validated delta cycles C: Delta bouts are shown in darker green)



PART IV

Model

Résumé de l'article Bien que l'on pense classiquement que le sommeil à mouvements oculaires rapides (REM) génère une activité désynchronisée similaire à l'éveil, il a été constaté que certaines régions du cerveau peuvent exprimer une activité à ondes lentes (SWA), un schéma qui est normalement typique du sommeil à ondes lentes. Pour en étudier le mécanisme sous-jacent, nous introduisons un modèle computationnel du cortex entier de souris en sommeil paradoxal. Des champs moyens exponentiels adaptatifs (AdEx mean-field) ont été connectés ensemble selon les données connectomiques du Allen Brain Institute et simulés à l'aide du simulateur The Virtual Brain (TVB). Pour comparer avec les données expérimentales, le potentiel de champ local est calculé dans chaque région du cerveau de la souris. Pour reproduire les expériences, nous supposons un niveau d'adaptation hétérogène dans différentes régions corticales. Dans ces conditions, le modèle reproduit une partie des observations expérimentales dans les aires somato-motrices et les autres aires corticales. Nous effectuons ensuite des expériences de stimulation dans le modèle pour tester la réactivité corticale. Prédissant les réponses des zones avec différents niveaux d'adaptation, le modèle soutient l'idée que le REM SWA est lié à la réactivité réduite observée pendant cet état. Comme l'adaptation est liée au niveau de neuromodulateurs tels que l'acétylcholine, nous concluons que des niveaux de neuromodulation hétérogènes peuvent expliquer la coexistence d'ondes lentes avec une activité désynchronisée dans le sommeil paradoxal.

WHOLE-BRAIN COMPUTATIONAL MODEL OF REM SLEEP IN MICE

A PREPRINT

✉ **Mathias Peuvrier**

French National Centre for Scientific Research (CNRS), Institute of Neuroscience (NeuroPSI)
Paris-Saclay university
91198 Gif sur Yvette, France
mathias.peuvrier@cnrs.fr

✉ **Paul Salin**

(CNRS), Institute of Neuroscience (Forgetting)
Lyon 1 University
69675 Bron, France
paul.salin@sommeil.univ-lyon1.fr

✉ **Alain Destexhe***

(CNRS), Institute of Neuroscience (NeuroPSI)
Paris-Saclay university
91198 Gif sur Yvette, France
Alain.Destexhe@cnrs.fr

April 1, 2022

ABSTRACT

Although classically Rapid-Eye Movement (REM) sleep is thought to generate desynchronized activity similar to wakefulness, it was found that some brain regions can express Slow Wave activity (SWA), a pattern which is normally typical of slow-wave sleep. To investigate possible underlying mechanism, we introduce a computational model of the mice whole cortex in REM sleep. Adaptive Exponential (AdEx) mean-fields were connected together according to connectomics data from the Allen brain institute, and simulated using The Virtual Brain (TVB) simulator. To compare with experimental data, the local field potential is calculated in each mouse brain region. To reproduce the experiments, we assume a heterogeneous level of adaptation in different cortical regions. In these conditions, the model reproduces some of the experimental observations in the somato-motor areas and the other cortical areas. We then run stimulation experiments in the model to test the cortical responsiveness. Predicting the responses of areas with different level of adaptation, it support the idea that REM SWA is related to the observed reduced responsiveness of this state. As adaptation is related to the level of neuromodulators such as acetylcholine, we conclude that heterogeneous neuromodulation levels can account for the coexistence of slow-waves with desynchronized activity in REM sleep.

Keywords REM sleep · Delta oscillation · Computational model

1 Introduction

Classically, brain states such as wakefulness (W) and Rapid-Eye Movement (REM) sleep are thought to generate essentially desynchronized activity, while slow-wave sleep (SWS) typically generates synchronized slow oscillatory waves [31]. However, it was found recently that slow-wave activity (SWA) can also be seen during quiet wakefulness in some brain areas [8, 40, 41, 14]. SWA can also be observed in REM sleep, in human [2, 4], and in mice [15, 38]. In their study, Funk et al showed local SWA in the superficial layers of primary areas of the mouse sensory cortex, while the activity in secondary sensory and associative cortical areas seemed desynchronized [15]. These results may suggest that SWA would be present in all primary sensory areas and filter sensory information during REM sleep.

*Use footnote for providing further information about author (webpage, alternative address)—*not* for acknowledging funding agencies.

Until now, most modelling efforts regarding REM aimed at building models concerning the genesis, maintenance or regulation of this sleep state in relation to the other states of vigilance [25, 19]. Surprisingly, little has been done to model cortical activity during REM, compared to the numerous computational works concerning SWS. Models of cortical dynamics of sleep (and wakefulness) with fine temporal precision rely on neuronal network models with single neurons, of various degrees of detail. Those models, and the thalamocortical models in particular, were very fruitful in describing the slow oscillatory Up and Down regime of the SWS [3, 12, 7, 18]. In such models the neocortex is composed of a few thousand neurons that would represent one to two cortical columns, with a specific connectivity, often inspired by biological observations [22, 20]. However, expanding such models to the whole cortex would require a lot (way too much) of computational power, making it almost impossible to run, but also extremely difficult to analyse. This is why we looked at population models, abstracting the neuron activity to drastically reduce the computational cost, while remaining completely relevant and very detailed in regard to experimental LFP recordings. It is a mesoscopic approach that describes the average collective properties of neuronal populations, instead of simulating each individual neuronal dynamics[9].

Furthermore, this modelling approach is inspired by the work of [17] that produced important features of global cortical dynamics comparable to W and SWS in human brain-scale simulation. Using TVB (<https://www.thevirtualbrain.org/tvb>) to integrate population models as the nodes of a network in which the connections are based on brain connectivity as defined from diffusion imaging experiments. In our model we will use the TVB mouse counterpart, The Virtual Mouse Brain (TVMB, [27]). TVMB can construct individual mouse brains from dMRI experiments or from tracer experiments realized by the Allen Institute. Thanks to that we could use a detailed connectome of the mouse cortex that fit well the level of description we have in our biological dataset.

To model neuronal populations, we used an AdEx mean-field model, as described in [13]. This biologically realistic mesoscale model was built to correctly predict the level of spontaneous activity observed in AdEx spiking neural networks with Asynchronous Irregular (AI) or Up and Down regimes. Two network regimes that are somehow the computational analogs of biological Wakefulness and SWS sleep respectively [11]. In those models, the spike-triggered adaptation parameter is sufficient to switch from one regime to the other. It is interesting to note that this adaptation parameter is strongly related to the type of adaptation produced by high-threshold calcium-gated current [1]. This current is known to mediate the spike frequency adaptation in cortical pyramidal neurons but also to be deactivated by Acetylcholine [26]. Therefore it is not surprising that in models with strong spike-triggered adaptation, the adaptation mediated by this current is strong, such as in a cortex without acetylcholine innervation, such as in SWS.

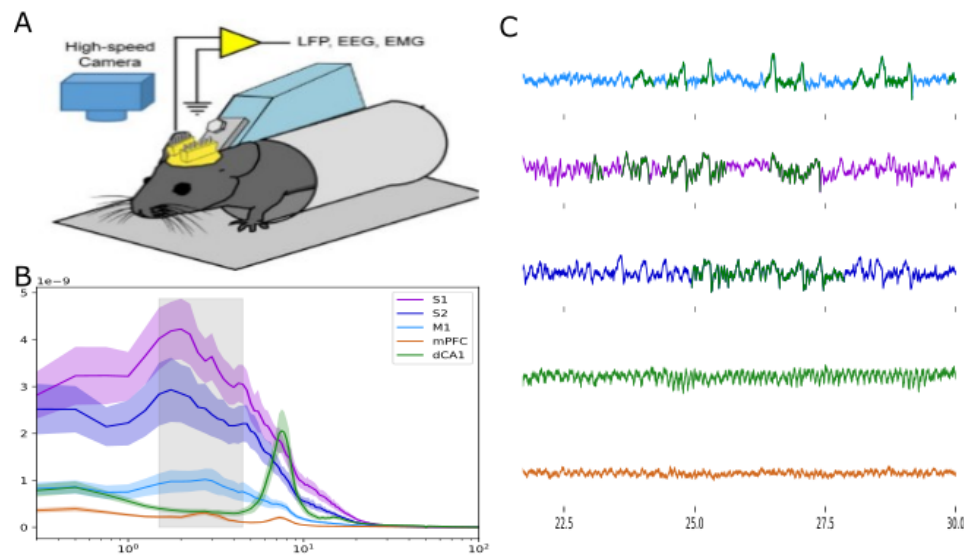


Figure 1: Experimental observation of mouse cortical activity in REM. This figure summarize some results of the experimental observations presented in a previous article (thesis chapter I). (A): Representation of the data presented in the column below. (B): Power spectrum observed for the different areas/adaptation values in the corresponding dataset. (C) Signal example showing the shape of LFP signal in the biological and simulated data

Using this model of the whole mouse cortex, we can simulate the transition from a Wake model (W-model) to a SWS model (SWS-model) by changing only the spike-triggered adaptation parameter. Yet there is no REM-model. Here we

present a whole-brain model that we tuned to fit LFP recording of mouse REM sleep . Figure 1 shows the summary of the LFP analysis from [14] and the first article of the thesis. Briefly we presented the cortical dynamics of the somatosensory primary and secondary cortices (S1 and S2), the primary motor cortex (M1), the medial prefrontal cortex (mPFC) and the hippocampus (dCA1), with a particular interest regarding the REM SWA as recently observed [15, 4, 36]. With these considerations to build our REM-model, we propose a simple topological organisation of the spike-triggered adaptation parameter in the model. This organisation allows the simulation of different patterns of activity across the cortex that reproduce a part of the diversity of activities we observed experimentally. Finally we also use this new model to predict the potential cortical response to stimulation in this state

2 Methods

2.1 Whole brain modelling

The models we discuss are whole brain models built at the neuronal population resolution and implemented in The Virtual Mouse Brain. It consists of a network of AdEx mean fields connected together following Connectome-based information from the brain Allen institute. In order to keep this section as short and simple as possible, we'll spare some mathematical details regarding the mean-field model or the TVB implementation. The corresponding informations could be found in DiVolo 2018 [13] and Goldman 2020 [17] respectively.

All simulations presented in the paper were run for ten seconds, with the first two seconds, the simulation initiation, being systematically excluded. The results presented for the brain state model in Fig. 2 (expected the spectrogram which average 4 simulations for each b value in this single figure) and the figure 4 are results from a single simulation. Results concerning the stimulation part are the average of multiple simulations. See the related part of the method.

The Virtual Mouse Brain We use the neuroinformatic framework The Virtual Mouse Brain (<https://www.thevirtualbrain.org/tvb>) to perform detailed connectome-based mouse brain simulations. With the Allen Connectivity Builder pipeline, experimental connectivity data from dMRI or tracer experiments are used to build a precise mouse connectome. The connectome is a square matrix (origin to target structure and vice versa) informed with connection strength and tract length. The Allen Connectivity Builder also provides a 3D matrix which represents the volume of the mouse brain to create a region volume mapping [27]. This framework allows us to virtualize a mouse brain with a population model at the nodes corresponding to a cortical column or a brain area, and edges corresponding to connection strength between regions. We use a connectome composed of 104 cortical nodes, such as proposed in [ref ??]. We selected this connectome over more detailed ones that includes thalamus and other subcortical nuclei for two principal reasons. First we don't have simultaneous recordings including subcortical areas in our dataset. Second, the population model we decided to use was built to match the dynamics of cortical spiking neuronal network models. Therefore more complex connectomic dataset are not more relevant regarding our biological dataset while it could induce some errors in the network dynamics.

Mean field model The population model used is an AdEx mean-field model such as described by DiVolo et al 2018 [13]. This mean-field model, based on a previous Master Equation formalism [5] was built to match the spontaneous activity of networks of 10000 Regular and Fast Spiking AdEx (Adaptive Exponential) neurons. It takes into account the nonlinear effects of the conductance-based synaptic interactions as well as the spike-frequency adaptation of excitatory regular spiking neurons. The mean-field has two neuron populations with different intrinsic properties. One is excitatory, called the "regular spiking" (RS), and is affected by the spike-frequency adaptation. The other is an inhibitory population called "fast spiking" due to its usually higher firing frequency. The dynamics of the two population firing rate and their covariance are computed as a function of the transfer function (TF; the firing rate of one population as function of the inputs it receives), which is itself dependent on the population adaptation variable W . This population adaptation has two important parameters: the sub-threshold adaptation a and the spike-triggered adaptation b . It should be noted that this parameter b affects only the excitatory population. Another difference in the dynamics of the two populations is the inputs considered in their transfer function. Indeed, only the excitatory population is affected by external noisy drive, while both populations are affected by external inputs (such as thalamic inputs).

This mean field describes the population dynamics of a single, isolated cortical column. The parameters used in our study are the same as in previous ones. They produce biologically realistic and sustained brain dynamics. With those parameters we can switch from an AI to an Up and Down model regime changing only the spike triggered adaptation parameter b . Therefore, except this single parameter b , all parameters are the same in every node and every simulation presented.

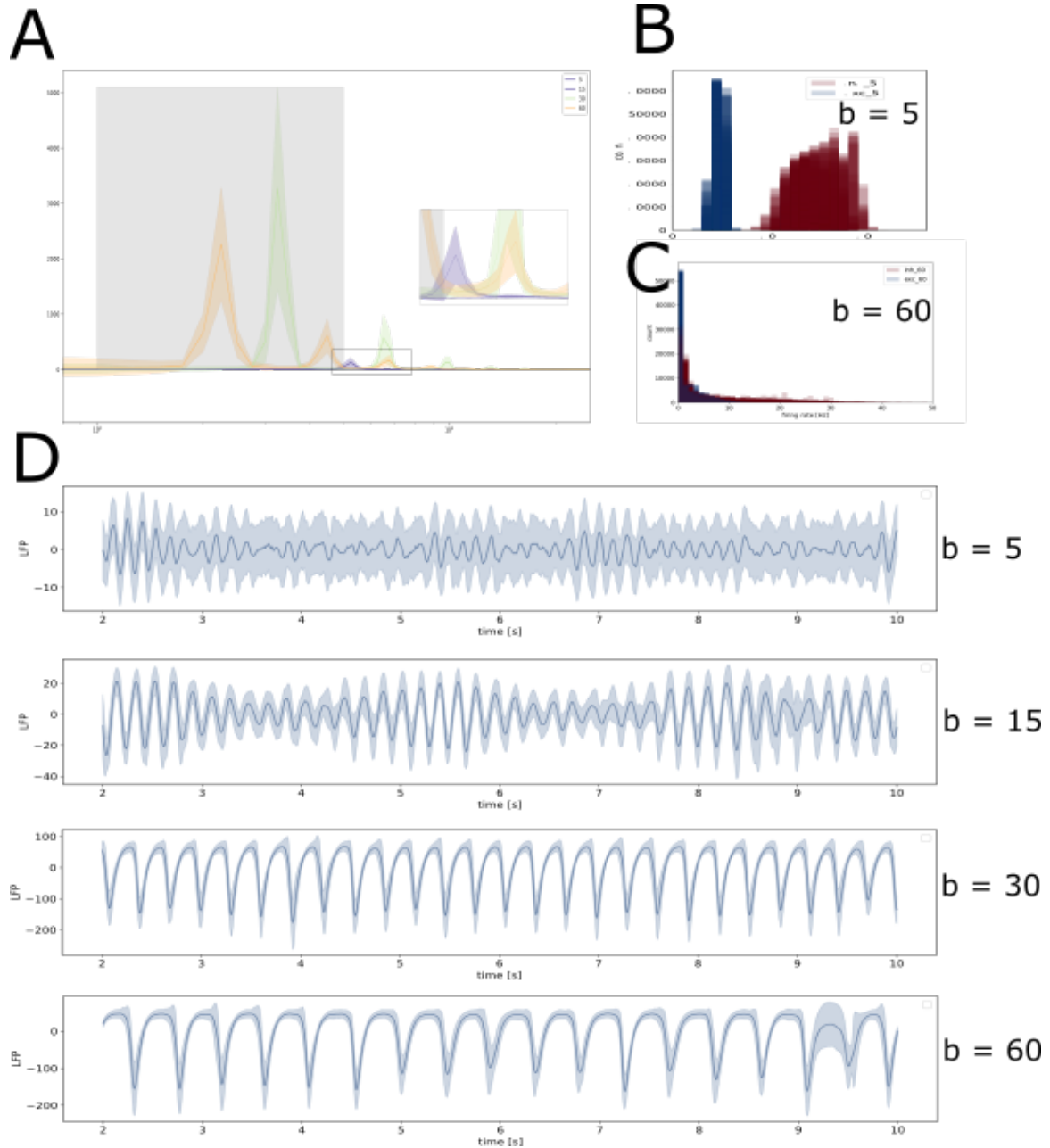


Figure 2: Classical model results with homogeneous adaptation (A): Power spectrum for the four adaptation values presented (B): Histogram of the mean firing rate at each nodes for excitatory and inhibitory populations (in Blue and Red respectively) for a W model with $b=5$. (C): Same as B but for the SWS model with $b=60$. (D): Mean signal and its deviation for the different value of adaptation discussed.

Networks of mean-field models In order to model large brain regions, we represent interconnected cortical columns as a network of mean-field models. The inter-cortical mean-fields connections are done by excitatory interactions only, while inhibitory connections remain locally within the column.

Therefore, once in the network, the dynamics of the single mean-field is changed as it is now impacted by the excitatory input exerted from multiple excitatory populations. The integration of all excitatory inputs is computed using the distance between the origin to target node and the axonal propagation speed to account for the delay of axonal propagation. Thus it is at this step that the connectomics information impacts and shapes the whole model dynamics.

REM-model spike-triggered adaptation parameter The REM model tries to account for the diversity of activity observed experimentally. We look to produce a simulation in which some areas marked by a Delta activity intertwined with periods of faster oscillations (in different proportions according to the area), while other areas would be closer to an ‘Awake-like’ activity. We hypothesize that regional variation of adaptation could be a key to get such a model as it is the parameter used to switch from Wake like to SWS like in the reference model.

In order to keep the model easy to use and describe, we present a model with only three different values of adaptation. This number is the smallest number of different values we found that produces a satisfying result. The different adaptation values used are 5nS (as for our reference W-model), 30nS and 60nS (as for our reference SWS-model). We decide to spatially arrange the adaptation to match with the observation of the decreasing prevalence of delta activity in the LFP going from S1 to S2 and to M1. Limited with the areas we observed experimentally, we place the maximum adaptation level at S1 barrel cortex, then 1.2cm away from it the level adaptation is decreased to 30nS, encompassing the S2 area, and again, 1.2cm further the adaptation parameter is decreased to 5nS, encompassing M1. We add some exceptions to this method of application of the b parameter regarding hippocampal (field CA and dentate gyrus) and prefrontal (cingulate and retrosplenial areas) areas that were parameterized with $b = 5nS$ disregarding their position in the model. We think that this setup is more in accordance with the literature [29, 21], although we did not look further into optimizing the activity of those regions.

REM shuffled as control With our REM model we introduce a mirror model that we’ll use as control: the REM shuffled. This model is built to have exactly the same number of nodes with the different values of adaptation. However in this model the topological arrangement is randomized, losing the spatial aspect of our parametrization for the adaptation. The goal of this model is to look at the importance of this spatial arrangement of adaptation parameter b . We use it to question if the phenomenon need the organized recruitment of multiple nodes, or if any node with high enough adaptation could produce the delta activity disregarding (or with randomized) the average input of the other cortical areas. Most results concerning this model are not shown to keep the results clear, although it should be considered that the results of those REM shuffled models are always more variable than any other model.

LFP measurement The estimate of the LFP signal of each node is computed with a Kernel-based method based on previous work [37]. First demonstrated in a neuron network and then extended to mean-field models, it relates the spiking of neurons to the LFP through efferent synaptic connections. The LFP is calculated as the convolution of the unitary LFPs waveforms modeled from the spiking activity of the field. This method also takes into account the relative contribution of the neuronal population to the signal according to the distance between the origin of the uLFP and the recording site.

In this paper the LFP signal is simulated as if originating from an electrode placed in a superficial layer of the cortex. It is about the equivalent of $400\mu m$ above the somas of layer IV in a human cortex. Thus the signal is inverted compared to the population firing rate. There was no horizontal contribution nor contribution from other mean-fields considered in the calculation of our LFP.

Stimulation With TVMB we used an external input in order to stimulate our model. The stimuli we used consist of a single pulse of 20ms produced by an external and repeated every 1.25sec (+250ms) and starting 3 seconds after the beginning of the simulation Fig. 3).

This external node is connected to its target with a specific connection weight that allows us to control the strength of the stimulus. Different connection weights were tested by stimulating S1 in our different state models. Looking at the kinetic of the evoked potential we found a point where the time to the first peak response is small and remains stable in all conditions for connection strength of 10-3 and above. Therefore all results presented in the main article have the same connection strength of 10-3.

The stimulation experiment shown in the article consists of a set of ten simulations in which the stimuli is provided to one node only, from the right hemisphere, with 5 or 6 stimulus repetition. For each we therefore have a set of above 50 Stimulus Evoked Potentials. We performed this stimulation experiments for the 5 areas we focus on this article (S1, S2, M1, mPFC (its equivalent is the anterior cingulate in the model), dCA1) in each model state (AI, UpDown, REM-model, REM-shuffled). The results presented is the average of the SEP obtained in each condition.

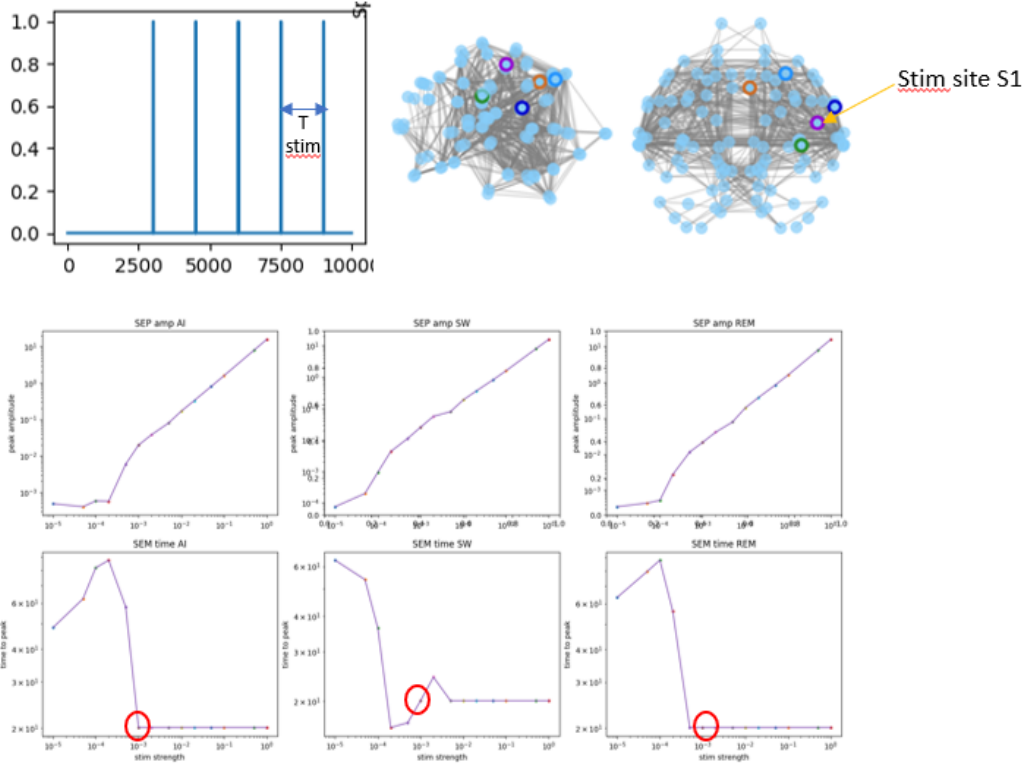


Figure 3: Method of stimulus experiment in the model. (A): Representation of the temporal repartition of the simulations in the protocol. Each stimulus lasts 20ms and is repeated every 1.25+0.25 seconds. (B): Peak amplitude of the Stimulus Evoked Potential (SEP) according to the strength of the stimulus (connection weight). On the Y axis is the amplitude of the response peak observed in the stimulated region. On the X axis is the connection weight between the stimulus source and the stimulated region. Both axis are shown in log. The three panels show the responses values in the different model state (W-model, SWS-model, REM-model from left to right). (C): Time to the peak of SEP according to the strength of the stimulus (connection weight). On the Y axis is the time to the first peak response observed in the stimulated region. On the X axis is the connection weight between the stimulus source and the stimulated region. Both axis are shown in log. The three panels show the responses values in the different model state.

3 Results

3.1 Computational models of REM sleep in mice

To investigate possible mechanisms to explain these local delta waves during REM sleep, we investigated computational models. We used The Virtual Brain platform (<https://www.thevirtualbrain.org/tvb>) to simulate the whole brain of the mouse (see Methods). The model was inspired from previous publications [17, 16] who used mean-field models with conductance-based synaptic interactions to simulate human wakefulness and slow-wave sleep using the TVB platform. Like the human model, the TVB mouse model simulated the asynchronous dynamics reminiscent of Wakefulness (Fig 2 B, Di), and the synchronized slow waves reminiscent of SWS (Fig 2 C, Div). In this model, the transition was driven by modulating the level of adaptation in excitatory populations, which mimics the action of neuromodulators such as acetylcholine, noradrenaline or serotonin, which strongly reduce adaptation in cortical neurons (reviewed in [26]).

In the wakefulness model (W-model), with low adaptation ($b=5$), the neuronal populations are constantly firing with higher firing frequencies for inhibitory cells as observed experimentally [10]. We also see that the different mean-fields are not synchronized together and don't exhibit clear patterns, thus causing asynchronous dynamics. While in the SWS-model with high adaptation ($b=60$), the neuronal populations alternate between periods of important firing (up to 50Hz) and periods of silence where the mean firing rate fall to 0(Hz), inducing a shift to inverted synchronized slow

waves in the LFP with Up and Down state dynamics. We also present the average LFP and spectrum of two intermediate adaptation values for this model. At an intermediate low value ($b=15\text{nS}$) most nodes engages in an oscillatory dynamics but it's less consistent and of smaller amplitude than the oscillations of the SWS-model and there is no real period of silence within the neuronal population. Then, with b at 30nS , a value that will be used in our REM model, the simulation is already in a regime similar to our SWS-model but with shorter periods of silence it oscillates faster.

Simulating REM sleep In order to simulate REM sleep, we hypothesized that the level of adaptation (or equivalently the action of neuromodulators) was inhomogeneous in cortex. In Figure 4 we see an example of heterogeneous distribution of the adaptation parameter b . Motivated by our experimental analysis, we assumed higher values of b in areas such as S1 and S2, and low values in association cortex.

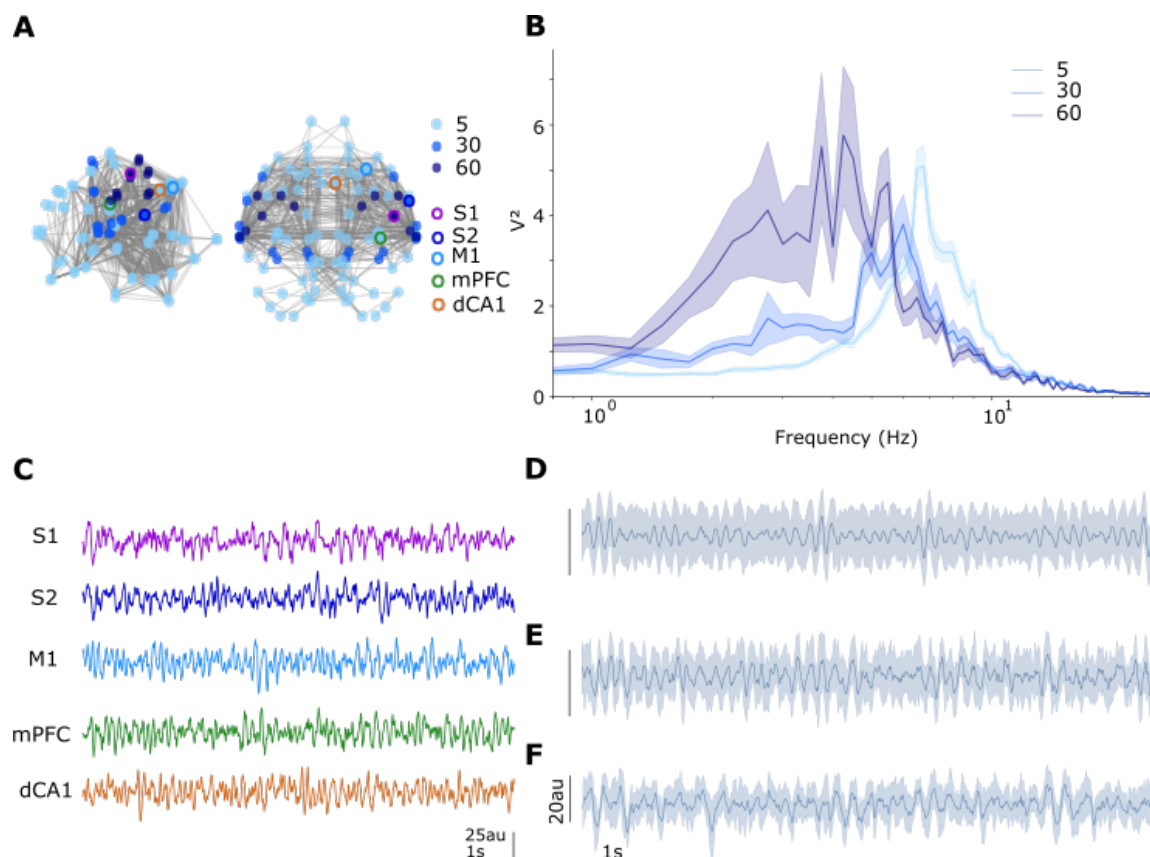


Figure 4: **Cortical model with heterogeneous B setting as model of REM.**

(A) Representation of the Mouse TVB network with nodes for each mean-field. The colour of each node corresponds to the Spike-Adaptation B parameter. Nodes surrounded by a colour circle (Purple, darkblue, lightblue, green and yellow) correspond to the areas studied in figure 1 from the biological dataset. (B) Mean power spectrum for each B parameter value in the model. Power spectrum is computed for each node LFP (with a time window of 4 sec and an overlap of 2 sec), and then averaged across nodes with the same b value. Averaged power spectrums are shown with the SEM. (C) Example 8 seconds of LFP signals from the REM model nodes highlighted in A. (D) Mean LFP signal and its deviation obtained at nodes with $b=5\text{nS}$. This corresponds to the adaptation value of the AI reference model. (E) Same as D for nodes with $b=30\text{nS}$. (F) Same as D for nodes with $b=60\text{nS}$. It corresponds to the adaptation value of the Up and Down reference model

This type of distribution produced the spatial patterns of local delta waves in the simulated REM sleep. In Figure 4B, the nodes with high adaptation display spectrums dominated by the power between 2 and 6 Hz, which could correspond to the model equivalent of the Delta band. It should be noted that there is an important contrast between this relatively broad power in the Delta band and the strong and sharp peak that the SWS-model produces (Fig 2). For nodes with intermediate level of adaptation, although the PSD peaks at a faster frequency, about 6Hz, there is significantly more power in the low frequencies (below 6Hz) compared to nodes with low adaptation.

In the simulated LFP example of the node corresponding to S1, with high adaptation, (Fig 4.C), we can see some slow fluctuations in the signal. This activity is not sustained along the whole simulation but few consecutive cycles could be observed around the 7th second of simulation. Those slower oscillations are of higher amplitude than the portions of the signal that oscillates faster. This slow activity is the model equivalent of the Delta activity we described in the previous analysis. It is harder to find such well defined Delta activity in the simulated LFP for S2. However we can see that the signal of nodes with intermediate level of adaptation, such as the node corresponding to S2, oscillates on average slightly slower and in a slightly more synchronized way than nodes with low adaptation (Fig 4.D,E).

In order to grasp the importance of the topological setup for the spike-triggered adaptation we propose a control model: REM-shuffle, with a random organisation of the parameter b . An example is shown in Fig 5 (D,E,F). As expected each REM-shuffle presents different global activity and the nodes with high b do not always present high slow frequency power ($<5\text{Hz}$). In the example we present, nodes with high b peak at faster frequencies, but some other REM-shuffle (data not shown) could produce dynamics more biased toward slower oscillations than our REM-model. The main point of this control is to show that the adaptation parameter alone is not sufficient to generate the dynamics we want to produce.

Our REM-model, with heterogeneous parametrization of the adaptation presents some sporadic slow activity in the nodes with high adaptation that is close to the Delta oscillation observed experimentally. Then we see that areas with intermediate level of adaptation oscillate slower than nodes with low adaptation of the reference model of wakefulness, and could be prone to produce a few delta events.

Stimulation in the REM model Finally, to investigate the possibility that Delta in primary sensory cortex impairs information integration and thus decreased responsiveness to sensory stimuli [39, 15], we used our model to compare the responsiveness of different brain states with respect to external inputs (Fig. 6, 7).

Stimulus response can be described as composed of two main parts. The first part is the important and fast negative deflection that occurs in less than 50ms after the stimulation. We can see in Figure 6 (and Fig 7,A), that this initial deflection is of higher amplitude in the SWS-model compared to the W-model. Then in a second time the LFP will return to the baseline level. In the W-model this return is fast and accompanied with a second much smaller negative peak in the LFP. In the SWS-model this second part is slower and is associated with a positive peak around 280ms. This reflects a post-stimulus suppression of the neuronal activity. Although the amplitude of the first peak response is exaggerated in our model and the response is a bit slower, the general kinetics are very similar to what could be observed experimentally [32, 28]. In our REM model, the response to stimulation in areas with high adaptation such as S1 is a bit different to what we saw for the W or SWS models. The amplitude of the first peak is between the two other model levels, although closer to W-model. Then, with a slow hyperpolarized return to the baseline, although without a clear positive peak, the second phase of the response is closer to what we observed in the SWS-model.

In Figure 7.B we can see in our different model states how the response to S1 stimulation propagates across the cortex. We can see that the response in the non-stimulated nodes is much smaller, when there is a clear response. For S2 we can see that the response follows at a smaller scale the dynamics seen in S1 for the W-model and SWS-model. However for the REM-model the second phase of the response in S2 is closer to a slower version of what we see in the W-model, with no clear post-stimulation hyperpolarization. For M1 and the other areas, the response is not clear except in the SWS-model because of amplitude issues. However in the SWS-model the response of M1 peaks later than for S2 and with a smaller amplitude. Such observation could be guessed for the two other states and it follows the response propagation pattern observed in the barrel cortex of awake mice [28]. We do not show stimulation responses in our control REM-shuffle for clarity, but when averaged over multiple simulations (therefore multiple random parametrization) the results are very close to what we observe in the W-model.

Finally we investigated whether our REM-model responds to stimulation in the same way when nodes with different adaptation values are stimulated. As we can see in the Figure 7.D, in homogeneous models such as the Wm or the SWS-model, the response to stimulation in the different areas is extremely similar. On the other hand, in our REM-model we can see that each of our adaptation values elicit a slightly different response. The high adaptation values have the largest first peak and the slowest second phase with marked hyperpolarization. The nodes with intermediate adaptation such as S2 have a faster and more pronounced return to the baseline in the secondary part of the response, but it is still relatively slow and there is no negative peak there. And then, the nodes with low adaptation respond to stimulus similarly to the W-model, with the second part of the response as a fast return to the baseline accompanied with a second negative peak. Those results exhibit the variability in stimulation responses one could expect when stimulating during REM, with some areas closely matching the W-model while others have a larger initial peak response and an hyperpolarized second phase as observed in SWS.

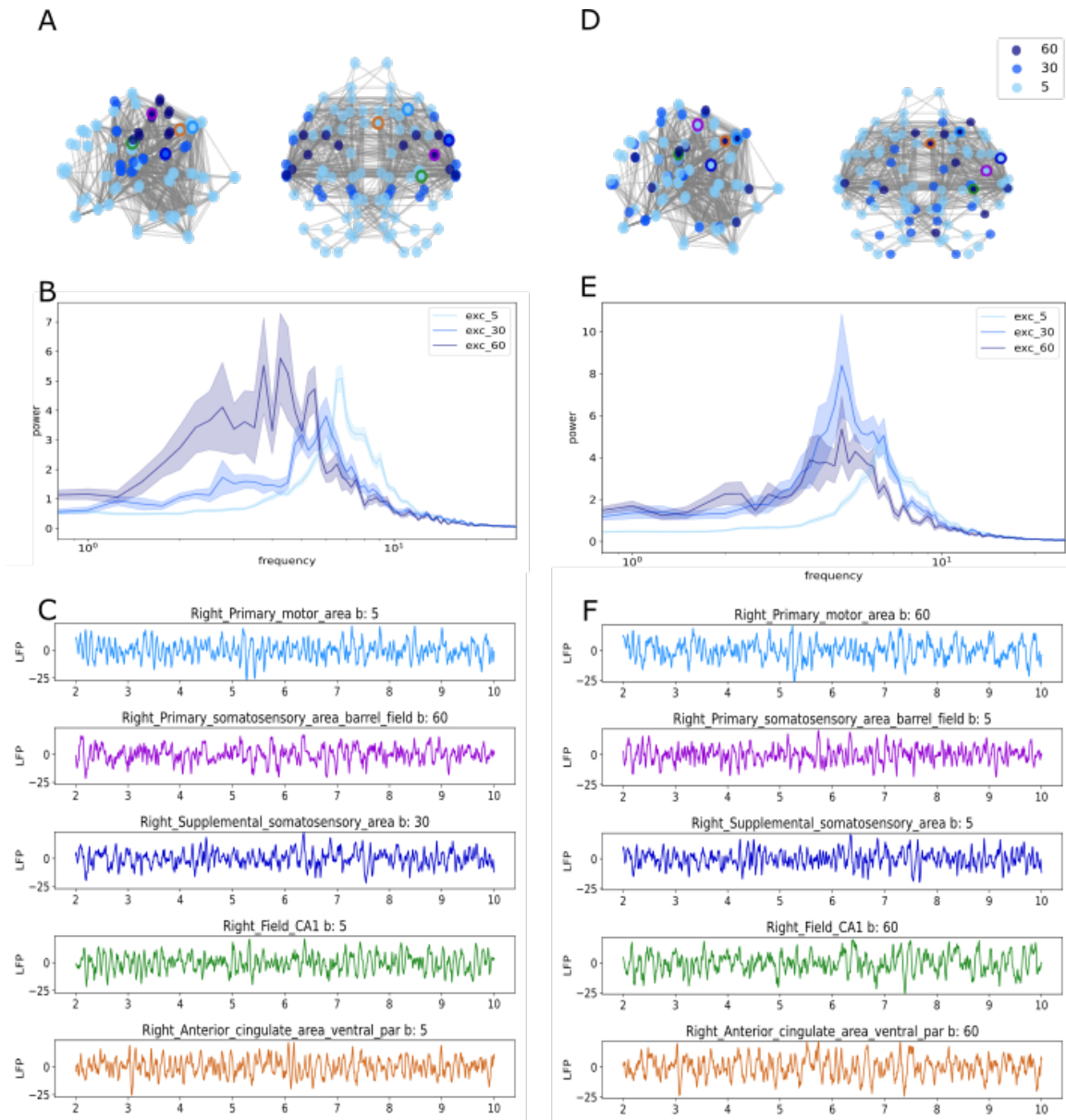


Figure 5: Heterogeneous REM-model vs REM shuffled. Left and Right panels represent the same aspects in two distinct models; the heterogeneous REM-model and its randomised equivalent the REM shuffled. (A/D): Topology of the adaptation parameter in the model. While a clear organisation can be seen in A, it is not the case of D where the setting of b is randomised. (B/E): Power spectrum of the three populations with different adaptation in each model. There is the same number of nodes that participate in the different populations of the two pannels. (C/E): Example LFP signals in the two models. As we can see in F, the b values of the sites of interest are randomised.

4 discussion

In this paper, we investigated a computational model of REM sleep in the mouse brain. The model was build assuming that the neuromodulatory drive, expressed with the adaptation parameter, is heterogeneous in REM sleep. The model showed that assuming such a heterogeneous neuromodulatory drive, there can be a coexistence between Delta activity and asynchronous activity in the same brain. Below we relate these findings to previous work and delineate possible perspectives to follow-up on this work.

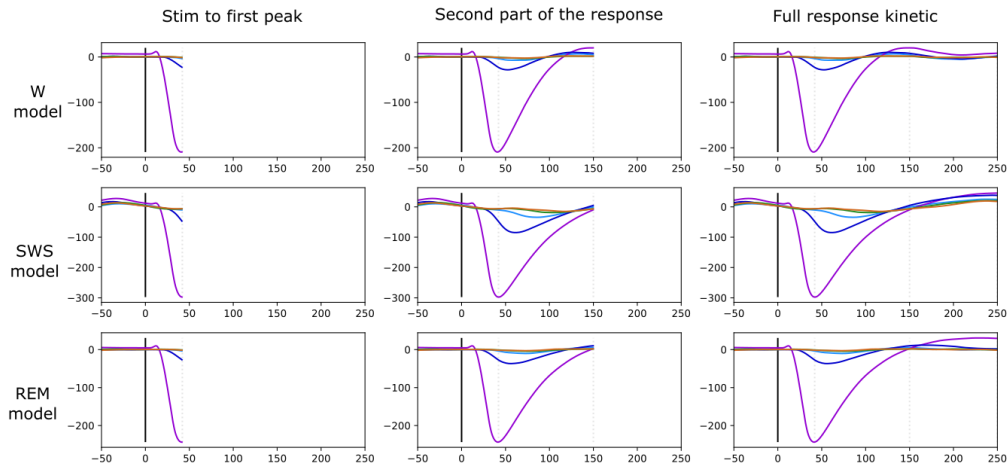


Figure 6: Kinetics of the response to stimulation. This figure shows the temporal evolution of the model in response to stimulation in the three different states. Each line shows one of the states and each panel shows one period manually selected: Panel 1: Response deflection. This panel shows the first part of the stimulus response, up to 42ms after the stimulation, we can see the large deflection of the signal in S1. Similar in duration, the amplitude vary according to the state. Panel 2: Second part of the response. This panel shows how the first response end as well as the the speed to the return to ‘averaged’ value is dependant of the model state. Panle 3: Complete picture of the response observed in the different areas.

The occurrence of local SWA was found before in humans [2, 4] and mice [15, 36]. Based on those observations we propose a new model of the whole cortical dynamics of REM sleep. It was built to relate the Delta waves observed in our analysis paper as well as the few previous observations of the phenomenon, and to this regard it is the first of such models. Along with the REM-model we propose a randomized control of our model showing that the simulations are not only the result of many single mean-field specially tuned but that of a larger network. It was used to show the importance of the considerations regarding the topological organisation of the adaptation we proposed. In the model, we could explain the delta waves by assuming a moderate neuromodulatory drive (using an heterogeneous adaptation) in some areas such as S1, S2, which then produce SWA at around 4 Hz. But those Delta waves we see in S1 are of small amplitude. We do not have Delta activity in M1, meaning that with such parametrization, the drive from the somatosensory cortex is not sufficient to produce Delta waves in the LFP. However, surprisingly, the temporal pattern of the Delta activity in S1, with Delta bouts alternating with faster activity, seems to be relevant compared to the experimental data although we do not tune the model looking for it. This could be studied more by analysing the delta cycles of an extended dataset of REM model simulations with an appropriate detection.

Our model was used to predict the response to sensory stimulation in the different states. While there are some issues with the responses we observed in the model (addressed later in discussion), the general dynamics of the response across the cortex is consistent with experimental data [32, 28]. In the REM-model, the responsiveness was modulated with the level of adaptation, evolving from similar to W-model for areas with low adaptation to somehow closer to SWS-model responses for the low to high adaptation levels respectively. In those areas, such as in S1, the peak response was smaller than in the SWS-model which might indicate that a smaller portion of the neuronal population is recruited for the response. But the slow hyperpolarized second phase of the response is very close to what is characteristic of the SWS-model second phase. It comforts the idea that in REM, when we stimulate an area that can present Delta oscillation such as S1, we should observe large peak response followed by an hyperpolarization that disrupts the propagation of activity. This support the idea that REM SWA lead to an impairment of information integration and thus decrease responsiveness to sensory stimuli [39, 15].

Such a prediction could be tested experimentally by applying whisker stimulation during REM sleep while recording multiple areas. But it should be noted that the stimulus we used in the model is not as natural as a whisker stimulation or a noise presentation done experimentally, but would be closer to TMS experiments such as those performed in humans [23, 24]. In a recent experiment, Massimini et al reported about TMS on the rostral part of the right premotor cortex. They report a response composed of two peaks close to what they see in wakefulness, but the first peak having a larger amplitude and the second peak a slower amplitude. In our data, M1 behaves very similarly in W-model and REM-model. But when compared to the mPFC or dCA1 we could notice a slight tendency toward a slower dynamics in the second

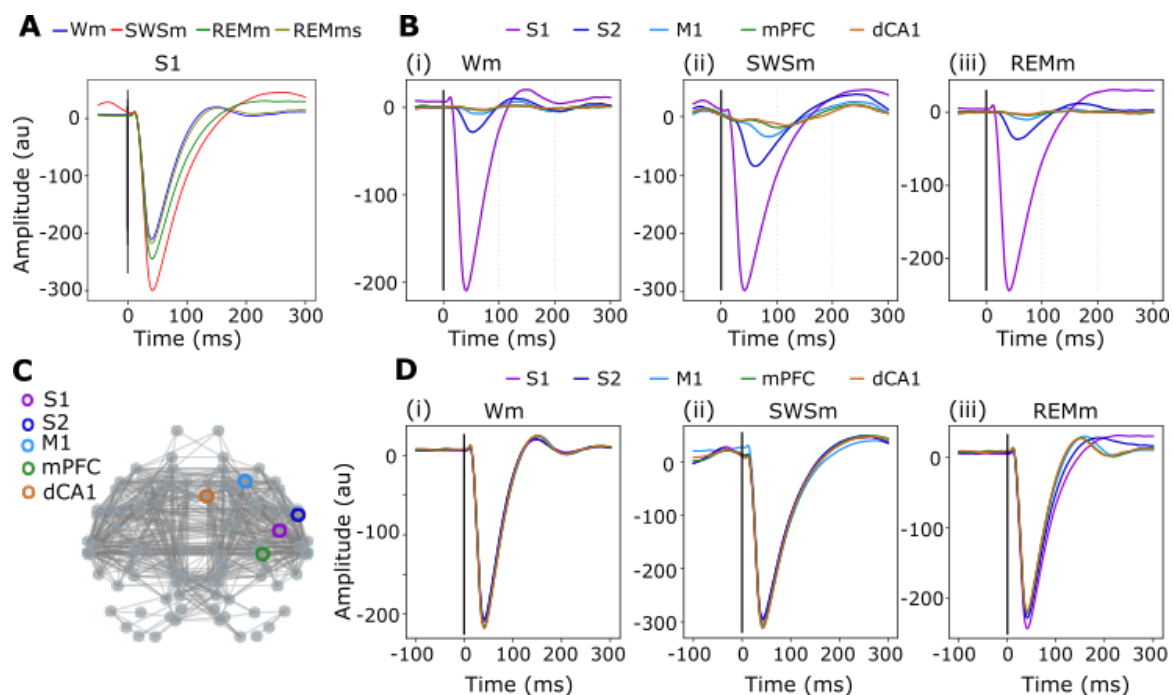


Figure 7: **Model response to stimulation in the different states.**

(A) S1 barrel response when stimulated in the different states (Red corresponds to up and down, Blue to Asynchronous Irregular, Green to REM-model and olive is REM-shuffled). (B) Cortical response to S1 stimulation in the different states. The average LFP response to stimulation in S1 is observed in the different areas of interest across the model states (i: W-model, ii: SWS-model, iii: REM-model). (C) Representation of the model network. Surrounded in colour the five nodes subjected to the stimulation experiment. (D) Response of cortical areas when stimulated across the model states. The colour code corresponds to the areas highlighted in panel C. Each line is the average response observed in an area when it's stimulated. Each sub-panel corresponding to a different state of the model (i: W-model, ii: SWS-model, iii: REM-model)

phase. We already reported that in our model M1 lack of delta activity compared to the biological data, but it seems likely that with some minor tuning for this node our model would be in accordance with such human results.

The model suffers from a number of limitations. First, it is a population model that cannot explain and detail the activity at the single-neuron level. Therefore such an approach cannot be easily related to experimental data at the cellular level but is more appropriate to relate to population-level variables, such as LFP, EEG or imaging. Second, we pointed to some differences between the model and the experimental analysis. The low Delta activity in S2 and its absence in M1 should be overcome with a larger area that encompasses M1 for the application of adaptation and some small tuning of the adaptation values used (using more different values seems an interesting approach from some testings, however it makes the model complex to examine). Third, we also pointed to some limits regarding the responses to stimulation. Indeed we have a very large response amplitude and a slightly slower dynamics. While the first issue might be addressed with a refinement of the stimulus used, the second would require to interact with the parameter of the temporal integration of the model, which would in turn require a complete verification of the different parameters used in the model.

The REM model we proposed can be improved in many ways. The topological parametrization of adaptation was kept simple and some issues could be addressed with finer tuning. But one could also think about more complex parametrization of the model that would take into account other aspects of REM sleep such as the characteristic theta activity [6, 30] in the hippocampus or the very active prefrontal areas [33, 21]. Also, the connectome we used in this model remains relatively limited. We used it for multiple practical reasons (easier to test, faster to run), but it lacks multiple brain regions, some of which, like the thalamus, might be critical to understand cortical delta oscillations or stimulus-response. Larger connectomes are now available with more regions and finer parcellation, but correctly integrating new regions according to this newly characterised phenomenon will require a large amount of research and the perspectives of this work are multiple.

First, one could perform a similar approach based on the human brain. One of the problems to overcome is that local slow-waves may not appear in the EEG, and would ideally require intracranial recordings. However, such recordings are usually rare in primary sensory areas, so one could use the model to simulate local slow-wave activity, use models to calculate the EEG and determine how such local slow-waves affect the EEG. The aim could be to find identifiable EEG signatures of local slow-waves in REM sleep.

Another possible outcome would be to use intracranial recordings in monkey to confirm the presence of slow-waves in some sensory areas, and test the response to stimuli. A TVB model of the macaque monkey brain is currently available based on the Cocomac database [35]. One could use this model constrained by intracranial recordings in monkey to further investigate the role of local slow-waves with respect to sensory or other stimuli in REM sleep.

A final, but not least follow-up would be to test the hypothesis behind our REM model: that the occurrence of Delta waves in REM is related to an heterogeneous level of neuromodulation. Because techniques now exist to measure cholinergic release locally [34], this question could be addressed experimentally. It would also be possible to use such data to construct a simulation where the level of adaptation (or cholinergic drive) is included not only spatially but also temporally, constrained by such data, leading to more realistic models of state transitions in brain activity during REM sleep.

References

- [1] M. Augustin, J. Ladenbauer, and K. Obermayer. How adaptation shapes spike rate oscillations in recurrent neuronal networks. *Frontiers in Computational Neuroscience*, 7, 2 2013.
- [2] B. Baird, A. Castelnovo, B. A. Riedner, A. Lutz, F. Ferrarelli, M. Boly, R. J. Davidson, and G. Tononi. Human rapid eye movement sleep shows local increases in low-frequency oscillations and global decreases in high-frequency oscillations compared to resting wakefulness. *eNeuro*, 5, 7 2018.
- [3] M. Bazhenov, I. Timofeev, M. Steriade, and T. J. Sejnowski. Model of thalamocortical slow-wave sleep oscillations and transitions to activated states. 1994.
- [4] G. Bernardi, M. Betta, E. Ricciardi, P. Pietrini, G. Tononi, and F. Siclari. Regional delta waves in human rapid eye movement sleep. *Journal of Neuroscience*, 39:2686–2697, 2019.
- [5] S. E. Boustani and A. Destexhe. A master equation formalism for macroscopic modeling of asynchronous irregular activity states. 2009.
- [6] G. Buzsáki, D. L. Buhl, K. D. Harris, J. Csicsvari, B. Czéh, C. Czéh, , and A. Morozov. Hippocampal network patterns of activity in the mouse. 2003.
- [7] A. Compte, M. V. Sanchez-Vives, D. A. McCormick, and X. J. Wang. Cellular and network mechanisms of slow oscillatory activity (<1 Hz) and wave propagations in a cortical network model. *Journal of Neurophysiology*, 89:2707–2725, 5 2003.
- [8] S. Crochet and C. C. Petersen. Correlating whisker behavior with membrane potential in barrel cortex of awake mice. *Nature Neuroscience*, 9:608–610, 5 2006.
- [9] G. Deco, V. K. Jirsa, P. A. Robinson, M. Breakspear, and K. Friston. The dynamic brain: From spiking neurons to neural masses and cortical fields. *PLoS Computational Biology*, 4, 8 2008.
- [10] N. Dehghani, A. Peyrache, B. Telenczuk, M. L. V. Quyen, E. Halgren, S. S. Cash, N. G. Hatsopoulos, and A. Destexhe. Dynamic balance of excitation and inhibition in human and monkey neocortex. *Scientific Reports*, 6, 3 2016.
- [11] A. Destexhe. Self-sustained asynchronous irregular states and up-down states in thalamic, cortical and thalamo-cortical networks of nonlinear integrate-and-fire neurons. *Journal of Computational Neuroscience*, 27:493–506, 2009.
- [12] A. Destexhe, D. Contreras, and M. Steriade. Spatiotemporal analysis of local field potentials and unit discharges in cat cerebral cortex during natural wake and sleep states. *Journal of Neuroscience*, 19:4595–4608, 1999.
- [13] C. di Volo, Romagnoni and Destexhe. Biologically realistic mean-field models of conductance-based networks of spiking neurons with adaptation. 2733:2709–2733, 2019.
- [14] L. M. Fernandez, J. C. Comte, P. L. Merre, J. S. Lin, P. A. Salin, and S. Crochet. Highly dynamic spatiotemporal organization of low-frequency activities during behavioral states in the mouse cerebral cortex. *Cerebral cortex (New York, N.Y. : 1991)*, 27:5444–5462, 2016.
- [15] C. M. Funk, S. Honjoh, A. V. Rodriguez, C. Cirelli, and G. Tononi. Local slow waves in superficial layers of primary cortical areas during rem sleep. *Current Biology*, 26:396–403, 2016.

- [16] J. S. Goldman, L. Kusch, B. H. Yalcinkaya, T.-A. E. Nghiem, V. Jirsa, and A. Destexhe. A comprehensive neural simulation of slow-wave 1 sleep and highly responsive wakefulness dynamics 2. 2021.
- [17] J. S. Goldman, L. Kusch, B. H. Yalcinkaya, D. Depannemaecker, T.-A. E. Nghiem, V. Jirsa, and A. Destexhe. Brain-scale emergence of slow-wave synchrony and highly responsive asynchronous states based on biologically realistic population models simulated in the virtual brain. *bioRxiv*, page 2020.12.28.424574, 2020.
- [18] S. Hill and G. Tononi. Modeling sleep and wakefulness in the thalamocortical system. *Journal of Neurophysiology*, 93:1671–1698, 3 2005.
- [19] C. Héricé, A. A. Patel, and S. Sakata. Circuit mechanisms and computational models of rem sleep. *Neuroscience Research*, 140:77–92, 2019.
- [20] J. Lübke and D. Feldmeyer. Excitatory signal flow and connectivity in a cortical column: Focus on barrel cortex. *Brain Structure and Function*, 212:3–17, 7 2007.
- [21] R. Maciel, R. Yamazaki, D. Wang, A. D. Laet, S. Cabrera, C. Agnorelli, S. Arthaud, P. A. Libourel, P. Fort, H. Lee, C. Queiroz, and P. H. Luppi. Is rem sleep a paradoxical state?: Different neurons are activated in the cingulate cortices and the claustrum during wakefulness and paradoxical sleep hypersomnia. *Biochemical Pharmacology*, 191, 9 2021.
- [22] H. Markram, M. Toledo-Rodriguez, Y. Wang, A. Gupta, G. Silberberg, and C. Wu. Interneurons of the neocortical inhibitory system. *Nature Reviews Neuroscience*, 5:793–807, 10 2004.
- [23] M. Massimini, F. Ferrarelli, S. K. Esser, B. A. Riedner, R. Huber, M. Murphy, M. J. Peterson, and G. Tononi. Triggering sleep slow waves by transcranial magnetic stimulation. 2007.
- [24] M. Massimini, F. Ferrarelli, M. J. Murphy, R. Huber, B. A. Riedner, S. Casarotto, and G. Tononi. Cortical reactivity and effective connectivity during rem sleep in humans. *Cognitive Neuroscience*, 1:176–183, 2010.
- [25] R. McCarley. Mechanisms and models of rem sleep control. 2004.
- [26] D. A. McCormick. Neurotransmitter actions in the thalamus and cerebral cortex and their role in neuromodulation of thalamocortical activity. *Progress in Neurobiology*, 39:337, 1992.
- [27] F. Melozzi, M. M. Woodman, V. K. Jirsa, and C. Bernard. The virtual mouse brain: A computational neuroinformatics platform to study whole mouse brain dynamics. *bioRxiv*, 4:1–14, 2017.
- [28] P. L. Merre, V. Esmaeili, E. Charrière, K. Galan, P. A. Salin, C. C. Petersen, and S. Crochet. Reward-based learning drives rapid sensory signals in medial prefrontal cortex and dorsal hippocampus necessary for goal-directed behavior. *Neuron*, 97:83–91.e5, 1 2018.
- [29] K. Mizuseki, S. Royer, K. Diba, and G. Buzsáki. Activity dynamics and behavioral correlates of ca3 and ca1 hippocampal pyramidal neurons. *Hippocampus*, 22:1659–1680, 8 2012.
- [30] S. Montgomery, A. Sirota, and G. Buszaki. Theta and gamma coordination of hippocampal networks during waking and rem sleep. *The Journal of . . .*, 28:6731–6741, 2008.
- [31] E. Niedermeyer. The electrocerebellogram. *clinical EEG and neuroscience*, 35, 2004.
- [32] Y. Nir, V. V. Vyazovskiy, C. Cirelli, M. I. Banks, and G. Tononi. Auditory responses and stimulus-specific adaptation in rat auditory cortex are preserved across nrem and rem sleep. *Cerebral Cortex*, 25:1362–1378, 2015.
- [33] L. Renouard, F. Billwiller, K. Ogawa, O. Clément, N. Camargo, M. Abdelkarim, N. Gay, C. Scoté-Blachon, R. Touré, P. A. Libourel, P. Ravassard, D. Salvat, C. Peyron, B. Claustrat, L. Léger, P. Salin, G. Malleret, P. Fort, and P. H. Luppi. The supramammillary nucleus and the claustrum activate the cortex during rem sleep. *Science Advances*, 1, 4 2015.
- [34] R. M. Santos, J. Laranjinha, R. M. Barbosa, and A. Sirota. Simultaneous measurement of cholinergic tone and neuronal network dynamics in vivo in the rat brain using a novel choline oxidase based electrochemical biosensor. *Biosensors and Bioelectronics*, 69:83–94, 2015.
- [35] K. Shen, G. Bezgin, M. Schirner, P. Ritter, S. Everling, and A. R. McIntosh. A macaque connectome for large-scale network simulations in the virtual brain. *Scientific Data*, 6, 12 2019.
- [36] S. Soltani, S. Chauvette, O. Bukhtiyarova, J. M. Lina, J. Dubé, J. Seigneur, J. Carrier, and I. Timofeev. Sleep–wake cycle in young and older mice. *Frontiers in Systems Neuroscience*, 13:1–14, 2019.
- [37] B. Telenczuk, M. Telenczuk, and A. Destexhe. A kernel-based method to calculate local field potentials from networks of spiking neurons. *Journal of Neuroscience Methods*, 344:108871, 2020.
- [38] I. Timofeev and S. Chauvette. *Neuronal Activity During the Sleep-Wake Cycle*, volume 30. Elsevier B.V., 1 edition, 2019.

- [39] G. Tononi and M. Massimini. Why does consciousness fade in early sleep? volume 1129, pages 330–334. Blackwell Publishing Inc., 2008.
- [40] V. V. Vyazovskiy, U. Olcese, E. C. Hanlon, Y. Nir, C. Cirelli, and G. Tononi. Local sleep in awake rats. *Nature*, 472:443–447, 2011.
- [41] E. Zaghera, A. E. Casale, R. N. Sachdev, M. J. McGinley, and D. A. McCormick. Motor cortex feedback influences sensory processing by modulating network state. *Neuron*, 79:567–578, 2013.



PART V

Discussion

2.3 Result summary

In this thesis we revisit the complex cortical activity of REM sleep using data analysis and modelling approaches. We first performed a close examination of a dataset of multi-site recordings of LFP in the mouse cortex by focusing on the newly discovered REM slow wave activity (SWA).

summary We show that this SWA differs from that of SWS. In REM, SWA is composed of bouts of a few seconds characterised by large delta waves but no slow oscillation ($<2\text{Hz}$). This activity is mostly present in S1 and S2 areas of the somatosensory cortex. The occurrence of delta bouts is loosely coordinated between these two cortical areas. SWA is more rarely observed in the motor cortex and is absent in the dorsal hippocampus (dCA1) and the medial prefrontal cortex (prelimbic area). We also showed that the occurrence of cortical Delta bouts in REM could be related to the hippocampal activity, and particularly to the phasic theta period of dCA1 (and also in the EEG)

Then we proposed a computational model to simulate the cortical activity we observed. The modelling approach builds upon a large theoretical framework encompassing multiple scales and a similar method was recently used to simulate the human brain with dynamical states resembling W and SWS. Here we propose to model the REM cortical activity by assuming a specific heterogeneous level of adaptation in the cortex. With this model we can observe that while most areas are in a regime resembling W we observe some sporadic delta waves in the somatosensory nodes. Using our model, we also tried to predict the cortical responsiveness in REM with a stimulation experiment, showing different stimulus responses according to the node's level of adaptation.

limits Our work suffers from several limitations and critics could be addressed. The use of referential LFP (with a referential electrode above the cerebellum) brings the risks of volume conduction. In general, volume conduction is still much debated among authors. However, the heterogeneous activity in the cortical signals recorded in neighboring cortical areas that we have analysed suggest that these risks are limited. Electrophysiology work, notably in mice, has shown that LFPs recorded in referential mode may be unlikely to be contaminated by volume conduction over a large distance (inferior to a cortical column, [53]). Moreover, as indicated in the Methods of the 1st article, the analysis of oscillations by the cycle-by-cycle method [23] relies on the arbitrary choice of values for certain parameters. Rather than developing a statistical approach, we preferred to do direct blind tests of delta oscillations detection by visual exploration of a sample of dataset aiming at confirming or not the detection capacities of these oscillations by the Bicycle algorithm. Finally, the model relies also on broad theoretical assumptions and simplifications. If, in this model, we have integrated several biological data (LFP activity of a certain number of cortical

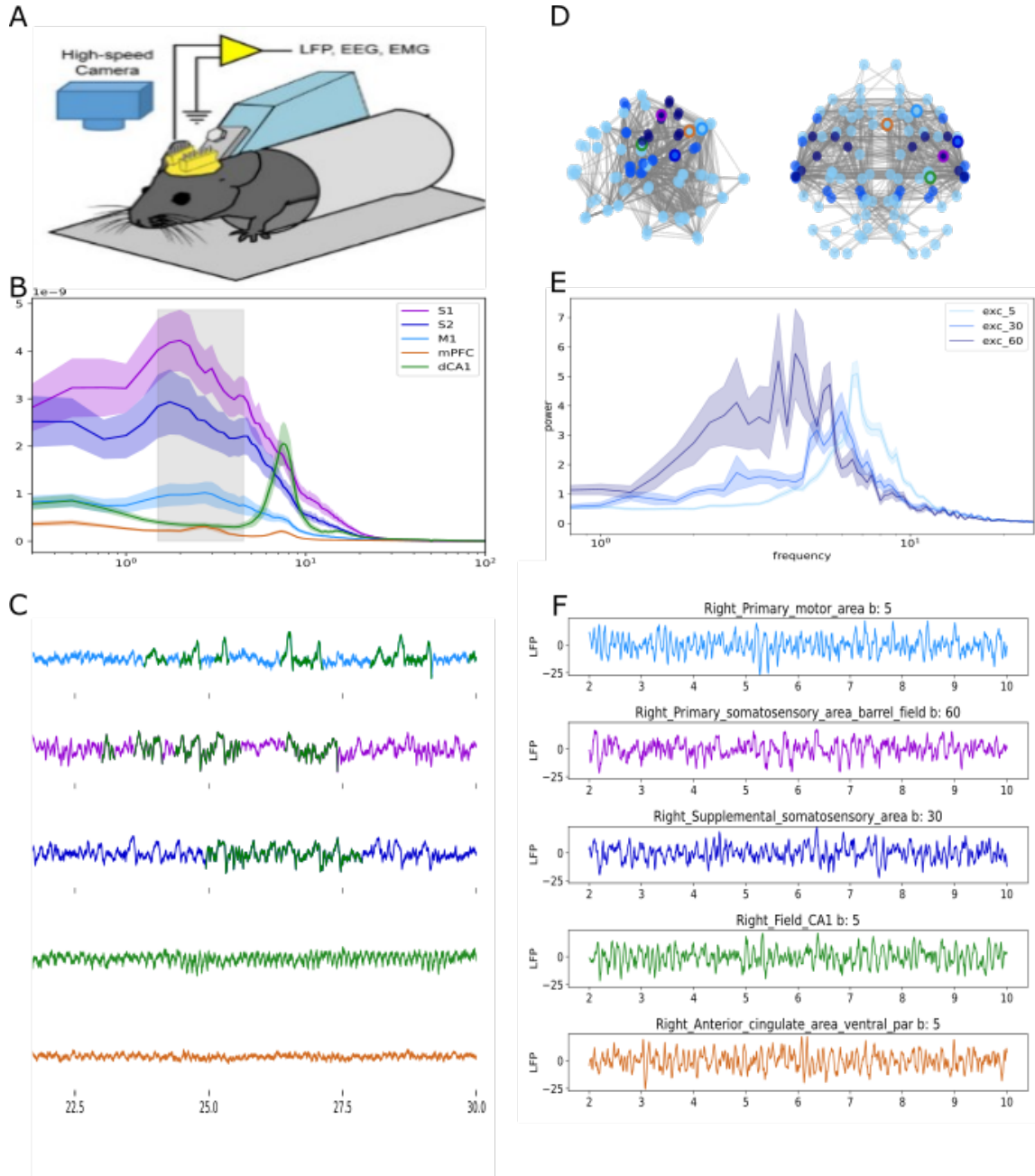


Figure 2.14: Dynamical response to stimulation in S1. This figure shows the different results of the analysis and the model presented in the article. (A/D): Representation of the data presented in the column below. (B/E): Power spectrum observed for the different areas/adaptation values in the corresponding dataset. (C/F) Signal example showing the shape of LFP signal in the biological and simulated data

areas and corticocortical connectivity), several data are missing which can be essential to the dynamics of the network activity during REM such as sub-threshold activity of cortical neurons which remains unknown during this brain state and thalamic activity. This work is a 1st attempt to describe the mouse cortical activity in REM and address potential mechanisms for this activity which has apparent similarities with wakefulness and SWS. Rather than a very detailed and complete description, we discussed different advances and findings, and how we could use them together to better understand REM sleep. More than the raw results, the interest of this work is about the methods and how they could be used, the questioning about the homogeneity and the global aspect of this brain state, and the various possible follow-up we pointed to.

Questioning the classical view

Pogler 2004: “the identity conditions for a thing [...] are the boundary conditions for that thing”

The classical view In neurosciences, theory closely interacts with data analysis and modelling, together with laboratory experiments [102]. We showed in the Introduction that classically REM sleep is defined from EEG as a brain-wide sleep state easily separable from SWS with emblematic neural activity programs and functions. But with the change of reference animal model (from cat and human to rodents) the study of REM became more delicate and the focus that was before on the study of a “dreaming state” faded. However, the picture of REM as an awake-like cortex producing dreaming content in a sleeping body, because of a protective atonia induced from the nucleus of the brainstem. The whole being is under close regulation from slow and global neuromodulatory signalling; still largely rely on early studies that were performed in humans and in cats [51, 42].

The contradictions In our analysis we presented recent findings that contradict the view of a brain-wide and relatively homogeneous state. The presence of strong delta waves in REM makes the distinction with SWS less clear [54], with some authors finding more SWS in some areas and more REM in others [88]. It also means that we can observe simultaneously very different oscillatory patterns: Delta that is usually related to SWS, and theta that is also related to exploratory W. Thus the paradox of REM can be seen from within the cortex. Other authors such as Simor [87] discuss the functional homogeneity of REM, and propose that it could be decomposed into tonic and phasic microstates determined from the eye movements in humans, similarly to what is done for the different stages of SWS. Of course this directly reminds of the tonic and phasic theta observed in the rodent hippocampus. Some articles as [14] says that the phasic REM is associated with both eye movements and phasic theta, but also with pontine waves, muscle

twitches and increased vegetative activity. If this was proven right it would largely support Simor's proposition as relevant, however, we do not know about studies that relate the different transient short events together. Thus it is still difficult to evaluate the relevance of functionally distinct microstates for REM

These different perspectives largely question the definition of REM as they contradict two important points: the brain-wide aspect that can be determined from the EEG and the homogeneity of the state as being only one single continuous brain state. These are propositions to redefine the beginning and end of REM episodes, either locally according to each cortical area activity or in general, splitting the episodes in smaller microstructure, thus changing the core definition of this state. But those two approaches might be difficult to conciliate and then to be used for scientists that are not interested in the very fine structure of REM. In addition we show that the two phenomena might be both related through the phasic hippocampal theta, and this might help to conciliate the different perspectives that tries to refine the definition of REM to fit the recent discoveries. In brief, the definition of REM should answer the following questions: How to take into account the heterogeneity of cortical activity? Do REM transient events reveal the microstructure of REM: do they imply very different mechanisms and brain functions?

What about neuromodulation? We already largely discussed another important conceptual shift would be about neuromodulation and how it regulates sleep and cortical activity. Traditionally considered as a slow and global phenomenon, our results, both experimental and from the model, supports the idea that it might be actually heterogeneous both spatially and temporally [84], and can regulate the cortical activity at a very short time-scale [30].

But this change in perspective we discuss brings another question: Is the Delta activity the result of local sleep in an awake brain, or is it the manifestation of an asleep brain with only some extremely active (/”awaken”) areas? What might seem like an odd question was actually a central concept for the topological organisation of our model! We implemented the first perspective, considering looking for local delta in an awake model, but the question should be asked and I still doubt the correct approach. Indeed, the first goes in line with the earlier studies and the corpus of study that is mostly based on animal EEG analysis. But the second might also be supported by previous studies [66, 82], suggesting only a small subset of cortical areas activated by ascending projections in REM. This would also be somehow more logical considering the classical view of neuromodulation: If this phenomenon is slow, it is more likely that REM, which occurs after SWS, would have a neuromodulatory background closer to SWS than W.

Personal hypothesis

The main point of this section is not to propose a new definition of REM that would consider the different phenomena that need to be better integrated into this definition, but to point toward the important aspects and questions such an updated definition should answer. Associated with it I believe that an approach defining sleep state locally as proposed by Soltani [88] or Tononi's group [36, 9, 85] might be too complex to be used in most studies as it almost makes the whole concept of sleep state caduc as it becomes specific to the observed neuronal population (and thus brings many issues similar to what was discussed in the introduction about the different model scales, and the associated limits in understanding the system). On the other hand, an approach such as proposed by Simor, based on detection of bursts of eye movements is much easier to use and could even be applied to previous studies. But this approach does not take into account other transient events of REM, such as the rapid whisking or the changes in respiratory rate, and those behavioral events are shown to affect the cortical activity in REM [43, 96]. Therefore it might be too simplistic and also difficult to translate to animal models such as rodents. However, if we established the relation between all short transient events of REM, either cerebral as for the phasic theta, or corporal as for the eye movements and whisker movements, then such an approach could be extremely useful.

Perspectives

We already discussed several possible follow-up to this thesis work and most of them are related to better answer the questions previously asked. Here I would like to emphasise on important aspects that would help to better understand the global picture of REM and that relate to ongoing investigations, and then remind how and why computational models of REM are extremely useful for future investigations.

The first important follow-up to remind is the study of the different transient events, behavioural and physiological and their relation. If we showed in this thesis that phasic theta can be somehow observed in the EEG, it is because of the idea that the EEG could be used as a proxy for hippocampal phasic events. Thus it could be used to revisit previous studies or extrapolate about future results, as 2.15, with both EEG and recordings of any corporal transient event that one wants to consider, is it a specific respiratory pattern of a burst of eye movement or whisking. Indeed in an ongoing study about the relation between REM whisking and the electrophysiology of the barrel cortex S1, Boscher and Urbain finds that in addition to a slight decrease of S1 SWA power, the whisking period of REM is also related to a faster theta in the EEG. Considering that EEG faster theta likely reflects hippocampal phasic theta period, it thus supports the yet unfounded idea that transient behaviour very closely matches the transient cortical event in mouse REM.

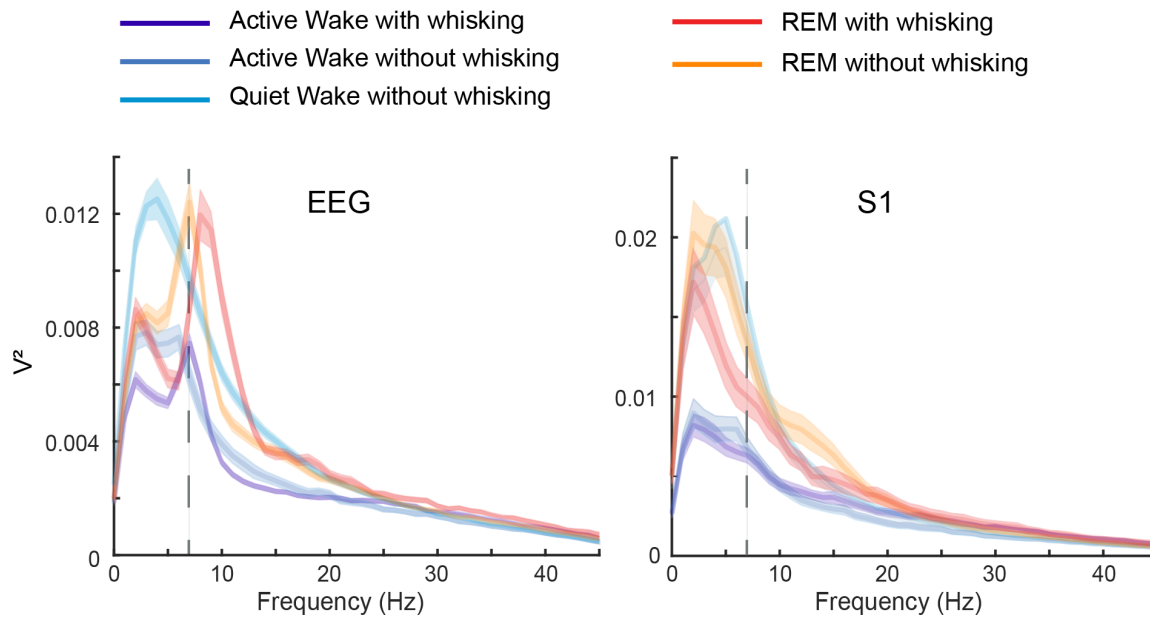


Figure 2.15: Periods of vibrissae movement during REM correspond to an increase in EEG theta frequency. Left, EEG power spectrum during wakefulness and REM (n=23 mice). During REM, in the absence and presence of rapid vibrissae movements (whisking) the theta frequency changes. Vertical dashed line indicates similar theta frequency in wakefulness with whisking and in REM without whisking. Right, power spectrum in area S1 during wakefulness and REM (n=23 mice). A slight spectral difference is observed between REM without whisking and with whisking. Vertical dotted line indicates theta frequency during REM without whisking. Communication from Boscher F and Urbain N « Cortical state dynamics across the mouse sleep wake cycle » Barrel cortex Congress (October 2020) and Congrès SFRMS, (November 2021). Thanks to F Boscher and N Urbain for sharing their results.

Another essential aspect to understand the cortical activity and integrate it into a larger REM framework, is the subcortical and especially the thalamic activity. Not wanting to extend much on this, it could be related to the vast majority of the different points discussed in the whole thesis. Thus knowing its functioning in REM is essential to define that state, as it is to understand W and SWS too, yet we lack information in its regard.

Finally, we saw that theories and models are tightly related and as we showed with our model it is possible to support experimental findings and test biological theories by doing predictions. Thus it helps by explicitly stating what should be looked for in future experiments. For our model, this can mean to look for the cortical distribution of the neuromodulatory drive in REM, and the different level of cortical responsiveness related to this modulation. One major issue with our model is that it is only built to consider REM delta waves and it does not relate well to hippocampal and thalamic activity or other phenomena discussed. Thus, in line with the many experimental studies to consider, we can see a lot of room for improvement of the model, that would go together with a refinement of the core definition of REM sleep.

We are at a time when REM needs to be reconsidered, much more complex than

sometimes thought. It is important to recontextualize the new findings into a larger framework, and computational approaches can help to formalize it.

Reference:



PART VI

Bibliography

Bibliography

- [1] Peter Achermann. “The two-process model of sleep regulation revisited”. In: *Aviation Space and Environmental Medicine* 75 (SUPPL.1 2004), pp. 37–43. ISSN: 00956562.
- [2] Antoine R. Adamantidis, Carolina Gutierrez Herrera, and Thomas C. Gent. “Oscillating circuitries in the sleeping brain”. In: *Nature Reviews Neuroscience* 20 (12 2019), pp. 746–762. ISSN: 14710048. DOI: 10.1038/s41583-019-0223-4. URL: <http://dx.doi.org/10.1038/s41583-019-0223-4>.
- [3] Byungik Ahn. “Implementation of a 12-Million Hodgkin-Huxley Neuron Network on a Single Chip”. In: 2020, pp. 1–8.
- [4] Moritz Augustin, Josef Ladenbauer, and Klaus Obermayer. “How adaptation shapes spike rate oscillations in recurrent neuronal networks”. In: *Frontiers in Computational Neuroscience* 7 (FEB Feb. 2013). ISSN: 16625188. DOI: 10.3389/fncom.2013.00009.
- [5] Sophie Bagur et al. “Breathing-driven prefrontal oscillations regulate maintenance of conditioned-fear evoked freezing independently of initiation”. In: *Nature Communications* 12 (1 2021), pp. 1–15. ISSN: 20411723. DOI: 10.1038/s41467-021-22798-6. URL: <http://dx.doi.org/10.1038/s41467-021-22798-6>.
- [6] Danielle S. Bassett, Perry Zurn, and Joshua I. Gold. “On the nature and use of models in network neuroscience”. In: *Nature Reviews Neuroscience* 19 (9 2018), pp. 566–578. ISSN: 14710048. DOI: 10.1038/s41583-018-0038-8.
- [7] Michaël Bazelot et al. “Unitary inhibitory field potentials in the CA3 region of rat hippocampus”. In: *Journal of Physiology* 588 (12 June 2010), pp. 2077–2090. ISSN: 00223751. DOI: 10.1113/jphysiol.2009.185918.
- [8] Maxim Bazhenov et al. “Model of Thalamocortical Slow-Wave Sleep Oscillations and Transitions to Activated States”. In: (1994).
- [9] Giulio Bernardi et al. “Regional delta waves in human rapid eye movement sleep”. In: *Journal of Neuroscience* 39 (14 2019), pp. 2686–2697. ISSN: 15292401. DOI: 10.1523/JNEUROSCI.2298-18.2019.
- [10] Mark S. Blumberg et al. “What Is REM Sleep?” In: *Current Biology* 30 (1 2020), R38–R49. ISSN: 09609822. DOI: 10.1016/j.cub.2019.11.045. URL: <https://doi.org/10.1016/j.cub.2019.11.045>.

-
- [11] Alexander A. Borbély et al. “The two-process model of sleep regulation: A reappraisal”. In: *Journal of Sleep Research* 25 (2 2016), pp. 131–143. ISSN: 13652869. DOI: 10.1111/jsr.12371.
- [12] Sami El Boustani and Alain Destexhe. “A Master Equation Formalism for Macroscopic Modeling of Asynchronous Irregular Activity States”. In: (2009).
- [13] R. Boyce et al. “Causal evidence for the role of REMs sleep theta rhythm in contextual memory consolidation”. In: *sleep research* 352 (2016), pp. 812–816. ISSN: 00167037. DOI: 10.1016/j.gca.2016.02.011.
- [14] Jurij Brankač et al. “Distinct features of fast oscillations in phasic and tonic rapid eye movement sleep”. In: *Journal of Sleep Research* 21 (6 2012), pp. 630–633. ISSN: 09621105. DOI: 10.1111/j.1365-2869.2012.01037.x.
- [15] A R Braun et al. “Regional cerebral blood flow throughout the sleep-wake cycle An H 2 15 O PET study”. In: 120 (1997), pp. 1173–1197.
- [16] Romain Brette and Wulfram Gerstner. “Adaptive exponential integrate-and-fire model as an effective description of neuronal activity”. In: *Journal of Neurophysiology* 94 (5 2005), pp. 3637–3642. ISSN: 00223077. DOI: 10.1152/jn.00686.2005.
- [17] Richard Brown. “What is a brain state?” In: *Philosophical Psychology* 19 (6 2006), pp. 729–742. ISSN: 1465394X. DOI: 10.1080/09515080600923271.
- [18] G Buzsaki. “The Hippocampo-Neocortical Dialogue”. In: (1996). URL: <http://cercor.oxfordjournals.org/>.
- [19] Reichert C. “The impact of sleep pressure, circadian phase and an ADA-polymorphism on working memory: a behavioral, electrophysiological, neuroimaging approach”. 2015.
- [20] M Carlu et al. “A mean-field approach to the dynamics of networks of complex neurons, from nonlinear Integrate-and-Fire to Hodgkin-Huxley models”. In: *J Neurophysiol* 123 (2020), pp. 1042–1051. DOI: 10.1152/jn. URL: www.jn.org.
- [21] Mary A Carskadon and William C Dement. *Chapter 2 - Normal Human Sleep : An Overview*. 2011, pp. 16–26. DOI: 10.1016/B978-1-4160-6645-3.00002-5.
- [22] Hannah Choi and Stefan Mihalas. “Synchronization dependent on spatial structures of a mesoscopic whole-brain network”. In: *PLoS computational biology* (2019). DOI: 10.1101/319830. URL: <https://doi.org/10.1101/319830>.
- [23] Scott Cole and Bradley Voytek. “Cycle-by-cycle analysis of neural oscillations”. In: *Journal of Chemical Information and Modeling* 53 (9 2018), pp. 1689–1699. ISSN: 1098-6596. DOI: 10.1017/CB09781107415324.004.

-
- [24] S Daan, D G Beersma, and a a Borbély. “Timing of human sleep: recovery process gated by a circadian pacemaker.” In: *The American journal of physiology* 246 (2 Pt 2 1984), R161–R183. ISSN: 0002-9513.
- [25] Ronald E. Dahl and Daniel S. Lewin. “Pathways to adolescent health: Sleep regulation and behavior”. In: *Journal of Adolescent Health* 31 (6 SUPPL. 2002), pp. 175–184. ISSN: 1054139X. DOI: 10.1016/S1054-139X(02)00506-2.
- [26] Subimal Datta. “Neuronal Activity in the Peribrachial Area: Relationship to Behavioral State Control”. In: *Neuroscience and Biobehavioral Reviews* 19 (1 1995), pp. 67–84.
- [27] Subimal Datta et al. “Localization of Pontine PGO Wave Generation Sites and Their Anatomical Projections in the Rat”. In: *Synapse* 30 (1998), pp. 409–423.
- [28] Gustavo Deco et al. “The dynamic brain: From spiking neurons to neural masses and cortical fields”. In: *PLoS Computational Biology* 4 (8 Aug. 2008). ISSN: 1553734X. DOI: 10.1371/journal.pcbi.1000092.
- [29] Alain Destexhe. “Self-sustained asynchronous irregular states and Up-Down states in thalamic, cortical and thalamocortical networks of nonlinear integrate-and-fire neurons”. In: *Journal of Computational Neuroscience* 27 (3 2009), pp. 493–506. ISSN: 09295313. DOI: 10.1007/s10827-009-0164-4.
- [30] Emmanuel Eggermann et al. “Cholinergic Signals in Mouse Barrel Cortex during Active Whisker Sensing”. In: *Cell Reports* 9 (5 2014), pp. 1654–1661. ISSN: 22111247. DOI: 10.1016/j.celrep.2014.11.005. URL: <http://dx.doi.org/10.1016/j.celrep.2014.11.005>.
- [31] Laura M.J. Fernandez et al. “Highly Dynamic Spatiotemporal Organization of Low-Frequency Activities During Behavioral States in the Mouse Cerebral Cortex”. In: *Cerebral cortex (New York, N.Y. : 1991)* 27 (12 2016), pp. 5444–5462. ISSN: 14602199. DOI: 10.1093/cercor/bhw311.
- [32] Luigi Fiorillo et al. “Automated sleep scoring: A review of the latest approaches”. In: *Sleep Medicine Reviews* 48 (Dec. 2019). ISSN: 15322955. DOI: 10.1016/j.smr.2019.07.007.
- [33] Nicolas Fourcaud-Trocmé et al. “Behavioral/Systems/Cognitive How Spike Generation Mechanisms Determine the Neuronal Response to Fluctuating Inputs”. In: (2003).
- [34] Paul Franken. “A role for clock genes in sleep homeostasis”. In: *Current Opinion in Neurobiology* 23 (5 2013), pp. 864–872. ISSN: 09594388. DOI: 10.1016/j.conb.2013.05.002. URL: <http://dx.doi.org/10.1016/j.conb.2013.05.002>.
- [35] Frigg et al. “Models in Science”. In: *Science* (2006).

-
- [36] Chadd M. Funk et al. “Local slow waves in superficial layers of primary cortical areas during REM sleep”. In: *Current Biology* 26 (3 2016), pp. 396–403. ISSN: 09609822. DOI: 10.1016/j.cub.2015.11.062. URL: <http://dx.doi.org/10.1016/j.cub.2015.11.062>.
- [37] Wulfram Gerstner and Richard Naud. “How good are neuron models?” In: *Science* 326 (5951 Oct. 2009), pp. 379–380. ISSN: 00368075. DOI: 10.1126/science.1181936.
- [38] F A Gibbs, H Davis, and W G Lennox. “THE ELECTRO-ENCEPHALOGRAM IN EPILEPSY AND IN CONDITIONS OF IMPAIRED CONSCIOUSNESS”. In: *Archives of Neurology & Psychiatry* 34 (6 1935), pp. 1133–1148. URL: <http://archneurpsyc.jamanetwork.com/>.
- [39] Jennifer S Goldman et al. “A comprehensive neural simulation of slow-wave 1 sleep and highly responsive wakefulness dynamics 2”. In: (2021). DOI: 10.1101/2021.08.31.458365. URL: <https://doi.org/10.1101/2021.08.31.458365>.
- [40] Jennifer S Goldman et al. “Brain-scale emergence of slow-wave synchrony and highly responsive asynchronous states based on biologically realistic population models simulated in The Virtual Brain”. In: *bioRxiv* (2020), p. 2020.12.28.424574. URL: <https://doi.org/10.1101/2020.12.28.424574>.
- [41] Jarrod A. Gott, David T.J. Liley, and J. Allan Hobson. “Towards a functional understanding of PGO waves”. In: *Frontiers in Human Neuroscience* 11 (Mar. 2017). ISSN: 16625161. DOI: 10.3389/fnhum.2017.00089.
- [42] Claude Gottesmann. “Discovery of the dreaming sleep stage: A recollection”. In: *Sleep* 32 (1 2009), pp. 15–16. ISSN: 01618105. DOI: 10.5665/sleep/32.1.15.
- [43] Maximilian Hammer et al. “Theta-gamma coupling during REM sleep depends on breathing rate”. In: *Sleep* 44 (12 Dec. 2021). ISSN: 0161-8105. DOI: 10.1093/sleep/zsab189.
- [44] Sean Hill and Giulio Tononi. “Modeling sleep and wakefulness in the thalamocortical system”. In: *Journal of Neurophysiology* 93 (3 Mar. 2005), pp. 1671–1698. ISSN: 00223077. DOI: 10.1152/jn.00915.2004.
- [45] Hobson and Friston. “Consciousness, dreams and inference”. In: *Journal of Consciousness Studies* 1-2 (21 2014), pp. 6–32.
- [46] J. A. Hobson and K. J. Friston. “Waking and dreaming consciousness: Neurobiological and functional considerations”. In: *Progress in Neurobiology* 98 (1 July 2012), pp. 82–98. ISSN: 03010082. DOI: 10.1016/j.pneurobio.2012.05.003.

-
- [47] J. Allan Hobson. “REM sleep and dreaming: Towards a theory of protoconsciousness”. In: *Nature Reviews Neuroscience* 10 (11 Nov. 2009), pp. 803–814. ISSN: 1471003X. DOI: 10.1038/nrn2716.
- [48] A L Hodgkin and A F Huxley. “A quantitative description of membrane current and its application to conduction and excitation in nerve”. In: *J. Physiol* (1952), pp. 500–544.
- [49] E.M. Izhikevich. “Simple model of spiking neurons”. In: *IEEE Transactions on Neural Networks* 14 (6 2003), pp. 1569–1572. ISSN: 1045-9227. DOI: 10.1109/TNN.2003.820440. URL: <http://www.ncbi.nlm.nih.gov/pubmed/18244602>.
- [50] Eugene M. Izhikevich. “Which model to use for cortical spiking neurons?” In: *IEEE Transactions on Neural Networks* 15 (5 2004), pp. 1063–1070. ISSN: 10459227. DOI: 10.1109/TNN.2004.832719.
- [51] M Jouvet et al. “Paradoxical Sleep - A Study of its Nature and Mechanisms”. In: (1961), pp. 20–62.
- [52] Akihiro Karashima et al. “Instantaneous acceleration and amplification of hippocampal theta wave coincident with phasic pontine activities during REM sleep”. In: *Brain Research* 1051 (1-2 July 2005), pp. 50–56. ISSN: 00068993. DOI: 10.1016/j.brainres.2005.05.055.
- [53] Steffen Katzner et al. “Local Origin of Field Potentials in Visual Cortex”. In: *Neuron* 61 (1 2009), pp. 35–41. ISSN: 08966273. DOI: 10.1016/j.neuron.2008.11.016. URL: <http://dx.doi.org/10.1016/j.neuron.2008.11.016>.
- [54] Jesse J. Langille. “Human REM sleep delta waves and the blurring distinction between NREM and rem sleep”. In: *Journal of Neuroscience* 39 (27 July 2019), pp. 5244–5246. ISSN: 15292401. DOI: 10.1523/JNEUROSCI.0480-19.2019.
- [55] Steven Laureys. “The neural correlate of (un)awareness: lessons from the vegetative state”. In: *TRENDS in Cognitive Sciences* 9 (12 2005), pp. 556–559. URL: www.sciencedirect.com.
- [56] Seung hee Lee and Yang Dan. “Review Neuromodulation of Brain States”. In: *Neuron* 76 (1 2012), pp. 209–222. ISSN: 0896-6273. DOI: 10.1016/j.neuron.2012.09.012. URL: <http://dx.doi.org/10.1016/j.neuron.2012.09.012>.
- [57] Daniel Levenstein et al. “On the role of theory and modeling in neuroscience”. In: (2020), pp. 1–24. ISSN: 2331-8422. DOI: 10.5281/zenodo.4497759. URL: <http://arxiv.org/abs/2003.13825>.
- [58] A Loomis, N Harvey E, and G Hobart. “Potential rhythms of the cerebral cortex during sleep”. In: *Science* 81 (1935), pp. 597–598.

-
- [59] BY L Alfred Loomis, E Newton Harvey, and Garret A Hobart. “CEREBRAL STATES DURING SLEEP, AS STUDIED BY HUMAN BRAIN POTENTIALS”. In: *Journal of Experimental Psychology* 21 (2 1937).
- [60] Kenway Louie and Matthew A Wilson. “Temporally Structured Replay of Awake Hippocampal Ensemble Activity during Rapid Eye Movement Sleep”. In: *Neuron* 29 (2001), pp. 145–156.
- [61] Jun Lu et al. “A putative flip-flop switch for control of REM sleep”. In: *Nature* 441 (7093 2006), pp. 589–594. ISSN: 14764687. DOI: 10.1038/nature04767.
- [62] Pierre Hervé Luppi and Patrice Fort. *Sleep-wake physiology*. Vol. 160. Elsevier B.V., Jan. 2019, pp. 359–370. DOI: 10.1016/B978-0-444-64032-1.00023-0.
- [63] Joachim Lübke and Dirk Feldmeyer. “Excitatory signal flow and connectivity in a cortical column: Focus on barrel cortex”. In: *Brain Structure and Function* 212 (1 July 2007), pp. 3–17. ISSN: 18632653. DOI: 10.1007/s00429-007-0144-2.
- [64] Karen J Maloney, Lynda Mainville, and Barbara E Jones. “Differential c-Fos Expression in Cholinergic, Monoaminergic, and GABAergic Cell Groups of the Pontomesencephalic Tegmentum after Paradoxical Sleep Deprivation and Recovery”. In: (1999).
- [65] M El Mansari, K Sakai, and M Jouvet. “Unitary characteristics of presumptive cholinergic tegmental neurons during the sleep-waking cycle in freely moving cats”. In: (1989).
- [66] P Maquet et al. “Functional neuroanatomy of human rapid-eye-movement sleep and dreaming”. In: *Nature* 383 (1996), pp. 163–166.
- [67] Henry Markram et al. “Interneurons of the neocortical inhibitory system”. In: *Nature Reviews Neuroscience* 5 (10 Oct. 2004), pp. 793–807. ISSN: 1471003X. DOI: 10.1038/nrn1519.
- [68] Henry Markram et al. “Reconstruction and Simulation of Neocortical Microcircuitry”. In: *Cell* 163 (2 Oct. 2015), pp. 456–492. ISSN: 10974172. DOI: 10.1016/j.cell.2015.09.029.
- [69] Massimini. “Neural communication breaks down as consciousness fades and sleep sets in”. In: *sciencemag* (2005).
- [70] M. Massimini et al. “Cortical reactivity and effective connectivity during REM sleep in humans”. In: *Cognitive Neuroscience* 1 (3 2010), pp. 176–183. ISSN: 17588928. DOI: 10.1080/17588921003731578.
- [71] Alberto Mazzoni et al. “Cortical dynamics during naturalistic sensory stimulations: Experiments and models”. In: *Journal of Physiology Paris* 105 (1-3 Jan. 2011), pp. 2–15. ISSN: 09284257. DOI: 10.1016/j.jphysparis.2011.07.014.

-
- [72] David A. McCormick and Thierry Bal. “Sleep and arousal: Thalamocortical mechanisms”. In: *Annual Review of Neuroscience* 20 (1997), pp. 185–215. ISSN: 0147006X. DOI: 10.1146/annurev.neuro.20.1.185.
- [73] David A. McCormick, Dennis B. Nestvogel, and Biyu J. He. “Neuromodulation of Brain State and Behavior”. In: *Annual Review of Neuroscience* 43 (2020), pp. 391–415. ISSN: 15454126. DOI: 10.1146/annurev-neuro-100219-105424.
- [74] Francesca Melozzi et al. “The Virtual Mouse Brain: A computational neuroinformatics platform to study whole mouse brain dynamics”. In: *bioRxiv* 4 (June 2017), pp. 1–14. ISSN: 2373-2822. DOI: 10.1101/123406.
- [75] SM Montgomery, A Sirota, and G Buzsaki. “Theta and gamma coordination of hippocampal networks during waking and REM sleep”. In: *The Journal of ...* 28 (26 2008), pp. 6731–6741. DOI: 10.1523/JNEUROSCI.1227-08.2008.Theta. URL: <http://www.jneurosci.org/content/28/26/6731.short>.
- [76] P.L. Parmeggiani. “REM sleep related increase in brain temperature: A physiologic problem”. In: *Archives Italiennes de Biologie* 145 (2007), pp. 13–21.
- [77] John Peever and Patrick M. Fuller. “The Biology of REM Sleep”. In: *Current Biology* 27 (22 2017), R1237–R1248. ISSN: 09609822. DOI: 10.1016/j.cub.2017.10.026. URL: <https://doi.org/10.1016/j.cub.2017.10.026>.
- [78] Martin Pospischil et al. “Minimal Hodgkin-Huxley type models for different classes of cortical and thalamic neurons”. In: *Biological Cybernetics* 99 (4-5 Nov. 2008), pp. 427–441. ISSN: 03401200. DOI: 10.1007/s00422-008-0263-8.
- [79] Salman E Qasim, Itzhak Fried, and Joshua Jacobs. “Phase precession in the human hippocampus and entorhinal cortex”. In: *2021* (). DOI: 10.1101/2020.09.06.285320. URL: <https://doi.org/10.1101/2020.09.06.285320>.
- [80] Rampon et al. *Synapse-specific modulation of synaptic responses by brain states in hippocampal 2 pathways*.
- [81] Andrew M. Reiter et al. “Finger twitches are more frequent in rem sleep than in Non-REM sleep”. In: *Nature and Science of Sleep* 12 (2020), pp. 49–56. ISSN: 11791608. DOI: 10.2147/NSS.S233439.
- [82] Leslie Renouard et al. “The supramammillary nucleus and the claustrum activate the cortex during REM sleep”. In: *Science Advances* 1 (3 Apr. 2015). ISSN: 23752548. DOI: 10.1126/sciadv.1400177.
- [83] Clifford B Saper et al. “Sleep State Switching”. In: *Neuron* 68 (6 2010), pp. 1023–1042. ISSN: 0896-6273. DOI: 10.1016/j.neuron.2010.11.032. URL: <http://dx.doi.org/10.1016/j.neuron.2010.11.032>.

-
- [84] Martin Sarter and Cindy Lustig. “Forebrain cholinergic signaling: Wired and phasic, not tonic, and causing behavior”. In: *Journal of Neuroscience* 40 (4 2020), pp. 712–719. ISSN: 15292401. DOI: 10.1523/JNEUROSCI.1305-19.2019.
- [85] Francesca Siclari and Giulio Tononi. “Local aspects of sleep and wakefulness”. In: *Current Opinion in Neurobiology* 44 (June 2017), pp. 222–227. ISSN: 18736882. DOI: 10.1016/j.conb.2017.05.008.
- [86] L Silva, Y Amitai, and B Connors. “Intrinsic oscillations of neocortex generated by layer 5 pyramidal neurons”. In: *science* 251 (1991), pp. 432–435. URL: www.sciencemag.org.
- [87] Péter Simor et al. “The microstructure of REM sleep: Why phasic and tonic?” In: *Sleep Medicine Reviews* 52 (2020). ISSN: 15322955. DOI: 10.1016/j.smr.2020.101305.
- [88] Sara Soltani et al. “Sleep–Wake Cycle in Young and Older Mice”. In: *Frontiers in Systems Neuroscience* 13 (September 2019), pp.1–14. ISSN: 16625137. DOI: 10.3389/fnsys.2019.00051.
- [89] M Steriade et al. “Different Cellular Types in Mesopontine Cholinergic Nuclei Related to Ponto-Geniculo-Occipital Waves”. In: *The Journal of Neuroscience* (1990), pp. 2560–2579.
- [90] M Steriade et al. “Neuronal Activities in Brain-Stem Cholinergic Nuclei Related to Tonic Activation Processes in Thalamocortical Systems”. In: *The Journal of Neuroscience* (1990), pp. 2541–2559.
- [91] R. Stickgold et al. “Sleep, learning, and dreams: Off-line memory reprocessing”. In: *Science* 294 (5544 Nov. 2001), pp. 1052–1057. ISSN: 00368075. DOI: 10.1126/science.1063530.
- [92] Bartosz Telenczuk, Maria Telenczuk, and Alain Destexhe. “A kernel-based method to calculate local field potentials from networks of spiking neurons”. In: *Journal of Neuroscience Methods* 344 (July 2020), p. 108871. ISSN: 1872678X. DOI: 10.1016/j.jneumeth.2020.108871. URL: <https://doi.org/10.1016/j.jneumeth.2020.108871>.
- [93] Bartosz Telenczuk et al. “Local field potentials primarily reflect inhibitory neuron activity in human and monkey cortex”. In: *Scientific Reports* 7 (May 2016 2017), pp. 1–10. ISSN: 20452322. DOI: 10.1038/srep40211. URL: <http://dx.doi.org/10.1038/srep40211>.
- [94] Igor Timofeev and Sylvain Chauvette. *Neuronal Activity During the Sleep-Wake Cycle*. 1st ed. Vol. 30. Elsevier B.V., 2019, pp. 3–17. ISBN: 9780128137437. DOI: 10.1016/B978-0-12-813743-7.00001-3. URL: <http://dx.doi.org/10.1016/B978-0-12-813743-7.00001-3>.

-
- [95] Igor Timofeev and Sylvain Chauvette. “Thalamocortical Oscillations: Local Control of EEG Slow Waves”. In: *Current Topics in Medicinal Chemistry* 11 (2011), pp. 2457–2471.
- [96] Adriano B.L. Tort et al. “Temporal relations between cortical network oscillations and breathing frequency during REM sleep”. In: *Journal of Neuroscience* 41 (24 June 2021), pp. 5229–5242. ISSN: 15292401. DOI: 10.1523/JNEUROSCI.3067-20.2021.
- [97] Capone di Volo Romagnoni and Destexhe. “Biologically Realistic Mean-Field Models of Conductance-Based Networks of Spiking Neurons with Adaptation”. In: 2733 (2019), pp. 2709–2733. DOI: 10.1162/NECO. URL: <http://arxiv.org/abs/1803.01446>.
- [98] Matteo di Volo and Alain Destexhe. “Optimal responsiveness and collective oscillations emerging from the heterogeneity of inhibitory neurons.” In: *arXiv* (2020), pp. 1–5. ISSN: 23318422.
- [99] Matteo di Volo et al. “Coherent oscillations in balanced neural networks driven by endogenous fluctuations”. In: *Chaos: An Interdisciplinary Journal of Nonlinear Science* 32 (2 Feb. 2022), p. 023120. ISSN: 1054-1500. DOI: 10.1063/5.0075751.
- [100] Ursula Voss et al. “Measuring consciousness in dreams: The lucidity and consciousness in dreams scale”. In: *Consciousness and Cognition* 22 (1 2013), pp. 8–21. ISSN: 10902376. DOI: 10.1016/j.concog.2012.11.001.
- [101] Xiao Jing Wang. “Neurophysiological and computational principles of cortical rhythms in cognition”. In: *Physiological Reviews* 90 (3 2010), pp. 1195–1268. ISSN: 00319333. DOI: 10.1152/physrev.00035.2008.
- [102] Xiao-Jing Wang et al. “PERSPECTIVE NEUROSCIENCE Computational Neuroscience: A Frontier of the 21 st Century”. In: 2020 (). DOI: 10.1093/nsr/nwaa129/5856589. URL: <https://academic.oup.com/nsr/article-abstract/doi/10.1093/nsr/nwaa129/5856589>.
- [103] Rafael Yuste. “From the neuron doctrine to neural networks”. In: *Nature Reviews Neuroscience* 16 (8 July 2015), pp. 487–497. ISSN: 14710048. DOI: 10.1038/nrn3962.
- [104] Yann Zerlaut and Alain Destexhe. “Enhanced Responsiveness and Low-Level Awareness in Stochastic Network States”. In: *Neuron* 94 (5 2017), pp. 1002–1009. ISSN: 10974199. DOI: 10.1016/j.neuron.2017.04.001. URL: <http://dx.doi.org/10.1016/j.neuron.2017.04.001>.
- [105] Yann Zerlaut et al. “Modeling mesoscopic cortical dynamics using a mean-field model of conductance-based networks of adaptive exponential integrate-and-fire neurons”. In: *Journal of computational neuroscience* 44 (1 2018), pp. 45–61. ISSN: 1573-6873. DOI: 10.1101/168385.